

DEVELOPMENT AND APPLICATION OF MOLECULAR APTAMER PROBES FOR
LUNG CANCER EARLY DIAGNOSIS

By

HUI CHEN

A DISSERTATION PRESENTED TO THE GRADUATE SCHOOL
OF THE UNIVERSITY OF FLORIDA IN PARTIAL FULFILLMENT
OF THE REQUIREMENTS FOR THE DEGREE OF
DOCTOR OF PHILOSOPHY

UNIVERSITY OF FLORIDA

2009

© 2009 Hui Chen

To my wife, Ling Wang

ACKNOWLEDGMENTS

I would like to express my gratitude to many people. This dissertation would not be possible without their continuous help and support. First, I would like to thank my advisor, Dr. Weihong Tan, whose knowledge and expertise in different areas guided me during my five year graduate study. Also his encouragement and patience supported me during my most difficult time. Many thanks go to Dr. Charles Martin, Dr. Jon Stewart, Dr. David Hahn, and Dr. Charles Cao. As my committee members, their encouragement and assistance are invaluable for my research all the time.

I must also acknowledge all former and current Tan group members for their help and friendship. I thank Dr. Dihua Shangguan, Dr. Gang Yao, Dr. Steven Suljak, Dr. Julia Xiaojun Zhao, Dr. Min Yang, Dr. Chaoyong Yang, Dr. Charles Cao, Dr. Hong Wang, Dr. Zhiwen Tang, Dr. Shelly John, Dr. Charles Lofton, Dr. Lisa Hilliard, Dr. Timothy Drake, Dr. Marie Vicens, Dr. Lin Wang, Dr. Joseph Phillips, Dr. Jilin Yan, Dr. Huanghao Yang, Dr. Alina Munteanu, Dr. Colin Medley, Dr. Joshua Smith, Dr. Prabodhika Mallikaratchy, Dr. Maria Carmen Estevez, Dr. Haipeng Liu, Dr. Yufen Huang, Dr. Xiaolan Chen, Dr. Xiaoling Zhang, Karen Martinez, Li Tan, Dosung Sohn, Youngmi Sohn, Parag Parekh, Ye Xu, Kwame Sefah, Yanrong Wu, Huaizhi Kang, Yan Chen, Meng Ling, Pinpin Sheng, Dalia Lopez-Colon, Jennifer Martin, Zhi Zhu, Hui Wang, O'Donoghue, Megan, Patrick Conlon, Xiangling Xiong, Dimitri Van Simaeys, Suwussa Bamrungsap, Basri Gulbakan, and Elizabeth Jimenez.

I would like to thank my parents for their support through my entire life. I must acknowledge my wife, Ling Wang, for her love, encouragement, and continuous support over the years.

TABLE OF CONTENTS

	<u>page</u>
ACKNOWLEDGMENTS.....	4
LIST OF TABLES.....	8
LIST OF FIGURES	9
LIST OF ABBREVIATIONS.....	12
ABSTRACT	13
CHAPTER	
1 INTRODUCTION.....	15
Lung Cancer and Early Diagnosis.....	15
Nucleic Acid Aptamers.....	18
Signal Transduction Mechanisms	21
Synthesis and Modification of Nucleic Acid Aptamers	23
Bionanotechnology	26
Aptamer-Based Bioassays	32
Biomarker Discovery	36
2 SELECTION AND CHARACTERIZATION OF APTAMERS FOR LUNG CANCER USING CELL BASED SELEX	38
Introduction	38
Principle of SELEX.....	39
Methods and Materials.....	44
Cell Based SELEX	44
DNA Library and Aptamer Synthesis	47
Chemicals and Reagents.....	49
Cell Culture	49
Polymerase Chain Reaction	50
Gel Electrophoresis.....	54
Single-stranded DNA Generation.....	55
Cloning and Sequencing.....	55
Flow Cytometry	58
Fluorescence Confocal Imaging	59
Results and Discussion	60
Selection of Aptamers	60
Sequencing and Alignment Results	67
Deconvolution of Specific Aptamers	67
Identification and Characterization of Aptamers.....	71
Enzyme Analysis of Aptamers.....	75

	Minimal Binding Motif Study	76
	Competition Study of Selected Aptamers	80
	Conclusions	81
3	VALIDATION OF APTAMERS FOR LUNG CANCER RECOGNITION	83
	Introduction	83
	Methods and Materials.....	84
	Chemicals and Reagents.....	84
	Cell Culture	84
	Cell Blocks and Tissue Arrays.....	85
	Flow Cytometry	85
	Fluorescence Confocal Imaging	86
	Array Scanning	86
	Results and Discussion	87
	Validation of Aptamers with Various Cancer Cells.....	87
	Cell Block and Tissue Array Tests.....	89
	Clinical Sample Tests.....	94
	Detection of Lung Cancer Cells in Whole Blood.....	96
	Conclusions	96
4	EXTRACTION AND DETECTION OF LUNG CANCER CELLS WITH APTAMER CONJUGATED NANOPARTICLES	100
	Introduction	100
	Methods and Materials.....	101
	Cell Culture	101
	Aptamer Synthesis.....	102
	Fluorescent Nanoparticle Synthesis.....	103
	Magnetic Nanoparticle Synthesis	104
	Conjugation of Aptamers with Nanoparticles.....	104
	Fluorescence Confocal Imaging	105
	Plate Reader Measurements	105
	Results and Discussion	105
	Aptamer Conjugated Nanoparticle Assay Development	105
	Characterization of Extraction and Detection Assay.....	107
	Conclusions	109
5	APTAMER-PCR ASSAY FOR CANCER CELL DETECTION USING APTAMERS FROM CELL BASED SELEX	112
	Introduction	112
	Methods and Materials.....	113
	Cell Culture	113
	Chemicals and Reagents.....	114
	Aptamer Synthesis.....	114
	Real-time PCR Reaction	116

Proximity Dependent Evolution of Paired Aptamers	116
Principle of Aptamer-PCR Assay	118
Detection and Quantification of Cancer Cells by Aptamer-PCR Assay	119
Development of Paired Aptamers for Ultra-Sensitive Aptamer-PCR Assay	125
Conclusions	127
6 SUMMARY AND FUTURE DIRECTIONS	129
Summary	129
Future Directions	131
Conclusions	132
LIST OF REFERENCES	134
BIOGRAPHICAL SKETCH	141

LIST OF TABLES

<u>Table</u>		<u>page</u>
2-1	Equilibrium dissociation constant of selected SCLC aptamers.....	75
3-1	Tests of developed aptamers with cultured cancer cell lines.....	88
5-1	Copy numbers (Log) of specific binding aptamers on different amount of cells	125

LIST OF FIGURES

<u>Figure</u>	<u>page</u>
1-1 Jablonski diagram illustrating the fluorophore relaxation from the excited state to the ground state with the emission of a photon.	22
1-2 The principle of automated solid state synthesis of nucleotides (detritylation, coupling, capping, oxidization).	25
1-3 Chromatograph of RP-HPLC purification of fluorophore labeled oligonucleotide.	26
2-1 Scheme of SELEX.	41
2-2 Magnetic bead based SELEX.	43
2-3 Scheme of cell based SELEX.	45
2-4 Progress of aptamer enrichment during cell based SELEX.	47
2-5 ABI 3400 DNA/RNA synthesizer.	48
2-6 Melting curve of PCR amplified DNA product with optimized PCR conditions.	52
2-7 Principle of real-time PCR reaction.	53
2-8 Gel electrophoresis picture of PCR product in a 3% agarose gel.	55
2-9 pCR 2.1-TOPO cloning vector map.	56
2-10 Sequencing results produced by 454 Life Sciences DNA sequencing unit, GS20.	57
2-11 Working principle of flow cytometry.	59
2-12 Growing patterns and cell morphology of small cell lung cancer and non-small cell lung cancer.	62
2-13 Cell based SELEX using small cell lung cancer cells as target cells and non-small cell lung cancer cells as control cells.	64
2-14 Principle of determining starting quantity of PCR template by using real-time PCR.	65
2-15 Flow cytometry monitoring of lung cancer cells with DNA library and selected pools along the progress of SELEX.	66
2-16 Multiple sequence alignment analysis of sequencing results with MEME Version 3.5.3.	68
2-17 Family of aptamer HCH07 shares the same consensus sequence and has high repeats.	69

2-18	Flow cytometry results of molecular aptamers binding specifically to SCLC cells.	70
2-19	Fluorescence confocal imaging of TAMRA labeled aptamer binding to small cell lung cancer cells.	71
2-20	Z axis imaging of different focal planes of SCLC cells bound with TAMRA labeled aptamer.	72
2-21	Computer software simulated secondary structures of aptamers HCA12, HCC03, HCH07, and HCH01.	73
2-22	Saturation analysis of aptamers.	74
2-23	Aptamer target protein studies with protease treatment.	77
2-24	Minimal binding motif study of aptamer HCH07.	79
2-25	Minimal binding motif study of aptamer HCA12.	80
2-26	Flow cytometry and fluorescence confocal imaging results of competition study of aptamer HCH07.	81
3-1	Cell blocks and tissue microarrays used for lung cancer aptamer validation.	89
3-2	Specific binding of molecular aptamers to formalin-fixed, paraffin-embedded SCLC cell blocks.	90
3-3	Recognition of SCLC fixed cells and live cells by fluorescent dye labeled aptamer.	91
3-4	Aptamer staining of tissue microarrays.	92
3-5	Fluorescence confocal imaging of core A7, A8 and core E7, E8 stained with TAMRA labeled aptamer.	93
3-6	Recognition of SCLC cells in patient sample (T06-06195) with aptamers.	94
3-7	Recognition of SCLC cells in patient sample (T6165) with aptamers.	95
3-8	Flow cytometry data processing of aptamer binding to small cell lung cancer cells in human whole blood.	98
3-9	Recognition of SCLC cells in whole blood with molecular aptamers.	99
4-1	Scheme of extraction and detection of lung cancer cells with aptamer conjugated nanoparticles.	101
4-2	Confocal images of extracted target cells.	107

4-3	Extraction and detection of SCLC cells for enrichment and early diagnosis with aptamer conjugated magnetic/fluorescent nanoparticles.	108
4-4	Confocal imaging of cells extracted by aptamer conjugated nanoparticles and ssDNA library conjugated nanoparticles.	109
4-5	Comparison of binding pattern with target cells between dye labeled aptamer and aptamer conjugated nanoparticles.	111
5-1	Comparison of cancer cell detection by tumor specific gene identification and cancer cell detection by tumor specific aptamer based real-time PCR quantification.	119
5-2	Standard curve of real-time PCR for calculating the amount of specific binding aptamers in aptamer-PCR assay.	121
5-3	Flow cytometry results of aptamer SGC8 and library bound to CEM and RAMOS cells	122
5-4	Sample layout of real-time PCR reaction	123
5-5	Real-time PCR results of standard DNA samples and unknown amount of specific binding aptamer SGC8 sequences for CEM cells.	124
5-6	Proximity dependent evolution of paired aptamer probes for ultra-sensitive aptamer-PCR assay.	127

LIST OF ABBREVIATIONS

SELEX	Systematic evolution of ligands by exponential enrichment
SCLC	Small cell lung cancer
NSCLC	Non-small cell lung cancer
PCR	Polymerase chain reaction

Abstract of Dissertation Presented to the Graduate School
of the University of Florida in Partial Fulfillment of the
Requirements for the Degree of Doctor of Philosophy

DEVELOPMENT AND APPLICATION OF MOLECULAR APTAMER PROBES FOR LUNG
CANCER EARLY DIAGNOSIS

By

Hui Chen

May 2009

Chair: Weihong Tan

Major: Chemistry

Lung cancer has the highest incidence and death rate among all types of cancer. It is rarely curable when lung cancer patients are mostly diagnosed at late stage. Early diagnosis is one way to improve lung cancer survival rate. However, no effective technique is currently available for the early diagnosis. Imaging based techniques are not sensitive to detect early stage lung cancer. Even some newly developed molecular approaches failed to improve this situation.

We have developed a new aptamer approach for the recognition of specific lung cancer cell surface molecular markers. Aptamers are single stranded DNA or RNA molecules, capable of forming 3-dimensional structures at the presence of target molecules. Aptamers have several advantages for molecular recognition. First, they have great specificity and affinity. Aptamers can be chemically synthesized and have long shelf life. They are robust for different types of modification and conjugation. Our approach relies on cell based systematic evolution of ligands by exponential enrichment (cell based SELEX) to evolve aptamers for whole live cells that express a variety of surface markers representing molecular differences among cancer cells. With cell based SELEX technique, aptamers can be readily developed for any types of cancer cells of interest, and can recognize the target molecules at their native state. More importantly, aptamers

can be developed without knowing the details of the target molecules. This is particularly useful for lung cancer study that is short of these knowledges.

In this work, we successfully developed several aptamers against small cell lung cancer (SCLC) cells. These aptamers were characterized and tested with different samples for validation. When applied to different lung cancer cells including patient samples, these aptamers could bind to SCLC cells with high affinity and specificity in different assay formats including flow cytometry, confocal imaging, and tissue microarray. Even in some complex biological environment such as human blood, the aptamers retained their binding ability. When the aptamers were conjugated with magnetic and fluorescent nanoparticles, the aptamer/nanoparticle complex could effectively extract SCLC cells from cell media for isolation, enrichment, and sensitive detection. We also developed aptamer-PCR assay for detection and quantification of small amount of cancer cells. This may become useful for detection of small amount of exfoliated lung cancer cells at early stage. Our studies demonstrated the potential of the aptamer approach for early lung cancer detection.

Besides early diagnosis, understanding the disease mechanism will also benefit from aptamers developed in this work. The aptamers developed here will be further used for identification of the target proteins on cancer cell surface to facilitate the progress of biomarker discovery for lung cancer and design appropriate treatment strategy. More validation tests and clinical trials are required to further evaluate the usefulness of the developed lung cancer aptamers.

CHAPTER 1 INTRODUCTION

Lung Cancer and Early Diagnosis

Cancer is a major health problem in the world. In the United States, about 25% of deaths are due to cancer. Among all cancer cases, lung cancer has the highest incidence and death rate. With 170,000 deaths every year in the United States, lung cancer causes more deaths than the sum of the next three leading cancers: breast, colon, and prostate. According to recent study, most of the lung cancer cases are related to smoking. Asbestos, radon, and other environmental factors also contribute to the incidence of lung cancer. Based on morphology difference under microscopy, lung cancer can be classified into two main categories: small cell lung cancer (SCLC) and non-small cell lung cancer (NSCLC). Non-small cell lung cancer can further be divided into sub-categories such as adenocarcinomas, squamous cell (epidermoid) carcinomas, bronchoalveolar carcinomas, and large cell carcinomas, based on the location where tumor originally rises from and other pathological features. In some cases, mixed lung cancer types can also be observed in patients.

Small cell lung cancer typically develops from central location. It has rapid growth rate and is infamous for early metastases. Because of this pathological feature, chemotherapy is more effective than surgery for small cell lung cancer while non-small cell lung cancer favors surgical resection. Non-small cell lung cancer varies from the location and has relatively better prognosis than small cell lung cancer. Generally, different sub-categories of non-small cell lung cancer have distinct clinical and pathological features.

The prognosis of lung cancer is the worst among all cancer types with the 5-year survival rate less than 15%.^[1] This poor prognosis is partly due to a lack of effective early diagnosis technique as well as efficient treatment strategy. As more than 75% of all lung cancer patients

are at late stage of the disease when diagnosed, it is quite difficult to cure them with current therapy.^[2] The early diagnostic ability for lung cancer is crucial to decrease the lung cancer mortality since most lung cancer patients are diagnosed at an advanced stage where treatments are rarely successful. This is especially important for small cell lung cancer. Among all the lung cancer subtypes, small cell lung cancer (SCLC) is the most aggressive one, although it only accounts for 14% of all lung cancer cases. It has the highest tendency for early dissemination and the shortest median survival (7-12 months) as a clinically distinct entity. More than 95% of patients eventually die from the cancer.^[3]

Survival of patients with lung cancer, especially SCLC, relies on early detection as well as effective treatment. However, a few clinical trials of lung cancer early detection performed in the last several decades were not successful. The first large scale clinical trial of lung cancer early detection used both sputum cytology and chest x-rays. It led to earlier diagnosis of lung cancer at some level, but the reduction in overall mortality could not be justified thereafter.^[4] Recently newly developed imaging based screening technologies such as spiral computed tomography (CT), optical coherent tomography, positron emission tomography (PET), virtual bronchoscopy, autofluorescence bronchoscopy, and confocal microscopy were used to improve this situation, but they all failed.^[5] The reason may be that morphological criteria used in all these imaging approaches are not sensitive for early diagnosis during the premalignant phase of lung cancer development.^[6, 7] For example, tumors with size below the resolution of CT scan (1-2mm) may already begin to disseminate cancer cells to distant sites. In addition, some tumors grow rapidly, which makes early detection even more difficult. For SCLC, which arises without morphologically recognizable preneoplastic lesions, imaging based detection method is almost impossible for early detection.^[8]

Recently, molecular approaches were exploited to complement imaging studies. Molecular abnormalities correlate with behavioral aspects of lung cancer, and therefore are more sensitive in detecting invasive malignant lesions in preclinical phase than imaging methods by which tumor sizes are revealed. Genetic and proteomic analysis are two major molecular-marker based early detection techniques.^[9] Detection of gene mutations, nuclear riboprotein, methylation related gene silencing, and malignancy associated changes are widely used for genetic level early detection. Although genetic changes can be detected reproducibly by PCR^[10] and genomic hybridization,^[11] they do not always correlate with changes at protein level. Therefore, people began to seek approaches for early detection of lung cancer at protein level. Proteomic analysis using immunostaining^[12] is the most used method. However it is limited by the lack of specific lung cancer antigens. For some existing antigens, normal epithelia cells also show positive for these antigens in some cases. Extra costs of health care and unnecessary treatment due to false positive diagnostic results are main concerns about this method.

Most recently, mass spectrometry^[13] became a new trend in lung cancer early detection. This method does not involve any molecular probe for the recognition of biomarkers. Instead, simple comparison of mass spectroscopic results between lung cancer patient sample and control sample was used to distinguish lung cancers with different clinical and pathological features. This novel method greatly complements the genetic approaches. However, there has been only limited success because the significant variation among different patients makes it very difficult to get accurate and predictive pattern for clinical trial. Overall, neither genomic nor proteomic approaches succeeded in developing sensitive and specific way for lung cancer early detection.^[14] Therefore, there is a demand of approaches that can generate specific molecular probes rapidly for detection and discovery of lung cancer biomarkers.

Here, we introduce a new nucleic acid probe based approach, in which a panel of DNA aptamers was purposely developed against the molecular differences among lung cancer cells to detect specific molecular markers of lung cancer. Our approach relies on cell based SELEX (systematic evolution of ligands by exponential enrichment) to ensure the specificity and widespread availability of aptamer probes, which are missing in antibody based methods. We will first focus on the development of cell based SELEX methodology using the leukemia as the model system, followed by the technique transfer to the lung cancer systems including small cell lung cancer and non-small cell lung cancer. These aptamer probes were developed without prior knowledge about their target proteins. They were tested for their ability to specifically bind both cultured cells and clinical samples of lung cancer in various assay formats. Aptamers were also exploited for detection and isolation of lung cancer cells, a critical step towards the goal of early detection. Several assay platforms for early detection were designed using the aptamers developed. Using selected aptamers for identifying the target proteins were also reviewed. Compared to other molecular recognition elements, aptamers used in this approach present several advantages for early detection. While aptamers' sensitivity leads to the detection of malignant cells, their specificity derived from cell based SELEX prevents cross reactivity with normal epithelial cells, resulting in fewer false positives. In practice, multiple aptamers can be readily developed for any cancer cells of interest without prior knowledge of cell surface markers, and are more predictive of cancer progression than single probes used in previous studies. In addition, low-molecular weight aptamers can be easily synthesized and modified to recognize the target proteins at their native state on cell surfaces reproducibly.

Nucleic Acid Aptamers

Molecular recognition is a unique biological phenomenon. In this phenomenon, many biological molecules can recognize/bind to certain molecules with high selectivity and affinity.

This recognition capability was explained as a lock-and-key system at molecular level. There are several known molecular recognition systems: antibodies/antigens, nucleic acids, and avidin (streptavidin)/biotin. Antibodies are protein molecules produced by immune systems of human or animals, typically composed of two heavy chains and two light chains of amino acids, which play key role in recognition of their target, antigen. In an immune system, all the intruders from outside are tagged as antigens by antibodies to be destroyed later. In order to recognize the intruders effectively, antibodies are evolved to have the great specificity for antigens. Because of their great recognition ability, antibodies have been widely used in biomedical studies since 1950s.

During the past few decades, nucleic acid probes emerge as a new type of molecular recognition element. Nucleic acid probes include deoxyribonucleic acid (DNA), ribonucleic acid (RNA), peptide nucleic acid (PNA), and other artificially synthesized nucleic acid. Nucleic acids are linear chains of nucleotides which are comprised of 5 different bases for DNA and RNA: adenine (A), cytosine (C), guanine (G), thymine (T), and uracil (U). Each nucleic acid is defined by the sequence of all bases which is also referred as primary sequence. With the primary sequence, nucleic acid can hybridize to another nucleic acid molecule with complimentary sequence through Watson-Crick base pairing rule.^[15] This binding event between the two nucleic acid molecules is highly specific, and is primary sequence dependent. Unlike the primary structure based hybridization mechanism of nucleic acid detection, nucleic acids can also form secondary structures, which give rise to the recognition ability for various targets such as inorganic/organic molecules. Aptamer is one of the most important nucleic acid probes based on secondary structures, targeting a variety of molecules including proteins, organic molecules, ions, virus, organelles, and even cells. These oligonucleotide ligands are referred as “aptamers”,

derived from the Latin word “aptus”, meaning “to fit”.^[16] Although the famous RNA world hypothesis proposes that nucleic acids can specifically interact with proteins to perform certain types of functions, it was until 1990 that people began to explore the possibility of using nucleic acids for targeting proteins. This discovery of aptamer greatly benefited from the rapid growing of combinatorial chemistry, the functional screening of large libraries of compounds, particularly in this case, nucleic acids. Nucleic acids are suitable for combinatorial selection because of their secondary, tertiary, and quaternary structures. In addition, they can be easily amplified by polymerase chain reaction (PCR). By interacting with amino acid residues, nucleic acids with certain primary sequences show great binding affinity and specificity for proteins. Combinatorial screening technique of nucleic acids was known as SELEX (Systematic Evolution of Ligands by Exponential enrichment). SELEX starts with a large population of 10^{13} - 10^{16} synthetic oligonucleotides. Each candidate has a different sequence, which folds into a different structure. Individual molecules are separated from each other based on their abilities to bind target molecules. The retained molecules are then PCR amplified and go through iterative rounds of selection. Eventually the post-selection pool will be dominated with molecules that can bind with target tightly. After cloning, sequencing, and de-convolution, the aptamer sequences will be tested and further optimized. In 1990, for the first time, Szostak’s lab selected RNA aptamers for dye molecules using *in vitro* selection technique.^[16] In the same year, Gold’s lab also obtained RNA aptamers for polymerase by SELEX.

Although aptamers and antibodies have comparable specificity and affinity, aptamers have several advantages over antibodies. First, aptamers can bind to more targets than antibodies.^[17] Second, their low molecular weight makes them penetrate into the tissue more easily. In addition, they are easily synthesized and modified so that they can maintain structures and

functions when exposed to undesirable conditions. Besides their applications in bioanalytical chemistry as basic molecular recognition element, aptamers have been more and more used for disease diagnosis and therapy in recent years. Single stranded nucleic acid aptamers can be evolved to have great specificity and affinity against different disease-related metabolites, biomarker proteins, even whole live cells that express a variety of surface biomarkers. When coupled with suitable signal transduction mechanisms, aptamers show great potential as a new tool for biomedical studies.

Signal Transduction Mechanisms

With SELEX technique, we can develop a panel of molecular aptamers for target molecules. However the molecular recognition element itself can't function without appropriate signal transduction mechanisms since these two components are indispensable parts of molecular sensing systems.

Fluorescence-based signal transduction mechanisms are among the most popular ones used with molecular aptamers for detection. Figure 1-1 shows a typical Jablonski diagram that illustrates the fluorescence principle. Generally, photons of excitation light are absorbed by fluorophore and the absorbed energy jumps up the electrons from ground state to excited singlet state. There will be an energy relaxation process involved between different vibrational energy levels. This is called internal conversion. After this internal conversion, the electron will return to the ground state, accompanied by photon emission. The emitted photon will have a longer wavelength than the original excited photon because of the energy loss during internal conversion. These fluorescence-based signal transduction mechanisms include direct fluorophore labeling,^[18] fluorescence resonance energy transfer (FRET), fluorescence quenching, fluorescence anisotropy, light-switching excimers, and etc. Among all these mechanisms, the direct fluorophore labeling is the first choice for rapid and simple biological assays because of its

inherent stability and sensitivity. For example, flow cytometry assay using fluorescent dye labeled antibodies is the most frequently used assay for cell detection and discrimination. Signal transduction mechanisms based on energy transfer effect are another popular categories, including fluorescence resonance energy transfer (FRET), fluorescence quenching, and fluorescence anisotropy. These mechanisms are extensively used for protein binding and interaction studies. Besides, there are a few other types of fluorescence-based signal transduction mechanisms reported in details elsewhere, such as light-switching excimer-based probes.

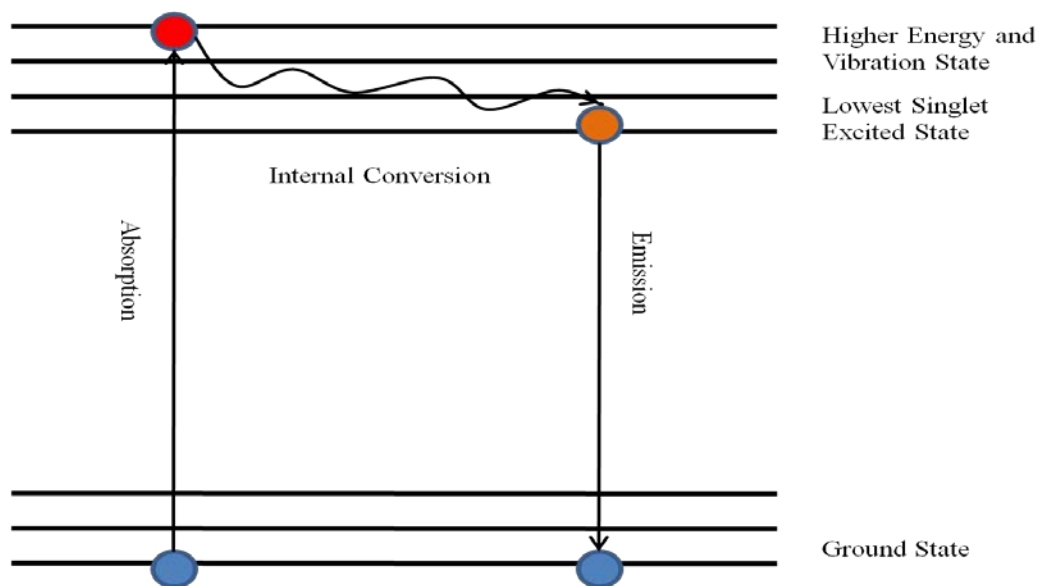


Figure 1-1. Jablonski diagram illustrating the fluorophore relaxation from the excited state to the ground state with the emission of a photon.

Besides various fluorescence-based signal transduction mechanisms, a few other signal transduction mechanisms were used with aptamers in different sensor designs. Aptamers for small molecules have been used in biosensors with mechanical readout mechanisms such as surface plasmon resonance technology,^[19] quartz crystal microbalance technology,^[20] and microfabricated cantilever technology.^[21] Electrochemical detection using aptamers as recognition molecules has been also reported previously.^[22] Recently single-walled carbon

nanotube-field effect transistors (SWNT-FETs) were used in the design of selective biosensor application to achieve signal transduction.^[23]

Synthesis and Modification of Nucleic Acid Aptamers

One of the most important advantages of using nucleic acid aptamers for sensor and biological applications is that they can be prepared *in vitro* by DNA/RNA solid state synthesis technology. Before the invention of automated nucleic acid synthesis technology, preparation of DNA/RNA relies on various molecular biology techniques such as PCR (polymerase chain-like reaction) and ligation. This costly process does not allow the preparation of large quantities of nucleic acid for applications. With the aid of automated nucleic acid synthesis technology, the preparation efficiency was greatly improved. Moreover, there is no involvement of animals in the production of aptamers. Easy modification is another important advantage of synthetic nucleic acid molecules. After the synthesis of nucleic acid, different functional groups can be linked to DNA/RNA molecules through on/off column coupling procedure with different conjugation strategies.

The core of automated oligonucleotide synthesis technology is the solid state synthesis via phosphoramidite chemistry. The solid state synthesis of oligonucleotides involves controlled-pored glass (CPG) beads as solid support which allows on-column washing and separation. As the direction of solid state synthesis of DNA/RNA is opposite to natural PCR reaction that is from 5' end to 3' end, the first nucleoside of 3' end is chemically linked to the support through 3'-hydroxyl group. The phosphoramidite synthesis method generally has four steps in a cycle (Figure 1-2) to add one DNA/RNA base: detritylation, coupling, capping, and oxidization. In order to retrieve the active 5' hydroxyl group of previous nucleotide for reacting with the next base, detritylation was done by incubating with either dichloroacetic acid (DCA) or trichloroacetic acid (TCA) in dichloromethane (DCM) to remove the trityl group that is

protecting the 5' hydroxyl group. After deprotection, the new monomer was linked to the nucleotides through the coupling step. Before that, the phosphoramidite derivative of nucleotide was activated by incubation with tetrazole that protonates the nitrogen of the diisopropylamine group on the 3'-phosphorous group. Following the tetrazole activation, a phosphoramidite derivative of the nucleotide was added to the growing chain on the solid support through the nucleophilic attack of active 5' hydroxyl group on the tetrazolyl phosphoramidite to form a phosphite linkage. Once the coupling step is finished, excess reagents are removed by washing the solid support thoroughly. Next, the capping step is introduced to treat the incomplete nucleotides which failed to elongate in last step. This can prevent the interference of these failed sequences during late elongation steps. To eliminate this effect, the 5'-hydroxyl groups of failed sequences are deactivated by capping with protective group. Acetic anhydride and N-methylimidazole are usually used for this step. The last step of the synthesis cycle is oxidization step when the unstable phosphite group is converted to the stable phosphate tri-ester by adding iodine as oxidizing reagent. By repeating these four steps, nucleotides are added one by one to the growing chain. After all nucleotides are added, the completed chains will be cleaved off from the solid support and deprotected by incubating with ammonium hydroxide for 2 hours at 65°C. In some cases, the product will be further treated to react with various functional phosphoramidites derivatives such as fluorophores, quenchers, and other functional groups. The automated nucleotide synthesis technology and the phosphoramidite chemistry confer the flexibility to the easy synthesis and modification of aptamers.

In our lab, the aptamers and other nucleic acid reagents were synthesized on an ABI 3400 DNA/RNA synthesizer using the above described standard phosphoramidite chemistry. After the completed synthesis, the oligonucleotides were deprotected and cleaved from the solid support.

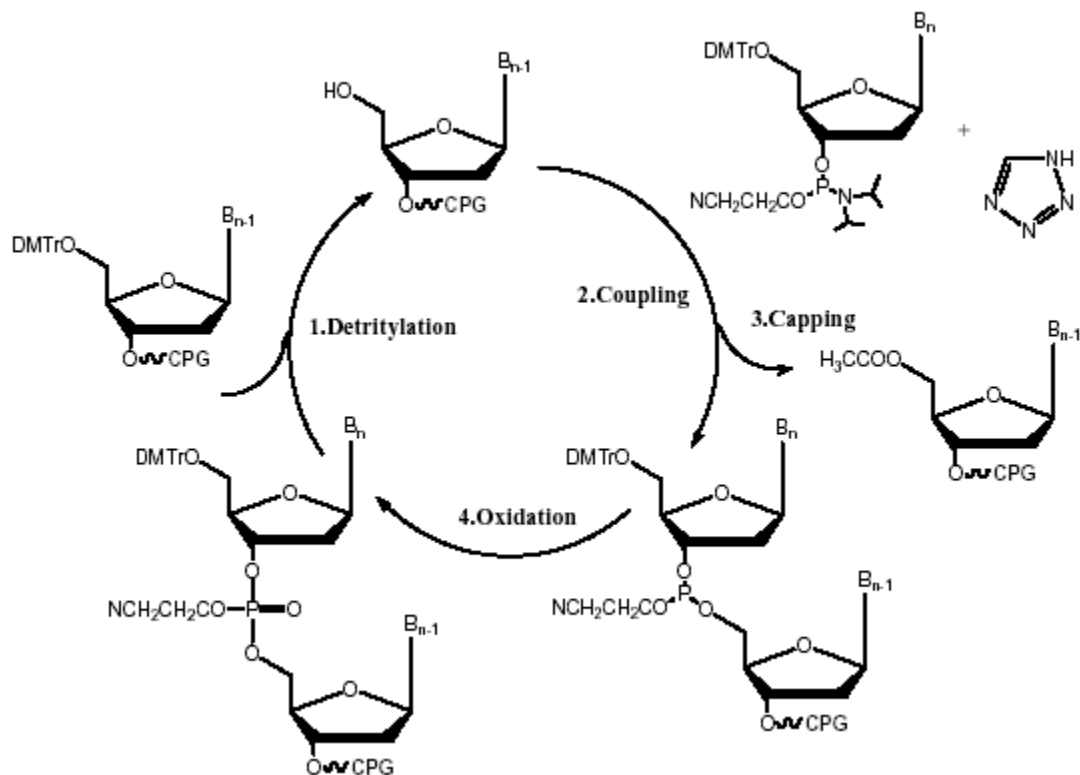


Figure 1-2. The principle of automated solid state synthesis of nucleotides (detritylation, coupling, capping, oxidization).

Because of the limit of yields, product needs to be purified to remove those incomplete sequences from completed sequences. Also in the case of labeling oligonucleotides with fluorophore or other functional groups, unlabeled sequences can significantly affect the final results. For example, if an aptamer molecule is not properly labeled with a fluorophore, it will not show fluorescent signal when it interacts with its target molecule. This will reduce the sensitivity of certain assays. The purification was normally achieved by reverse phase HPLC (RP-HPLC) on C18 column using optimized gradient in 0.1M TEAA since oligonucleotides as well as fluorophore labeled oligonucleotides are hydrophobic in most cases. Figure 1-3 shows a typical HPLC purification graph. PDA detector was used to measure the UV absorbance of different fractions of synthesized product. With the help of UV spectra, unlabeled

oligonucleotides and fluorophore labeled oligonucleotides can be distinguished from each other. As seen in Figure 1-3, two different fractions of synthesized product can help us get purified product. The purified product can be further conjugated with other materials such as nanoparticles. More details about this will be given in later sections.

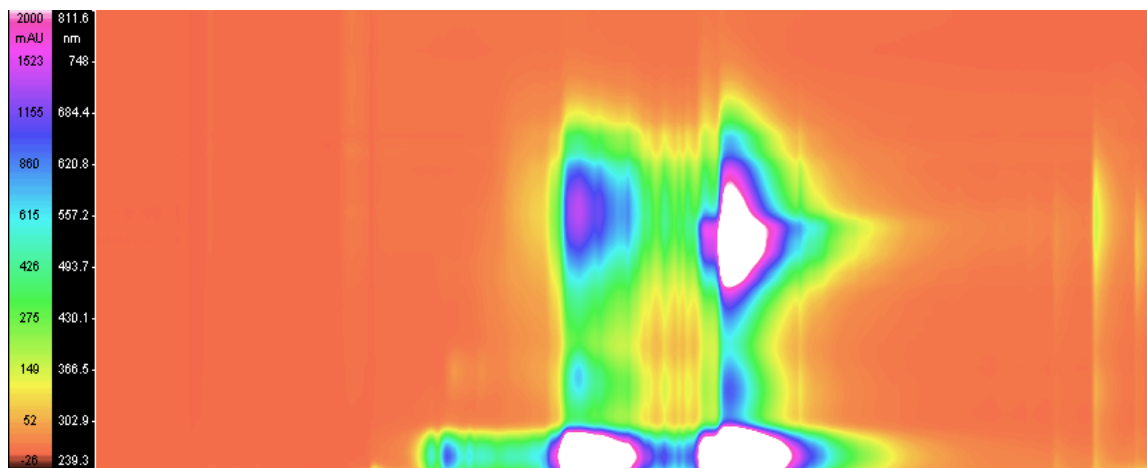


Figure 1-3. Chromatogram of RP-HPLC purification of fluorophore labeled oligonucleotide.

Bionanotechnology

Recent advances in nanotechnology have led to the rapid development of using nanotechnological devices for biomedical research, such as clinical diagnostics, cancer imaging, and drug delivery. The most popular nanotechnological devices used for biological studies include nanotube^[24], nanowire^[25], and nanoparticle^[26]. Among all these studies, nanoparticles have been extensively used because they are easy to prepare, flexible to modify, and effective to use. Nanoparticles can be classified into different categories based on different criteria such as shape, function, and material. There are two major categories of nanoparticles based on the materials: inorganic material based nanoparticles^[27] and organic material based nanoparticles^[28]. Inorganic materials used for nanoparticles include semiconductors^[29], magnets^[30], as well as

metals that are mainly gold^[31], silver^[32], silica^[33], and carbon^[34]. Organic materials used for nanoparticles include various polymers and dendrimers.

For nanoparticles based on semiconductor materials, it was reported that these nanometer-sized semiconductor quantum dots (QDs) can be covalently linked to various biorecognition molecules including antibodies, peptides, and nucleic acid probes to prepare fluorescent probes for biomedical applications.^[35-39] Most recently, multifunctional nanoparticle probes based on semiconductor quantum dots have been prepared for *in vivo* cancer targeting and imaging.^[40] Quantum dot nanoparticles have unique optical and electronic properties that make them the ideal material for biomedical applications^[41]. Quantum dots have both size and composition-tunable fluorescence emission wavelengths ranging from visible to infrared. They also have superior brightness and photostability ideal for fluorescent labeling purposes. Their broad excitation wavelengths and narrow emission wavelengths result in excellent multiplexing capability for biological systems.^[42] When conjugated with biorecognition molecules, quantum dots do not interfere with the binding events. In addition, the large surface area and functionalities of quantum dots are suitable for modification with multiple diagnostic and/or therapeutic agents.

Gold and silver are the two most frequently used materials for metal based nanoparticles because of their unique properties. Reduction of H₂AuCl₄ by citrate is the most widely used way to prepare gold nanoparticles.^[43] With this method, gold nanoparticles can be synthesized to the size of 1 nm to 200 nm reproducibly. These nanoparticles can be easily modified with many different functional groups, ligands, and biomolecules such as carboxylic acids^[31], amines^[44], phosphines^[45], proteins^[46], oligonucleotides^[47], enzymes^[48], and small drug molecules^[49]. Theoretically, incident light can result in the plasmon excitation of noble metal nanoparticles,

which involves the light-induced motion of the valence electrons. The cross section of gold for elastic light scattering in nanoparticles is much larger than any other materials. Also, this plasmon resonance is strongly dependent on size and shape.^[50] This size dependent color variation property provides a useful signal transduction mechanism for biological detection.^[51] It has been reported that aggregation of gold nanoparticles by DNA or other organic molecules can be used for spectroscopic detection system. When many gold nanoparticles are close to each other, their plasmon resonances couple to each other, which makes the plasmon resonance shift to higher energy. This mechanism is extremely useful for the detection of nucleic acids.^[52] Gold nanoparticles also show strong surface enhanced Raman scattering (SERS) effect that can be used to achieve multiplexing detection of a wide range of biological molecules.^[53]

Nanoscale magnetic systems are another important type of nanoparticles. They are widely used in biological separation and detection systems^[54]. Other important applications of magnetic nanoparticle includes magnetic resonance contrast enhancement agents.^[55] Intensive studies have moved from small magnetic systems^[56] to magnetic phenomena in individual nanoparticles.^[57] Magnetic nanoparticle itself can be treated as a single magnetic domain, in which all the spins create a giant magnetic moment together. At a high temperature, the nanoparticle becomes superparamagnetic because the magnetic moment wanders randomly. Magnetic nanoparticle also has a critical size, above which the nanoparticle becomes ferromagnetic since the magnetic moment is locked in a fixed direction. This critical size for iron oxide, a commonly used magnetic material, is about 25 nm.

Materials for preparation of magnetic nanoparticles include iron oxide, cobalt, MgFe_2O_4 , MnFe_2O_4 , CoFe_2O_4 , CoPt_3 , and FePt . For the frequently used iron oxide, co-precipitation is the most popular method to synthesize magnetic nanoparticles.^[58] The composition and size of the

synthesized nanoparticles depend on different aspects of the preparation reaction: temperature, pH, and the ionic strength.^[59] Polymer materials usually are added to the reaction as stabilizer to prevent prepared magnetic nanoparticles from forming aggregates.^[60]

Besides co-precipitation method, several common methods are also used for the preparation of magnetic nanoparticles. One of these is the thermal decomposition method. Magnetic nanoparticles can be prepared through the decomposition of organometallic compounds in boiling organic solvents containing certain stabilizing surfactants. This method is widely used for nanoparticles containing different magnetic materials such as Fe, Co, Mn, Ni, and Cr. Size and shape of nanoparticles depend on the temperature, reagent ratio, and type of additive. Microemulsion method is another method for magnetic nanoparticle synthesis.^[61] In this method, reactant solutions are dispersed in oil droplets and mixed with each other to prepare nanoparticles. The nanoparticles are then precipitated and washed by centrifugation. A wide variety of magnetic nanoparticles have been synthesized via microemulsion method. However, the nanoparticles synthesized by this method are less uniform in terms of size than those prepared by other techniques. In addition, the yield of this technique is not satisfying compared to others. The hydrothermal synthesis method is also worthy to mention as a common way to prepare magnetic nanoparticles. This method uses solid metal linoleate, ethyllinoleic acid, and water/ethanol solution as reactants under different temperatures to complete the synthesis.^[62] This method is based on phase transfer and separation phenomena occurring at the interfaces of liquid, solid, and solution phases during the synthesis.

Generally, magnetic nanoparticles need post synthesis coating procedure to stabilize the nanoparticles and prevent aggregation of nanoparticles. Both polymers and metals have been used for this coating procedure. During this coating procedure, functional groups can be

introduced to the surface of the particles to fulfill different tasks. This is extremely useful in numerous biomedical applications including magnetic nanoparticle assisted cell separation,^[63] automated DNA extraction,^[64] gene targeting,^[65] drug delivery,^[66] magnetic resonance imaging,^[67] and hyperthermia.^[68] Recently, biorecognition molecules such as antibody and oligonucleotide have been modified to the surface of magnetic nanoparticles to achieve highly sensitive immunoassay^[69] and gene detection.^[70]

Fluorescence is a phenomenon in which photon energy is absorbed by fluorophore at certain wavelength and emitted at different wavelength as previously shown in Figure 1-1. It is a widely used tool in biology. Fluorescence labeling of biological entities is extensively used to visualize the unit or the interaction between different units. Before, fluorescence labeling was done by chemically linking fluorescent dye molecule to molecular recognition element. However, conventional dye molecules impose stringent requirements on the detection system. In order to have brighter fluorescence for sensitive detection, two possible solutions are available: first, to improve the quantum yield; second, to increase the density of fluorescent dye for labeling. It is often advantageous to increase the amount of fluorescent dye molecules on single molecular recognition molecule. Recently, fluorescent silica nanoparticles are prepared to replace the organic dyes for biological labeling. One fluorescent silica nanoparticle can be treated as a single labeling molecule, although it has thousands of single dye molecules embedded in it. Therefore, it has much higher fluorescence signal than normal dye molecule has. In fluorescent nanoparticles, the dye molecules are typically embedded in silica or polymer based nanoparticles. Compared with the conventional dye molecules, these dye doped nanoparticles overcome some known disadvantages of single dye molecules in biological applications. For example, dye doped nanoparticles gain improved photostability and pH stability without compromising conjugation

flexibility. In our lab, we focused on making and using silica based fluorescent nanoparticles because of their well established preparation method and modification scheme.

The two most popular synthesis methods for silica based fluorescent nanoparticles are the microemulsion method^[71] and the Stober method.^[72] The microemulsion method is a method in which tetraethyl orthosilicate is hydrolyzed in a mixed environment of water, oil, and surfactant. In the microemulsion method, water droplets containing dye molecules are surrounded by hydrophobic surfactant and serving as the supply of fluorescent dye. In the droplets, the ammonium hydroxide hydrolyzes tetraethyl orthosilicate into solid silica while the dye molecules are entrapped in the silica matrix by electrostatic interaction. After condensation, synthesized fluorescent dye doped silica nanoparticles can be separated from reaction mixture by washing and centrifugation. Another synthesis method for silica based fluorescent nanoparticles is the Stober method. Instead of trapping dye molecules in synthesized silica matrix, the Stober method covalently links dye molecules to silica material.^[72] In the synthesis process, fluorophore in the form of isothiocyanate or succinimidil ester is first covalently linked to silane, followed by addition of tetraethyl orthosilicate. Hydrolysis then happens in solution containing water, ethanol, and ammonium hydroxide. During this process, both tetraethyl orthosilicate and fluorophore linked silane are hydrolyzed to form dye doped silica nanoparticles.

Once fluorescent silica nanoparticles are synthesized, they are usually required to be further modified with functional molecules or biorecognition molecules. A relatively simple way for modification is absorbing avidin on the surface of nanoparticles, followed by the addition of biotinylated ligands. Conjugation involving covalent linking is more complicated and versatile. Carboxy, amine, and thiol are most common active groups for conjugation. It has been reported that antibodies,^[73] oligonucleotides,^[74] peptides^[75] were conjugated with these fluorescent silica

nanoparticles. After bioconjugation, these nanoparticles can be used for a variety of applications including sensing and imaging.^[76]

Polymer based nanoparticles are another important type of nanoparticles, particularly useful in drug delivery as well as controlled drug release. Nanoparticles mentioned here mainly function as vehicles that encapsulate drugs. These encapsulated drugs can be released in a controlled manner that depends on the specialized property of nanoparticles. In addition, targeted delivery capability is desirable for treating cancer and other diseases because most cancer drugs have poor specificity and are cytotoxic to the surrounding non-cancerous cells over an extended period. This is solved by conjugation nanoparticles with targeting agents such as antibodies and aptamers, which can recognize tumor specific biomarkers. Polymer based nanoparticles also have other merits for biomedical studies. They are engineered to be biocompatible, biodegradable, and complied with Food and Drug Administration (FDA) regulations for potential clinical use. How to improve the up-take efficiency and bio-availability of these nanoparticles by biological systems is another important task. Recently, people developed drug encapsulated pegylated PLA nanoparticles that conjugated with PSMA aptamer for targeted drug delivery to treat prostate cancer.^[26]

Aptamer-Based Bioassays

Nucleic acid aptamers, selected from random sequence pool by SELEX, have been shown to bind with targets ranging from small molecules to proteins. The great specificity of aptamers allows the discrimination between even closely related molecules. Thus aptamers are suitable for development of various bioassays. For disease diagnostics, there is indeed the need of technologies to realize specific detection and precise quantification of biomarker molecules. In the past two decades, numerous aptamer based assays have been developed. These assays include sandwich assay,^[77, 78] flow cytometry assay,^[79, 80] fluorescence assay,^[81, 82] capillary

electrophoresis assay,^[83, 84] proximity-dependent ligation assay,^[85] aptamer array^[86]. In this section, some of these works such as sandwich assay, flow cytometry assay, proximity-dependent ligation assay, and immuno-PCR assay will be reviewed.

Sandwich assay is one of the most commonly used assays in biomedical studies. In this approach, the target is captured by two ligands simultaneously. One of the capturing agent molecules serves as signaling molecule or the substrate of secondary signaling mechanism. This assay was first demonstrated with antibodies. Aptamers have also been tested in sandwich assays. For example, VEGF aptamers were used to detect VEGF in the serum sample by sandwich assay.^[78] Besides the free capturing agents in solution, there are a few successful demonstrations of immobilization of them on the solid support. The two capturing agents in sandwich assay are not all aptamers. Instead, one of them can be antibody. This is due to the lack of multiple aptamers for single target molecule. Only a few systems such as thrombin, which has non-overlapping binding aptamers, are available.^[87] However, this situation can be greatly improved by carefully designed SELEX strategy. A previously identified aptamer can be used to direct the selection of new aptamers bound to the same target with modified SELEX technique.

Flow cytometry is another assay format for aptamer widely used in cell biology and particle science. It is able to measure a set of different parameters such as size, smoothness, and fluorescence of cells or particles in very short time. Because the data set is from thousands to hundreds of thousands of cells or particles, the results have statistical meaning, which is very important for interpretation of diagnostic assay results. Flow cytometry is also an attractive platform for multiplex analysis. With multiple excitation sources and emission filters, fluorescence signals from different labeling molecules can be detected. Aptamers has been used to detect target molecules presenting on the surface of cells or particles. In most cases, this was

demonstrated on the particle surface where target molecules were immobilized.^[88] The flow cytometry assay faces the same problem as sandwich assay. Only a few examples of aptamers can target the cell surface proteins. One example is the aptamer for PSMA that is a protein biomarker for prostate cancer. This aptamer has been validated to be an effective probe in flow cytometry assay. Recently we have made great progress in developing cell based SELEX for selecting aptamers against cell surface markers.^[18] Multiple aptamers can be selected for any type of cells given by using this strategy. Study has shown that these aptamers can easily identify certain cancer. They can even classify subtypes of cancer with high accuracy.^[89] With this breakthrough, the use of flow cytometry assay can be expanded to more detection systems using aptamers.

Proximity dependent ligation assay is a new assay format for protein detection by aptamers. In this technique, a set of two target binding ligand molecules are in close proximity, which facilitates the ligation reaction between DNA reporter sequences. This ligated reporter sequence can then be detected by real-time PCR. This proximity dependent ligation assay is similar to the sandwich assay in terms of binding pattern. However, the proximity dependent ligation assay adds an extra ligation event to the binding system. This can eliminate the background signal brought by nonspecific binding of oligonucleotides as shown in sandwich assay. Thus, it has much higher specificity than normal sandwich assay. This assay format requires the availability of multiple probes for non-overlapping binding sites of the same target, and these two binding sites should be in close proximity for ligation to happen. Previously, antibodies conjugated with oligonucleotides were used as binding ligands. Recently, aptamers are directly used for this assay to serve as both binders and reporter sequences, which significantly simplified the assay and greatly improved its performance.^[85] The proximity

dependent ligation assay can be applied to different sample formats. For high-throughput analysis, homogenous protein detection can be done with this assay. In an example of using aptamers for homodimer of the B form of platelet-derived growth factor (PDGF-BB), all the components including those for ligation and amplification were added without washes. The detection limit was proved to be 1000-fold lower than traditional enzyme-linked immunosorbent assay (ELISA). With this sensitivity, the proximity dependent ligation assay can be applied for trace amount protein detection, which is critical for early detection of certain diseases. Besides homogenous assay format, this new method also applies to localized protein detection as well as solid-phase detection in which one binder is immobilized on a solid support to capture the target molecule. In summary, the proximity dependent ligation assay brings paired aptamers probes, enzymatic ligation, and PCR reaction together to fulfill the task of minute amount protein detection.

Immuno-polymerase chain reaction (immuno-PCR) assay is another technique. Immuno-PCR^[90] and other similar techniques such as immunodetection amplified by T7 RNA polymerase (IDAT)^[91] are all variations of the sandwich ELISA assay but with improved sensitivity. Antibody-based sandwich assay is a powerful tool and widely used in biomedical studies. However the sensitivity of this assay is not satisfactory for the rapid growing demands. To further improve the detection sensitivity, immuno-PCR assay was developed. Polymerase chain reaction (PCR) is a technique using enzyme to amplify specific DNA segment with the help of primers. The amplified product can be easily detected by numerous methods and is proportional to the starting quantity of the template molecules. In immuno-PCR, the antibody with the recognition capability for certain target is conjugated with a DNA report sequence. By above mentioned PCR mechanism, the quantity of target molecules bound with antibody-DNA

complex can be calculated from the number of PCR amplified DNA reporter sequences. This mechanism can greatly avoid the generation of false signal from the nonspecific binding of both antibody and DNA in the system. In addition, other types of signal transduction mechanisms such as rolling-circle PCR^[92] and IDAT^[91] can be introduced to the system to further reduce the background signal resulted from nonlinear amplification of PCR.

Although antibodies have been the most widely used molecular recognition reagent in bioassays for several decades, aptamers with great affinity and specificity now are expected to have more impact in this field. This requires the discovery of new aptamers for various targets, and relies on the rapid development of the SELEX technology for aptamer selection.

Biomarker Discovery

Biomarkers are the indicators of specific biological states. They can be used to diagnose disease or monitor the progress of disease. Ideally they can serve as the guide of therapy.^[93] Biomarkers were usually physiological parameters. Recently, new types of biomarkers such as transcriptional profiling and DNA methylation have been introduced to the clinical practice.^[94] Biomarkers can be classified into different categories based on their purposes. These categories include disease biomarkers, surrogate endpoints, efficacy biomarkers, mechanism biomarkers, pharmacodynamic biomarkers, target biomarkers, and toxicity biomarkers.^[95] Typically, biomarker discovery is a comprehensive process including several essential steps: candidate discovery, biomarker validation, and assay development.^[96] Candidate discovery generally means seeking differences between groups that respond to stimulus and those that don't. Since protein biomarker is likely the most relevant to the disease, proteomics methods, especially those based on mass spectrometry, have become the trend of novel biomarker discovery. Human plasma has been the preferred material to look for important biomarker proteins. However it still remains poorly characterized. This is mainly due to the lack of high throughput tools for such a

complicated system which contains thousands of types of proteins with variable concentrations.^[97] Besides blood, cell homogenates, tissue lysates, and biofluids are also used in many studies for biomarker discovery.

For biomarker discovery, mass spectroscopy is the principal technique to use. There are mainly two types of MS based methods. The first one is pattern based methods that produce MS-derived protein pattern. Surface-enhanced laser desorption ionization (SELDI),^[98] matrix-assisted laser desorption ionization (MALDI),^[99] and electrospray^[100] are the main MS techniques used in this type of methods. The other type of methods is identity based methods that give rise to peptide sequences of digested proteins. Liquid chromatography (LC)-MS/MS is the main technique to use in this category.^[101, 102] Because of the intrinsic variations among different samples, it is very difficult to get universal biomarkers for general diagnostic purposes from pattern based methods. Thus the identity based methods are more reliable for proteomic biomarker discovery at this point. Recently several novel biomarker discovery techniques have emerged, such as aptamer assisted cell surface biomarker discovery. While the new aptamers are being selected for cell surface biomarkers using cell based SELEX strategy, these aptamers can also be used to purify and identify the target biomarkers.^[103, 104] After the molecules of interest have been selected and identified, the relevance of these molecules to the disease needs to be evaluated. Only after the newly identified biomarkers have been validated, can they be further used for animal study and clinical trial.

CHAPTER 2 SELECTION AND CHARACTERIZATION OF APTAMERS FOR LUNG CANCER USING CELL BASED SELEX

Introduction

Effective diagnosis, therapy, and prevention of diseases require the understanding of diseases at the molecular level, which relies not only on the genetic character but also on the proteomic character of diseases, especially for cancer, the number one killing disease of humans. For the diagnosis of cancer, accurate and flexible criteria are indispensable for the classification of types as well as subtypes of certain cancers to support the appropriate treatment and the detection of minimal residual disease. Current criteria for cancer diagnosis based on genetic and morphological features instead of proteomic features are complicated and insufficient for clinical practice, which is partially because of the lack of well-defined cancer biomarker proteins and specific molecular probes to recognize and identify them.^[105, 106] Although cancer diagnosis by recognition of molecular signatures is relatively simple and direct, it is very challenging to discover enough cancer biomarker proteins for conclusive diagnosis because of the limits of current biomarker discovery techniques. Therefore, it is highly desirable to have an efficient and reliable method to develop specific molecular probes to distinguish the differences among cancer cells at the molecular level without prior knowledge of target biomarker proteins. In addition, with these molecular probes, more biologically meaningful biomarker proteins can be revealed to provide greater insight of cancer.

Molecular level differences are presenting among different cells. For example, normal cells and tumor cells can be differentiated from each other by a set of molecular markers at both genetic and proteomic level. Even for subtypes of certain cancer, molecular differences are distinctive. These molecular differences are directly related with the biological mechanism of tumors, thus can be highly useful for diagnosis and therapy of cancer. Proteomics are the current

trend to realize the disease diagnosis based on molecular differences since genetic changes are not always related to the protein changes that directly exert the influence on the disease. Among all the proteins, the extracellular proteins, especially those cell surface membrane proteins are of great interest for cancer study such as immune response, inter-cell signaling, and cell migration. Practically, cell surface membrane proteins are easier to access than intracellular proteins, can be handled and studied at their native state without disturbing the cell activity or destructing the cells. Therefore, they are naturally good target molecules for molecular difference study. In other words, the membrane protein targets can represent the molecular level differences between different cancer cells. These molecular signatures expressed on live cell membranes may imply important disease mechanisms if validated as biomarkers. In our lab, we tried to select aptamers targeting these cancer cell surface proteins using a novel *in vitro* selection method, cell based SELEX. By using this cell based SELEX technique, we expect to select aptamers against whole live cancer cells which exclusively express certain protein targets on cell surface, but not on other types of cells. The membrane protein targets of the selected aptamers represent the molecular level differences between the given cell lines and can be used for diagnostic purposes.

Principle of SELEX

In modern pharmaceutical industry, most of the drugs are designed and developed through a complicated process. This is done by screening the synthetic library of compounds with the drug target in different assays. Combinatorial chemistry plays an important role in selecting the best drug candidate for further investigation. Similar to drug, biopolymers are also found to bind with enzyme, receptor, or other protein targets. These biopolymers include peptides, proteins, and nucleic acids. Selection is a well established method to identify the specific biopolymers. The selection process usually begins with a random library, followed by incubation with target molecules. After removing non-binding or weak-binding molecules, the selected binders are

amplified *in vitro* or *in vivo*. Iterative selection cycles are required to reinforce the selection strength and let different binders compete with each other. Eventually this process will result in a small population of binding species that has highest binding affinity or efficacy against a given target molecule. For peptide and protein, *in vivo* selection techniques such as phage display and hybridoma technique are involved in most cases^[107-111]. As synthetic molecules, nucleic acid probes such as aptamers can be identified using the *in vitro* selection. The *in vitro* selection method was first used to develop aptamers in 1990s and is generally relevant to combinatorial chemistry.^[112, 113] The invention of automated DNA synthesis machine for the first time allowed the preparation of diverse, random library to be used for the selection. In addition, the *in vitro* amplification techniques such as the polymerase chain reaction (PCR) enabled researchers to realize the idea of iterative selection. In 1990, single-stranded nucleic acids were used to select aptamers using a well defined *in vitro* selection technology, SELEX (the Systematic Evolution of Ligands by Exponential enrichment).^[114, 115]

As shown in Figure 2-1, the SELEX experiment begins with a chemically synthesized DNA or RNA library. During the solid state synthesis, equal amounts of A, T, G, and C phosphoramidites are added at each step to make a totally randomized pool, resulting in a total number of 10^{13} to 10^{16} different sequences. Each member of the library has a different sequence that can form different secondary structure, and has different binding ability. These synthesized nucleic acid pools are then subjected with HPLC purification to remove those truncated or failed sequences from the pool. The length of the randomized sequences varies from 15 to 60 bases. There are two flanked constant sequence regions at two ends of randomized sequence region, serving as primer binding sites for PCR amplification. For RNA aptamer selection, the synthesized single-stranded DNA library needs to be transformed to single-stranded RNA

library. This is done by adding a promoter sequence in the primer binding site for reverse transcription.

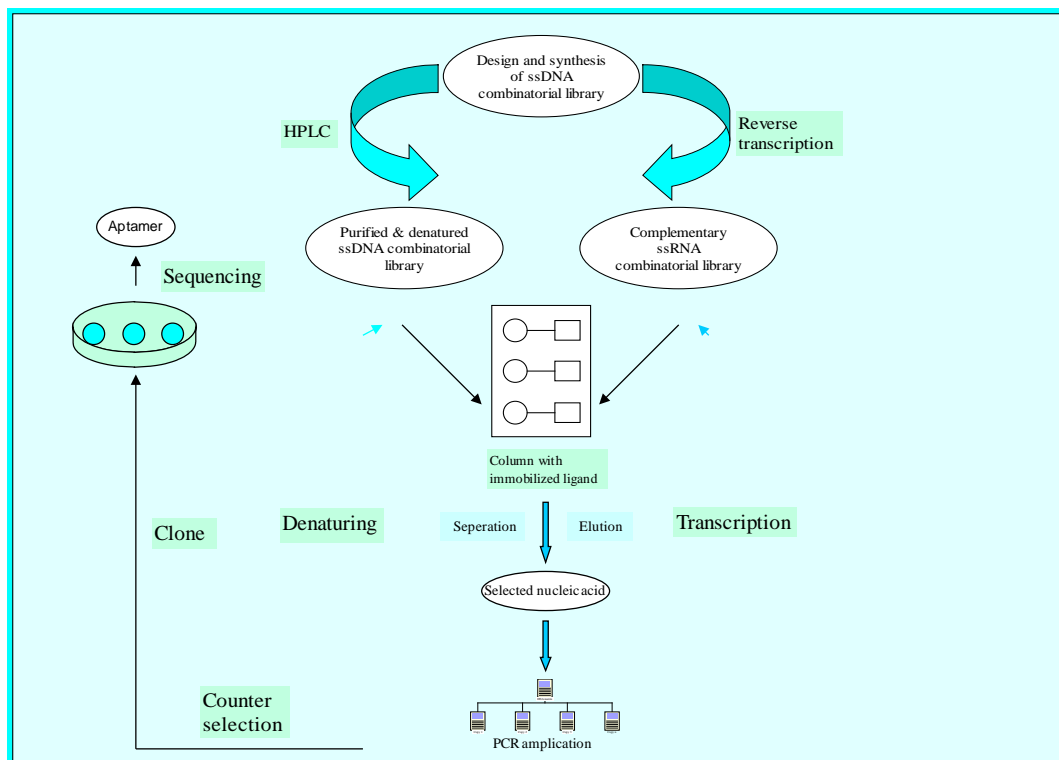


Figure 2-1. Scheme of SELEX. Like other combinatorial chemistry techniques, SELEX involves three steps: preparation of DNA/RNA library, selection and screening, deconvolution and analysis of the selected aptamers. The selection step needs to be repeated a few times to enrich probes with highest affinity.

In order to select aptamers from the synthesized pool, many separation methods have been used for aptamer selection. There are generally two major categories of methods. The first category is based on the difference of mobility between free and target bound molecules, including electrophoretic mobility shift assay and equilibrium dialysis. For example, native polyacrylamide gel is a method commonly used for aptamer selection of protein. The difference of migration ability between unbound species and bound complex allows the separation to happen. Another major category is immobilization of target molecules on a carrier or stationary phase of chromatography through covalent bonding or absorption. For single protein aptamer

selection, the nucleic acid pool is allowed to interact with the target on nitrocellulose filters, followed by washing to remove those unbound nucleic acid sequences from the binding complex of aptamer and protein. Affinity chromatography is usually used for small molecule aptamer selection. By using chromatography technique, the unbound species can be washed off and the bound sequences can be eluted later on. Recently, a few new separation techniques are introduced to this field for aptamer selection. For example, capillary electrophoresis has great number of theoretical plates and therefore has excellent separation capability for protein. The small volume of CE experiment is also an advantage for aptamer selection against some small amount samples. With CE technique, the unbound species can be well separated from bound species and the efficiency is much better than traditional chromatography based selection techniques.^[116] Another new SELEX technique is magnetic bead based SELEX. Before the selection experiment, the protein molecules are immobilized on the surface of magnetic beads using conjugation methods through certain amino acid residues. The magnetic beads are commercially available maghemite/magnetite material commonly used for separation and MRI. It has several properties suitable for aptamer selection: the high capacity allows enough proteins to be immobilized on the surface; and they are very easy to be conjugated with protein; also the magnetic bead will not have any effect on the later PCR amplification experiments. As shown in Figure 2-2, protein targets immobilized on the magnetic beads interact with nucleic acid pool first, followed by washing away unbound sequences with the help of magnetic extraction. This strategy allows easy separation and recovery of sample during SELEX experiment. The consumption of the target protein is also very low. More importantly, there is no decay of aptamer/ protein complex during the separation as observed in CE-SELEX, which makes the selection highly reproducible, and thus suitable for automation of the whole process.

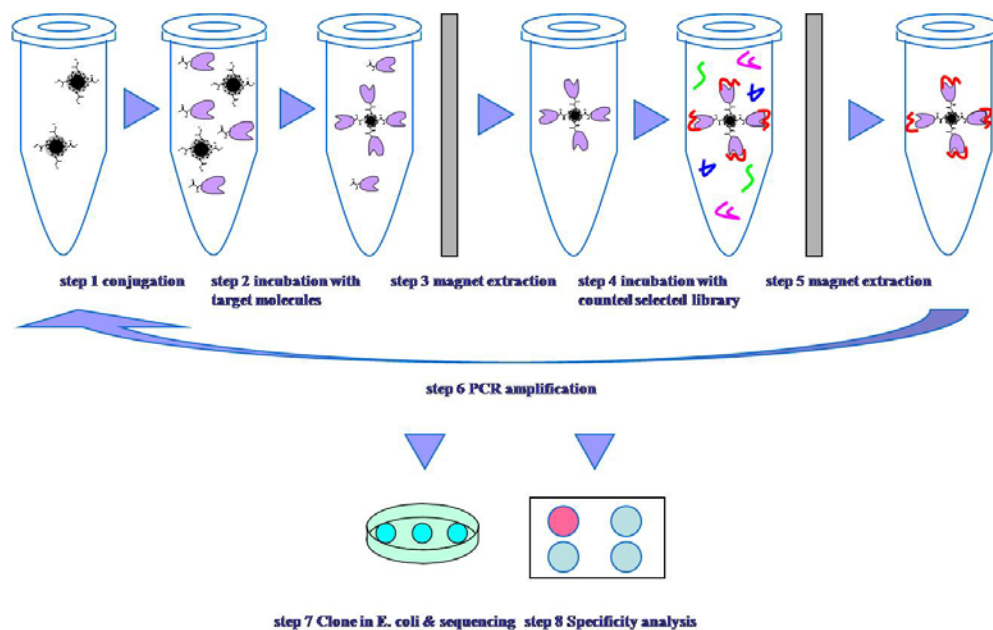


Figure 2-2. Magnetic bead based SELEX. Target proteins are immobilized on the surface of prefabricated magnetic beads. After purification and conjugation, unbound protein is removed from protein-magnetic particle complex. Following its incubation with nucleic acid library, protein-magnetic particle complex with bound aptamers will be removed from free nucleic acid by the magnetic extraction. PCR amplification of selected aptamers then can be performed directly at the presence of magnetic beads.

After the incubation and separation steps, only a few sequences will remain in the pool.

Molecular biology methods are then used to amplify the selected nucleic acid molecules.

Typically PCR technique is used to amplify DNA pools. For RNA pools, reverse transcription takes place first, followed by DNA amplification by PCR. For later selection, amplified DNA can be converted back to RNA via *in vitro* transcription. In order to have binding species compete with each other to obtain the aptamers with highest affinity, multiple rounds of selection are required. Along with the selection progress, the stringency of aptamer selection is varied, including the concentration, incubation time, and the volume of wash. The number of cycles of selection depends on many factors such as nature of target, degree of randomization, and selection stringency. The entire process can take a few weeks, about 15-25 rounds of selection. Between cycles of selection, the resulted pool will be screen to monitor the progress of

enrichment of aptamers. Once the binding reaches to a plateau and the pool population narrows down enough, the pool will subject to cloning and sequencing to identify the individual sequences. The sequences of selected pool will then be aligned with the help of software to sort consensus sequences that are expected to have more chance of being prospect aptamers. The de-convolution experiments will then be performed to test the aptamer candidates.

Methods and Materials

Cell Based SELEX

Unlike the SELEX techniques for small molecules and pure proteins, the *in vitro* selection for complex target is far more difficult. In such a selection experiment, an array of proteins is targeted, instead of a single purified protein. During the selection, the composition of selected pool is dominated by both concentration ratio of different target proteins and their affinities to corresponding aptamers. Recently a mathematic simulation of SELEX against complex target was performed.^[117] This study revealed the relationship among the protein concentration, partitioning efficiency, and protein affinity in the selection experiment. In addition, the SELEX against complex target requires particular effort for de-convolution of aptamers targeting different target proteins. In the past a few years, there were a few demonstrations of SELEX against complex system using organelle or subpopulations of cells as target. Red blood cell membranes and live trypanosomes have been tested and aptamers were successfully developed.^[118, 119]

To select aptamers targeting membrane proteins on live cell surface, we developed a new cell based SELEX method. This method is different from previous attempts of SELEX against complex systems such as isolated cell membranes, organelles, and purified proteins.^[118, 120-122] The new cell based SELEX method uses whole live cell as complex target for aptamer selection. Another distinct aspect of this methodology is the use of a counter-selection strategy to screen

out those aptamers bound to common target proteins expressed on the cell membranes of different cancer cells. As shown in Figure 2-3, cell based SELEX were established to develop aptamer probes for molecular differences between different cancer cells. In this specific case, two different leukemia cell lines were chosen as a model system to develop the methodology.

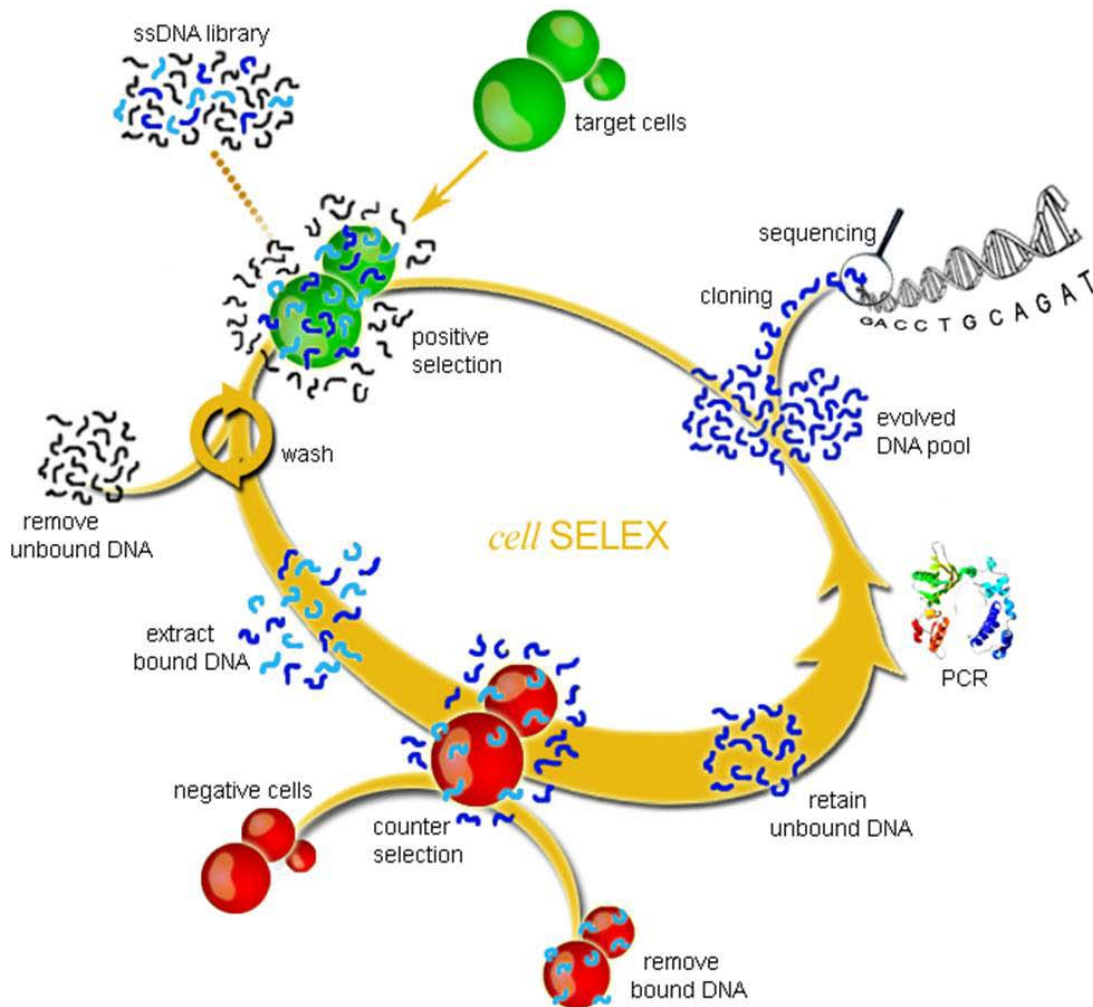


Figure 2-3. Scheme of cell based SELEX. The single stranded DNA pool was incubated with target cells. After washing, the binding species were eluted by heating. The eluted DNAs were then incubated with negative cells for counter-selection. The supernatant containing specific DNA for only target cells was collected for PCR amplification. After single stranded DNA generation, the sequences were used for next round of selection. The selected pool will be cloned and sequenced for individual aptamer identification after the last round selection.

A cultured precursor T-cell acute lymphoblastic leukemia (ALL) cell line, CCRF-CEM, was used as a positive target and a cultured B-cell human Burkitt's lymphoma cell line, Ramos, was used as the negative control.

Leukemia cell lines were chosen to demonstrate the cell based SELEX concept because they are homogeneous cell suspension that is easy to handle during experiments. Also the viability of leukemia cell lines is greater than 99%, which will not have negative effect on the SELEX efficiency, since the dead cells often nonspecifically uptake DNA molecules. In addition, there are many antibodies specific for leukemia cell surface antigen recognition. These antibodies are available for comparison with selected aptamers. At the beginning of the SELEX experiment, the single-stranded DNA pool was incubated with target cells to allow the binding. The unbound DNA or weak binders were then removed by washing the cells. After washing, the bound DNAs were eluted by heating. These DNAs were then incubated with negative cells for counter-selection. The DNAs specific for target cells were left in the supernatant after counter-selection and collected by centrifugation. The collected DNAs were amplified by PCR reaction. In the next step, the PCR product containing double stranded DNAs was separated to single stranded DNAs for next round of selection. After the last round of selection, the selected pool will be cloned and sequenced to identify the individual aptamers.

After iterative binding with both positive and negative cell lines, a panel of aptamer probes becomes enriched. Flow cytometry assay was used to screen the binding ability of selected pools along the progress of selection. The DNA sequences were labeled with fluorophore by using fluorophore modified primers in PCR reaction. After incubation with dye -labeled pools, the fluorescence intensity of DNA bound cells measured by flow cytometry represents the binding capacity of the aptamers to the cells as shown in Figure 2-4. Along with the progress of selection

experiment, we can see the gradual increase of the binding ability of selected pool. This means that the population of strong binders has been enriched. The later cloning and sequencing experiment confirmed this result. A few aptamers against different cell surface target proteins were discovered and used for probing the molecular signatures of different leukemia cells in a direct and simple manner. Not only are these discovered aptamers as accurate as, if not better than, the antibodies for the differentiation of subtypes of leukemia, they also reveal more subtle molecular-level differences. Theoretically, any molecular level variance among different types or subtypes of cancer cells could be revealed by a similar methodology that was previously impractical.

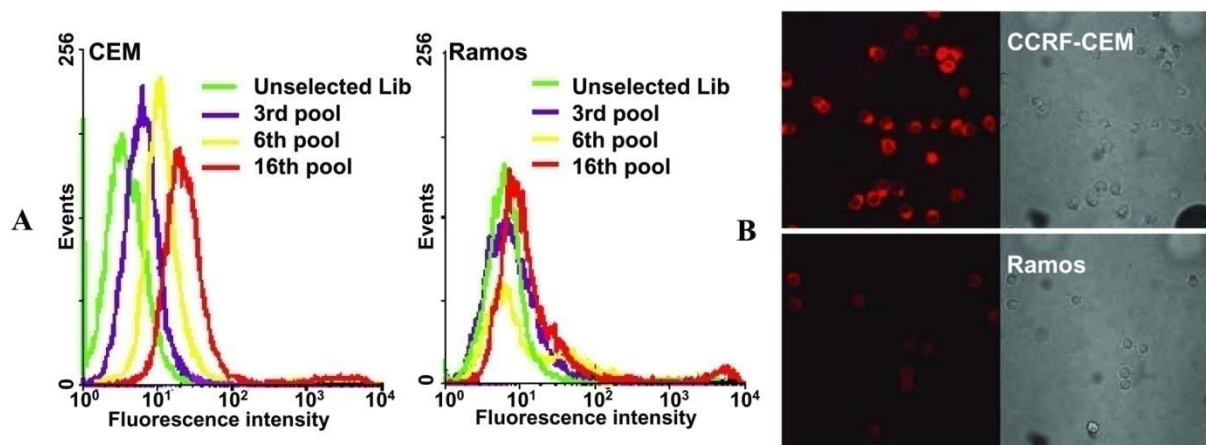


Figure 2-4. Progress of aptamer enrichment during cell based SELEX. A) Flow cytometry assay of FITC-labeled selected pools with CCRF-CEM target cells and Ramos control cells. The green curve represents the non-specific binding of unselected DNA library. For target cells, there were gradual increases in binding capacity of the DNA pools as the selection progressed, whereas there was little change for the control cells. B) Confocal imaging results of TMR-labeled selected pools with CCRF-CEM target cells and Ramos control cells. Target cells were stained by the dye labeled DNA pools on the membrane region, while only little background signal can be observed on the control cells.

DNA Library and Aptamer Synthesis

After we successfully established the methodology of cell based SELEX, we applied this new approach to the aptamer selection for lung cancer cells. We designed a 71mer single-

(Econosil, 5 μ , 250 \times 4.6 mm) from Alltech (Deerfield, IL) and optimized elution gradient in 0.1M TEAA solution. The HPLC-purified product was then dried, trityl group deprotected, and re-suspended in water for quantification. Quantification was done by measuring the UV/Vis absorbance on a Cary Bio-300 UV spectrometer (Varian, Walnut Creek, CA). A 1 cm path length square quartz cuvette was used for absorption measurements. Then the product was titrated and suspended in buffer for experimental uses.

Chemicals and Reagents

Controlled-pored glass (CPG) beads, phosphoramidite, dichloroacetic acid (DCA), tetrazole, acetic anhydride, iodine, and other reagents used for DNA synthesis were purchased from Glen Research (Sterling, Va.). DNA labeling reagents were purchased from Molecular Probes and Glen Research. Solvents for DNA synthesis and HPLC purification such as acetone nitrile, dichloromethane (DCM), and water with different purity were purchased from Fisher Scientific. Ammonium hydroxide, TEAA, ethanol, were also purchased from Fisher Scientific. All other chemicals were purchased from Sigma–Aldrich and Fisher Scientific. Agarose, agar, PBS buffer were purchased from Fisher Biotech.

Washing buffer was prepared by dissolving glucose (4.5 g/L), MgCl₂ (5 mM), and bovine serum albumin (1 mg/mL) in Dulbecco's PBS (pH 7.3). Yeast tRNA (0.1 mg/mL) was added in washing buffer to prepare binding buffer to minimize the nonspecific binding effect.

Cell Culture

NCI-H69 (small-cell carcinoma), NCI-H661 (large-cell carcinoma), NCI-H146 (small-cell carcinoma), NCI-H128 (small-cell carcinoma), NCI-H23 (adenocarcinoma), NCI-H1385 (squamous-cell carcinoma), CCRF-CEM (T-cell acute lymphoblastic leukemia), and Ramos (B-cell human Burkitt's lymphoma) cells were purchased from American Type Culture Collection (ATCC), and maintained at 37°C and 5% CO₂ in RPMI 1640 medium (ATCC) supplemented

CTGACGCATTCGGTTGAC - 3'. The primers were designed under the general guideline of primer requirement with the help of Oligo Analyzer software (Integrated DNA Technologies, Coralville, IA) and PrimerPremier 3.0 software (PremierBiosoft). The primers have melting temperature difference within 1 degree, and have no apparent intra-primer homology (homodimer), inter-primer homology (primer dimer), internal secondary structure, repetitive sequence, and poly-nucleotide stretches. The sequences and parameters of primers are as following.

Forward primer: 5'-TACCAGTGCGATGCTCAG (length: 18 base; GC content: 55.6 %; melting temperature: 54.6°C; molecular weight: 5499.6 g/mole; extinction coefficient: 171500 L/(mole·cm); nmole/OD260: 5.83; µg/OD260: 32.07; strongest secondary structure folding T_m: 25 °C).

Reverse primer: 5'-GTCAACCGAATGCGTCAG (length: 18; GC content: 55.6 %; melting temperature: 54°C; molecular weight: 5508.6 g/mole; extinction coefficient: 176400 L/(mole·cm); nmole/OD260: 5.67; µg/OD260: 31.23; strongest secondary structure folding T_m: 33.1°C).

Melting temperature settings are oligo concentration: 0.25 µM; Na⁺ concentration: 50 mM monovalent salt.

The designed PCR primers were then synthesized on DNA synthesizer and purified with RP-HPLC before experiment. Unlabeled forward and reverse primers were used for real-time PCR experiments in which the intercalating dye, SYBR green was used for signal detection. FITC labeled forward primer and triple-biotinylated (trB) reverse primer were used to generate PCR product for flow cytometry assay. TAMRA labeled forward primer and triple-biotinylated (trB) reverse primer were used to generate PCR product for confocal imaging experiments.

PCR reaction conditions were then optimized for the designed primers. The parameters include concentrations of primers and template, concentrations of Taq polymerase and dNTP, concentrations of Mg^{+} and other salt, annealing temperature and time, extension temperature and time, PCR cycles. PCR parameters consisted of 3 minutes of Taq activation at 95°C, and 15 cycles of PCR at 94°C for 30 s, 52°C for 30 s, 72°C for 15 s, followed by 5 minutes of extension at 72°C. Specificity of PCR amplification was verified by melting curve analysis as shown in Figure 2-6. Amplification products were also resolved by agarose gel electrophoresis and visualized by ethidium bromide staining. The optimized PCR reaction conditions were then used in SELEX experiments except the template DNA amount, which will be determined by real-time PCR experiment after every round of selection.

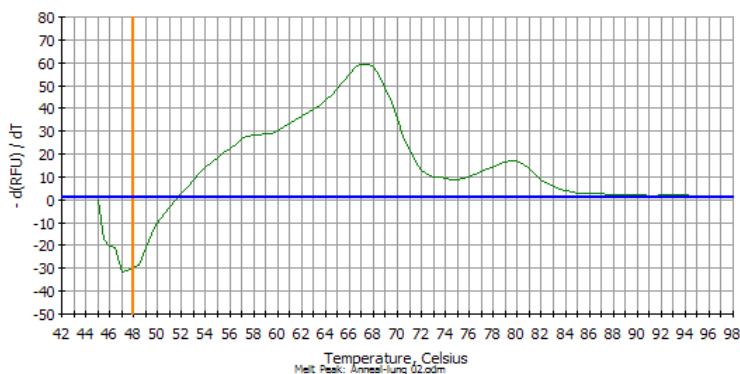


Figure 2-6. Melting curve of PCR amplified DNA product with optimized PCR conditions. The left peak represents the specific PCR product, the right peak represents the small amount of non-specific PCR product such as low molecular weight primer dimer or high molecular weight over-amplified DNA.

Because the amount of template DNA used in PCR reaction is an important parameter to avoid non-specific PCR amplification, and the amount of bound DNA sequences after every round of selection is variable, real-time PCR was used in SELEX experiment to determine the amount of DNA molecules to be amplified after every round of selection. Real-time PCR is a PCR system using fluorescence based detection system to measure the amount of amplified

products through the use of DNA intercalating dye or other probe chemistry. In contrast, amplified products were measured by end point analysis system in regular PCR reaction. By using real-time PCR, people can monitor the PCR reaction to avoid the linear increase range after initial exponential increase range. Also, the starting quantity of template molecules can be measured by determining the number of cycles required to reach a set level of product. Typically, the fluorescence based detection system of real-time PCR uses intercalating dyes or hybridization probes. For intercalating dyes, the fluorescence is hundreds of times brighter when bound to double stranded PCR product than bound to single stranded DNA template, as illustrated in Figure 2-7.

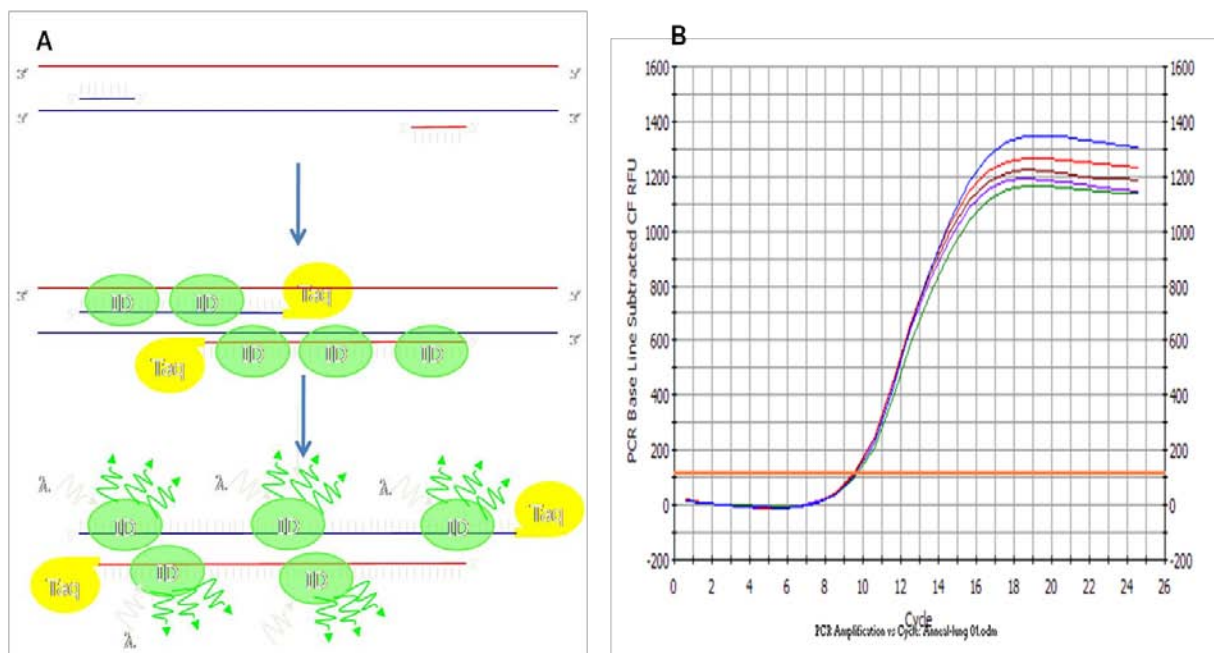


Figure 2-7. Principle of real-time PCR reaction. A) Intercalating dyes bind to double stranded PCR product and give out bright fluorescence signal for detection. B) Fluorescence profile of real-time PCR along with PCR cycles.

In SELEX experiment, we used iTaq DNA polymerase (Bio-Rad) and a MyiQ real-time PCR system (Bio-Rad) to perform real-time PCR experiments. SYBR green (Molecular Probes) was used for the detection of PCR products by intercalating into double stranded DNA product

of PCR reaction. PCR cycles were optimized according to the determined template amount. The bulk of target cell specific DNA molecules harvested from selection experiment were then amplified with the optimized conditions in regular PCR.

Gel Electrophoresis

After PCR reaction, the amplified selection products were analyzed by gel electrophoresis. Typically, agarose gel was used for the visualization of relatively short double stranded DNA. This is achieved by forcing the negatively charged DNA molecules to move through agarose matrix with an electric field. Shorter sequences move faster than longer ones. By running together with a standard DNA ladder, the size of DNA product can be estimated. In our experiments, we prepared 3% agarose gel by dissolving 1.35 g agarose in 45 mL 1X Tris/Borate/EDTA (TBE) buffer (Fisher Scientific), followed by heating twice in microwave oven for 1 minute. The solution was then allowed to cool down to 60°C and poured in gel rack to form the gel. Once the gel is ready, the DNA samples mixed with loading dye (bromophenol blue and glycerol) were added in gel wells for running. At the same time, ethidium bromide (EtBr) was added for staining the DNA for visualization after electrophoresis. We typically used constant voltage of 100V for electrophoresis. After the electrophoresis, the gel was put on UV lightbox to visualize DNA bands in the gel. The locations of DNA bands to be detected were then compared with DNA ladder (molecular weight marker) to estimate the size of the DNA as shown in Figure 2-8.

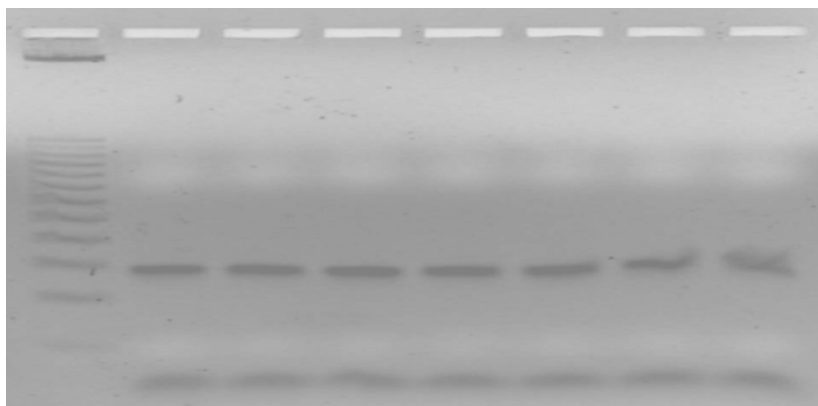


Figure 2-8. Gel electrophoresis picture of PCR product in a 3% agarose gel. The DNA is 70 base long in the length, which is close to the 75 base marker in the DNA ladder lane.

Single-stranded DNA Generation

PCR reaction amplifies single stranded DNA sequences to double stranded DNA sequences. To generate single stranded DNA from PCR product for next round of selection, the sense ssDNA was separated from the biotinylated anti-sense ssDNA using streptavidin-coated sepharose beads (Amersham Pharmacia Biosciences). We prepared affinity columns filled with streptavidin-coated sepharose beads. The PCR products then went through the column 3 times to allow the biotinylated anti-sense ssDNA to bind with streptavidin-coated beads. After elution with alkaline solution (0.2 M NaOH), the sense ssDNA was desalted with a Sephadex G-25 column (NAP-5, Amersham Pharmacia Biosciences). The recovered single stranded DNAs were then quantified by UV measurement, and dried in a SpeedVac. The products were finally re-suspended in buffer to be used for next round of selection.

Cloning and Sequencing

To isolate individual aptamers from selected pool, cloning was performed after a few rounds of selection. The most selected ssDNA pool was PCR amplified with unlabeled primers, and inserted into the pCR 2.1-TOPO TA Cloning vector (Invitrogen) (Figure 2-9). The TOPO TA Cloning kits are designed for cloning PCR products directly from a PCR reaction in short

time. They use a pCR-TOPO vector with covalently bound topoisomerase I for fast cloning and recombinants. To insert DNA pool into the vector, a 6 μ L TOPO cloning reaction was set up by mixing 4 μ L PCR products with 1 μ L TOPO vector in salt solution and incubating for 5 minutes at room temperature. The prepared cloning vector was then transformed into One Shot competent *Escherichia coli* cells by incubation together for 30 minutes on ice. The cells were then heat shocked at 42°C for 30 seconds. After well mixed with room temperature S.O.C medium, the transformed cells were spread onto pre-warmed and sterilized LB plates containing 50 μ g/mL ampicillin and 40 mg/mL X-gal in dimethylformamide (DMF). The cloning plates were then incubated at 37°C for the cells to grow. After 8 to 12 hours, the blue/white screening can be performed to pick the colonies. An efficient TOPO cloning reaction should produce several hundred colonies. Among them, white or light blue colonies were picked up for extracting the plasmids for sequencing.

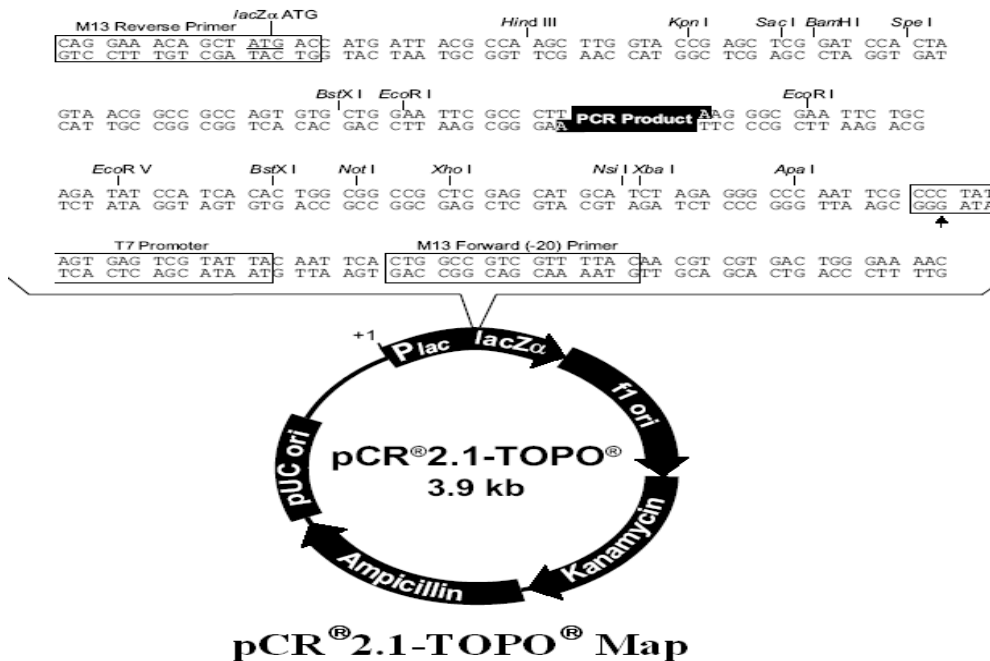


Figure 2-9. pCR 2.1-TOPO cloning vector map.

White colonies from cloning reaction were then heated to lyse the cells. The plasmid DNA was isolated using plasmid preparation kit. The isolated plasmid DNA was further amplified by rolling cycle amplification reaction (RCA) and analyzed by gel electrophoresis. The RCA products from every colonies were then sequenced with 454 Life Sciences DNA sequencing unit, GS20, at Interdisciplinary Center for Biotechnology Research (ICBR) of the University of Florida (Figure 2-10). The 96 well plates containing individual colonies were taken back and used as DNA template for PCR amplification to prepare individual sequences ready for binding tests with cells based on the sequence analysis results.

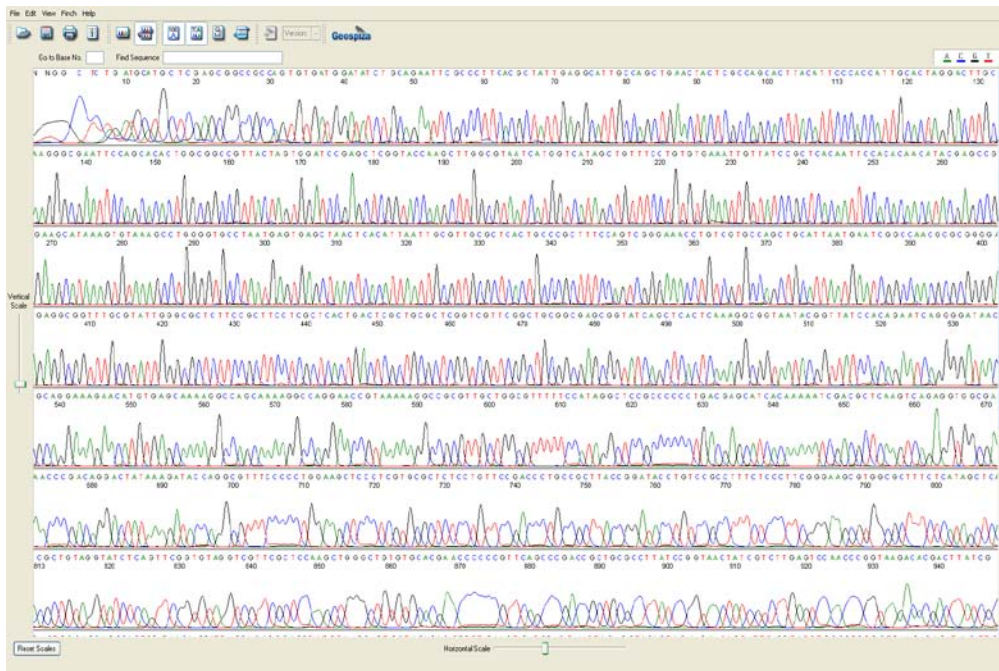


Figure 2-10. Sequencing results produced by 454 Life Sciences DNA sequencing unit, GS20.

The sequencing results were subjected to the multiple sequence alignment analysis with the MEME/MAST SYSTEM, version 3.5.3 (developed by Timothy Bailey, Charles Elkan, and Bill Noble at the UCSD Computer Science and Engineering department with input from Michael Gribskov at Purdue University, <http://meme.nbcn.net>) to discover highly conserved motifs in groups of selected DNA sequences. The discovered consensus sequences with high repeats

among selected pool were then prepared using RCA product from sequencing experiment as PCR template and tested for specificity and affinity. The aptamer candidates obtained in this way were then chemically synthesized on DNA synthesizer for further screening.

Flow Cytometry

Flow cytometry is a popular tool widely used in cell biology measuring various parameters of cells, which include forward scattering signal, side scattering signal, and fluorescence signal, as shown in Figure 2-11. During the experiment, the monodispersed cells are brought by sheath flow through the focal point of laser one by one. The signals resulted from the shining of laser are collected simultaneously for every cell. The forward scattering signal usually represents the size of the cells while the side scattering signal represents the smoothness of the cell surface. These two parameters generally describe the physical characteristics of cell. If the cells are stained with fluorescent molecules such as binding to dye labeled aptamers, the fluorescence signal can be collected at the same time. To monitor the enrichment of aptamers along with the progress of SELEX, FITC labeled ssDNA pools were incubated with 1×10^6 cells in 400 μ L binding buffer at 4°C for 30 minutes. Cells were washed twice after incubation and analyzed by flow cytometry. The binding of selected aptamers to SCLC cells, NSCLC cells, leukemia cells, and liver cancer cells were similarly analyzed. Flow cytometry was performed on a FACScan cytometer with CellQuest software (Becton Dickinson Immunocytometry Systems, San Jose, CA). Typically, 30000 cells were measured for every sample. Flow cytometry data were analyzed by WinMDI 2.9 software (Joe Trotter, <http://facs.scripps.edu/software.html>).

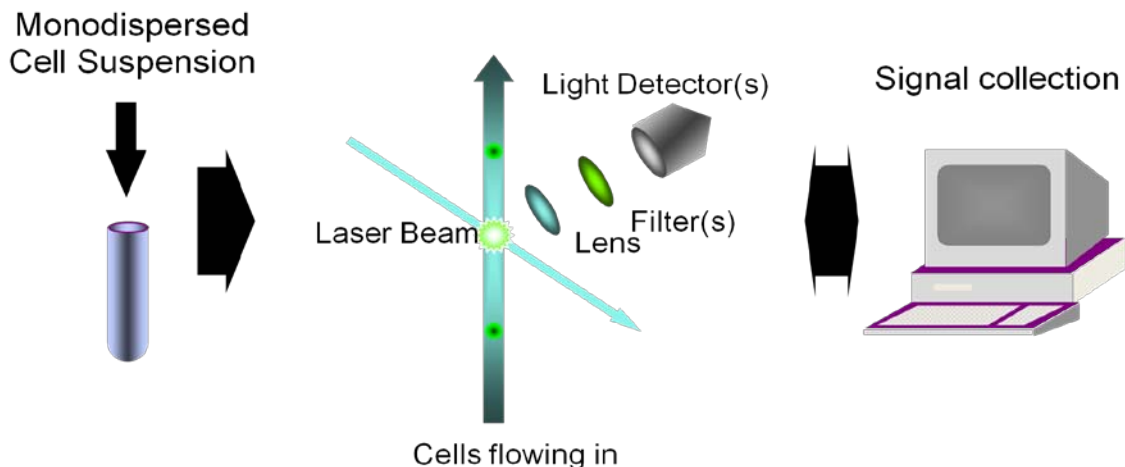


Figure 2-11. Working principle of flow cytometry. Forward scattering signal, side scattering signal, and fluorescence signal are collected for every cell.

Fluorescence Confocal Imaging

The binding of selected ssDNA pools and individual aptamers to SCLC cells were evaluated by fluorescence confocal imaging. Cells were incubated with 250 nM TAMRA labeled aptamers in 100 μ L binding buffer at 4°C for 30 minutes. After washing, 20 μ L of solution was dropped on a covered glass slide for examination with confocal microscope. Fluorescence confocal imaging was performed on a Fluoview 500/IX81 inverted confocal scanning microscope system (Olympus). A 5-mW, 543-nm He-Ne laser was used as excitation source for TAMRA dye. The objective used for imaging was a 60 \times oil-immersion objective (PLAPO60XO3PH) with a numerical aperture of 1.40 (Olympus). A 20 \times objective with a numerical aperture of 0.7 (Olympus) was also used for imaging of large field. Images were taken after a five to ten second period during which the instrument was focused to yield the highest intensity from the fluorescence channels. Staining of cell line tissue array by fluorescent aptamers and extraction of SCLC cells by aptamer conjugated nanoparticles were evaluated by confocal imaging in a similar way as described above.

Results and Discussion

Selection of Aptamers

With the developed cell based SELEX technique, we applied this approach to the system of our main interest, lung cancer. We expected to select some aptamers targeting the cell surface markers of various lung cancer cells, which may be used in future applications such as early diagnosis and targeted therapy of lung cancer. We first picked small cell lung cancer as the system to select aptamers using cell based SELEX because it is the most aggressive subtype of lung cancer with greater than 95% mortality in a few years, and has the shortest life expectancy among all lung cancer subtypes.^[123, 124]

To develop cell specific aptamer probes, live cancer cells were directly used as the target for cell based SELEX, an approach established in our lab. We chose to develop aptamer probes targeting classic small cell lung cancer (SCLC) in initial study as it possesses the worst clinical presentation among all lung cancer phenotypes. Non-small cell lung cancer (NSCLC, large cell) was adopted as a control for cell based SELEX to generate aptamers exclusive to the cell surface markers of SCLC. These cell surface markers are so exclusive to SCLC that normal lung epithelial cells are also not expected to bear them and cross-react with developed aptamers, as observed in previous studies with antibodies.^[7] With counter-selection against control cells, the aptamers achieve great selectivity for the reliable detection of lung cancer antigens.

The cell based SELEX approach was first adapted in a few aspects to work with floating aggregates of SCLC and adherent monolayers of NSCLC, which are two typical growth patterns of lung cancer cell culture. Because of their heterogeneous population and poor viability, it is more challenging to perform cell based SELEX with lung cancer than leukemia in previous study.^[18] The leukemia cells have several advantages to be used as a model system to demonstrate cell based SELEX. However, the developed aptamers are relatively less significant

for leukemia diagnosis or therapy than the aptamers for lung cancer. Leukemia cells are generally homogeneous cell suspension, so that they are easy to handle during the selection process. They also have very good viability that has minimal effect of nonspecific DNA absorption. In some cases, the dead cells can nonspecifically trap large amount of DNA, which could be amplified together with specific binding DNA during PCR reaction. This effect will significantly compromise the selection efficiency. In addition, the leukemia cells have short doubling time, which makes it easy to supply cells during selection.

In contrast, lung cancer cells have very diverse growing patterns as well as growing curves. Typically, small cell lung cancer grows as cell aggregates with various sizes in cell suspension, as shown in Figure 2-12 (A). This heterogeneous cell population can cause the aptamers to bind with cell aggregates of different sizes in a complicated manner. And the histogram results of fluorescence signals measured by flow cytometry are too broad to be used for comparison of binding ability among different selected DNA pools. The cell viability of lung cancer is also a concern for cell based SELEX, especially for small cell lung cancer. Generally, small cell lung cancer cells grow with a viability of 70% (30% cells are dead cells). The dead cells will fall off the cell aggregates to become single dead cells mixed with other live cell aggregates. These dead and/or dying cells can non-specifically absorb large amount DNA molecules during experiments. This effect was confirmed by both flow cytometry and fluorescence confocal imaging results. The biggest challenge of dead cells mixed with healthy cells for cell based SELEX experiment is that the cells trapped in dead cells can be PCR amplified together with those specific aptamer DNA, compromising the enrichment efficiency of aptamers. With these disadvantages, we preferred to treat the cell aggregates into single cells in solution before experiment. The small cell lung cancer cell suspension was filtered using a film with proper size to remove the single

dead cells in solution. The healthy cell aggregates were retained to be treated with non-enzymatic cell dissociation reagent, and were further broken apart by mechanical method such as pipetting the solution. The resulted single cell suspension was finally washed several times to remove the EDTA in non-enzymatic cell dissociation reagent, which may affect the formation of aptamer secondary structure. In addition, small cell lung cancer cells have relative longer doubling time, so that we studied their growing curve and optimized their culture condition to assure the supply of cells for SELEX experiments. Non-small cell lung cancer cells generally grow as adherent monolayers in cell flask, as shown in 2-12 (B). Instead of doing SELEX experiment with cell suspension, we incubated DNA pools with cells directly on the wall of cell flask without peeling them off using trypsin since the trypsin may destroy some cell surface proteins.

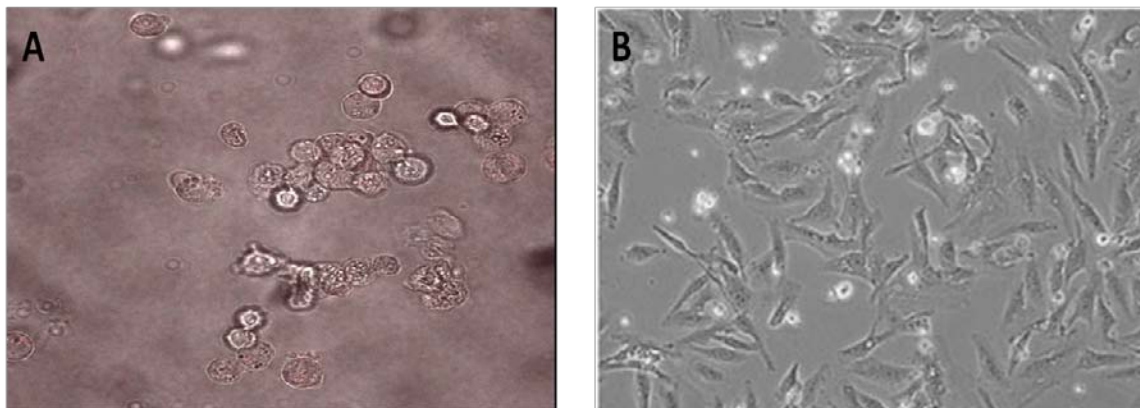


Figure 2-12. Growing patterns and cell morphology of small cell lung cancer and non-small cell lung cancer. A) SCLC cells grow as cell aggregates in suspension. B) NSCLC cells grow as adherent monolayer.

However, we often treated NSCLC cells with non-enzymatic dissociation reagent to make them single cells in suspension for flow cytometry experiments. Unlike SCLC cells, NSCLC cells have very good cell viability. The dead cells fall off the flask wall while healthy cells attach to

flask wall. The dead cells thus can be easily removed by washing before experiment. NSCLC cells have short doubling time, which makes cell culture relatively easier than SCLC cells.

In the actual selection (Figure 2-13), a cultured SCLC cell line, NCI-H69, was first incubated with a 71-base synthetic single stranded DNA library. Target cell (NCI-H69) and control cell (NCI-H661) were counted and tested for viability before experiments. Target cells were treated in the way described above: dead cells were filtered away, and cell aggregates were broken apart to individual cells. The synthesized ssDNA library (10 nmol in 1 mL binding buffer) was first denatured at 95°C for 5 minutes and kept on ice for 10 minutes. 2×10^6 target cells were washed, dissociated (0.53 mM EDTA/PBS), and then incubated with ssDNA library at 4°C for 30 minutes. After 3 times of stringent washing, the DNA sequences that bound to target cells were eluted to 300 μ L binding buffer by heating at 95°C for 5 minutes. The cell debris was removed by centrifugation, and DNAs in supernatant were collected. A cultured NSCLC cell line, NCI-H661, was now introduced as control cell to separate aptamers with affinity to both the target and control cells from those aptamers recognizing only target cells in the eluted DNA pool. The eluted DNAs were incubated with excess control cells at 4°C for 30 minutes for counter selection (eliminated in first round of selection). After counter selection, the DNAs that don't bind to control cells were collected, desalted, and used as template in PCR reaction for amplification.

Because the amount of harvested DNA from every round of selection is variable due to changing conditions, it is always wise to quantify the exact amount of DNA to be used as template in PCR reaction. Too little template can cause insufficient material for next round of selection; however, too much template may lead to non-specific amplification, resulting in by-

product in PCR. We developed a novel real-time PCR method to determine the amount of target bound DNA after selection.

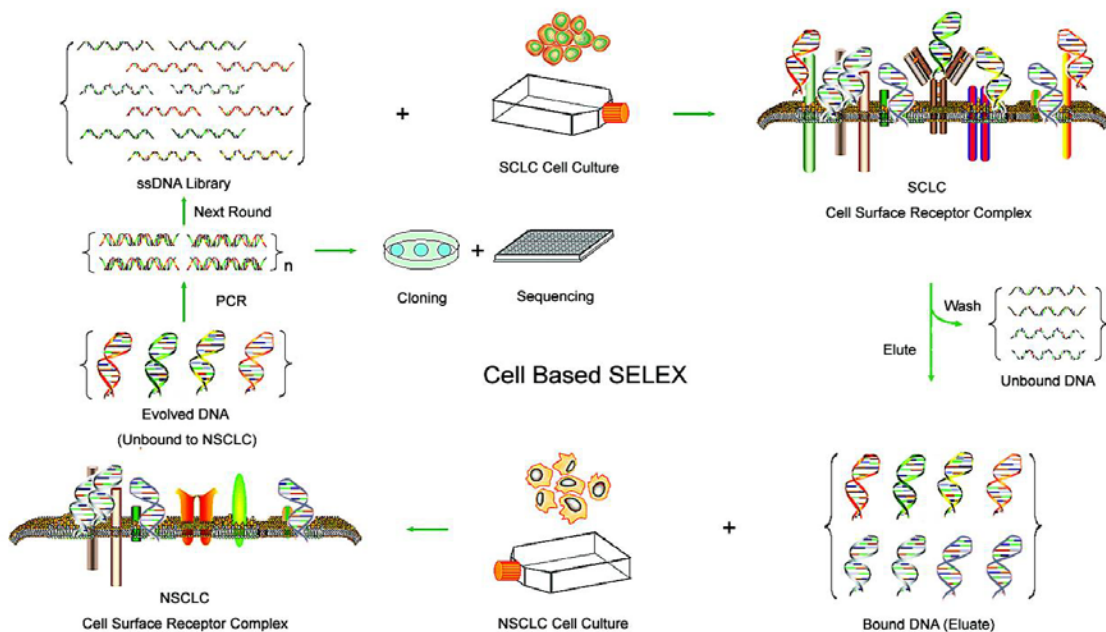


Figure 2-13. Cell based SELEX using small cell lung cancer cells as target cells and non-small cell lung cancer cells as control cells. DNA library was first incubated target cells in dish, followed by washing away non-specific binding sequences. A number of DNA molecules from the ssDNA library bind to SCLC cells after incubation and are retained for counter-selection with NSCLC cells. Target bound sequences were then incubated with control cells to remove those sequences bind to both target and control cells. The SCLC-specific DNA molecules are subsequently PCR amplified for the next round of selection, or for cloning and sequencing to identify individual aptamers in the most selected pool.

Besides using this data for bulk PCR, it can also be used to compare the binding ability of different pools during the SELEX. More DNA sequences left after selection generally means stronger binding pool. This can be correlated with the flow cytometry data to monitor the enrichment process of aptamers.

In our experiments, we took a portion of DNA from the selection product for real-time PCR test. This DNA template with unknown amount was accompanied by a series of standard

DNA samples with known amount in real-time PCR reactions, as shown in Figure 2-14 (A). Since the starting quantity of DNA template in real-time PCR is proportional to the threshold cycles, the unknown sample amount can be determined by comparison with standard known sample as shown in Figure 2-14 (B). Once we knew the amount of DNA in selected pool, we decided the reaction volume for bulk PCR reaction to be used with the previously optimized PCR conditions including cycles and temperatures. From our results, real-time PCR does show great advantages in cell based SELEX. It is both time and cost effective, without running several rounds of PCR and gel electrophoresis to optimize the PCR condition in every round. The quality of PCR product can be easily identified by melting curves.

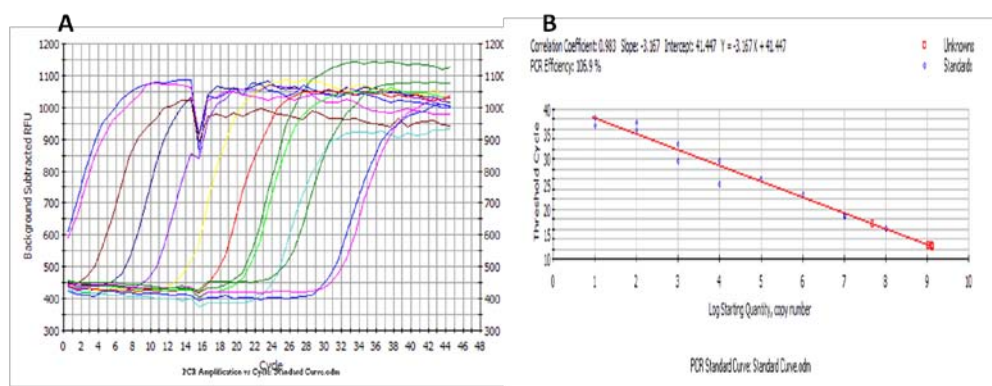


Figure 2-14. Principle of determining starting quantity of PCR template by using real-time PCR. A) Unknown amount sample was used as template in real-time PCR reaction, accompanied by a series of standard DNA samples with known amount. B) The starting quantity of DNA template in real-time PCR is proportional to the threshold cycles, the unknown sample amount can be determined by comparison with standard known sample.

After we amplified the selected pool with FITC and biotin labeled primers in bulk PCR reaction, the PCR product of first round of selection was then processed as described before to generate single stranded DNAs using streptavidin beads for next round of selection. For the second round of selection, all product of first round was dissolved in 200 μ L binding buffer as starting ssDNA pool. To increase the stringency of selection, the washing strength was enhanced

by gradually increasing washing time (from 1 to 10 minutes), washing volume (from 1 to 3 mL), and washing round (from 3 to 5 times). Meanwhile, the SELEX progress was monitored by flow cytometry and fluorescence confocal imaging.

From the results of flow cytometry (Figure 2-15) and confocal microscopy (data not shown), the binding ability of DNA pools from each round of selection was assessed.

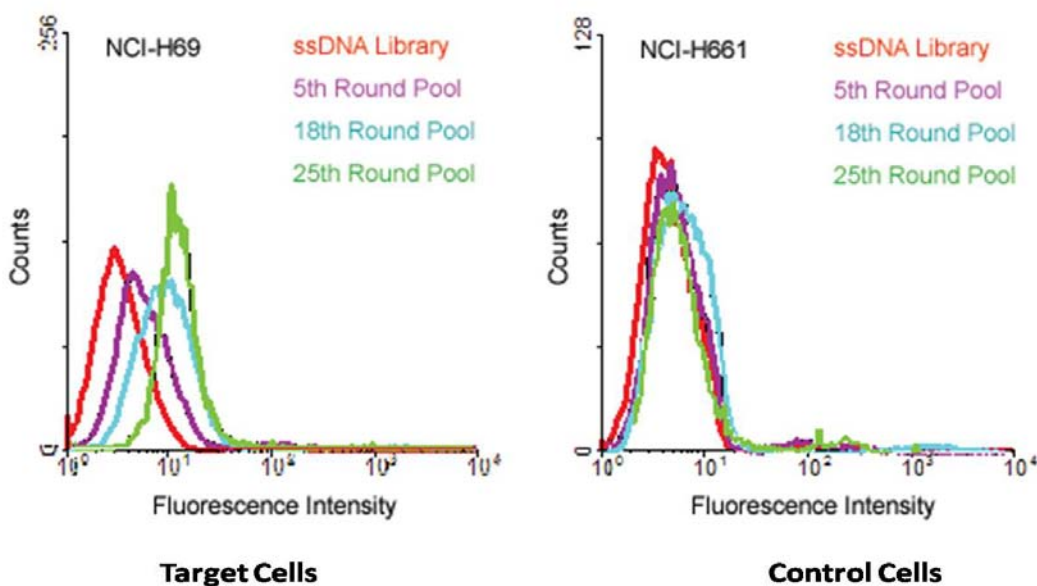


Figure 2-15. Flow cytometry monitoring of lung cancer cells with DNA library and selected pools along the progress of SELEX. The FITC-labeled ssDNA library and selected DNA pools were tested for binding to NCI-H69 (SCLC) and NCI-H661 (NSCLC) cells by flow cytometry. The binding ability of selected DNA pools gradually increased for SCLC, and no significant change was observed for NSCLC: red) ssDNA library, purple) 5th round pool, green) 18th round pool, blue) 25th round pool.

The increase in the fluorescence intensity of the dye labeled DNA pools bound to target cells is gradual and steady along with the progress of selection, indicating a successful evolution of high affinity aptamers. By contrast, no significant change was observed in the response to the control cells during the selection process, demonstrating the specificity of selected DNA pools. A panel of aptamer probes eventually evolved to have great specificity and high affinity for SCLC along

with the SELEX progress. After 25 rounds of selection, the binding ability of selected DNA pool reached a plateau, and cloning was performed to isolate individual aptamers in the most selected DNA pool.

Sequencing and Alignment Results

To isolate and purify individual DNA aptamers from the enriched pool, we PCR amplified the most enriched 25th round pool for cloning. The PCR products were inserted into the cloning vector and transformed into bacterial cells. The resulted monoclonies containing individual sequences were treated to extract the plasmids. The plasmids were further amplified by RCA reaction for sequencing. About 400 DNA sequences were obtained, and analyzed by multiple sequence alignment software (MEME/MAST SYSTEM, version 3.5.3) to check for any consensus sequence. As shown in Figure 2-16, we found that the majority of aptamers in the selected pool belong to several families based on the consensus sequences they have. In some families, many sequences have identical or similar sequence, and have high repeats (Figure 2-17). These families were thought to have the biggest chance to become the aptamers targeting cell surface markers, so that they were synthesized for testing their binding ability to SCLC cells.

Deconvolution of Specific Aptamers

From the sequencing and alignment results, we synthesized the following sequences as potential aptamer candidates.

HCA12:5'TACCAGTGCGATGCTCAGGTGGATTGTTGTGTTCTGTTGGTTTTTGTGTTGT
CCTGACGCATTCGGTTGAC3'
HCC03:5'TACCAGTGCGATGCTCAGCCGGGGACCGGGGCACCGGGGGCCAGTGGCAC
GGACTGACGCATTCGGTTGAC3'
HCH07:5'TACCAGTGCGATGCTCAGGCCGATGTCAACTTTTTCTAACTCACTGGTTTT
GCCTGACGCATTCGGTTGAC3'
HCH01:5'GTCAACCGAATGCGTCAGCTGGATCTTAAAGATTGCATGCGCTCACTATGG
GACTGAGCATCGCACTGGTA3'

Multiple sequence alignment analysis (selected sequences studied in this work)

Motif 1	NAME	START	P-VALUE	SITES
	C2-7-40-A12	2	1.92e-16	G TGGATTGTTGTGTTCTGTTGGTTTTTGTG TTGTC
	C2-8-40-F10	2	1.92e-16	G TGGATTGTTGTGTTCTGTTGGTTTTTGTG TTGTC
	C2-4-20-E08	2	1.92e-16	G TGGATTGTTGTGTTCTGTTGGTTTTTGTG TTGTC
	C2-2-20-G02	5	5.07e-13	GGTG TGTGTTTTTGTGTTTTGCTTGGTGTGTTG TG TC
	C2-4-20-F04	6	3.46e-11	GCGGT TCTGTGGTTGTTGTTGTGTTGTTTTTTG G
	C2-4-20-G08	7	4.06e-11	GGTCGG TGTGTTTTGTTGTTTTTTGTGCTTTTTTC
	C2-3-20-D02	1	6.41e-11	GGGTGTGTTGTTTTGTTGTTCTTTGGTG ATTTG
	C2-4-20-F03	4	6.73e-11	CGG TGTGTTTCGTCGTGTTTTGTTGTATGTG TG
Motif 2	NAME	START	P-VALUE	SITES
	C2-5-40-C03	7	3.44e-15	TCCGTG CCACTGGCCCCCGGTGCCCCGGTCCCCGG
	C2-5-40-C09	7	3.44e-15	TCCGTG CCACTGGCCCCCGGTGCCCCGGTCCCCGG
	C2-5-40-A10	7	3.44e-15	TCCGTG CCACTGGCCCCCGGTGCCCCGGTCCCCGG
	C2-2-20-H12	1	2.16e-10	ACACCAGCGTACCTTGGTGCGGGTCCCTGG GCGCAT
	C2-8-40-G03	3	2.35e-10	GC ACCTTCGTACCCCCACCTCCGGGCCCGTGC TCC
	C2-8-40-G06	3	2.35e-10	GC ACCTTCGTACCCCCACCTCCGGGCCCGTGC TCC
	C2-2-20-G06	1	2.35e-10	ACACCAGCGTACCTTGGTGCGGGTCCCTGC TCTGAT
	C2-5-40-B08	2	1.12e-08	C CACCCGACACTTCGTGCGTCCGTCCCCTTT TCCCG
	C2-3-20-B05	5	1.12e-08	CCGA CCTCTCGTTCCTCGTGTCCCATCCCCCG CT
	C2-2-20-F09	4	1.21e-08	GGC TCCGTTACCCTCGTTCGACCTGCCCCCGC GTG
Motif 3	NAME	START	P-VALUE	SITES
	C2-6-40-H02	5	1.89e-18	GCCG ATGTCAACTTTTTCTAACTCACTGGTTTT GC
	C2-7-40-C06	5	1.89e-18	GCCG ATGTCAACTTTTTCTAACTCACTGGTTTT GC
	C2-2-20-E04	5	1.89e-18	GCCG ATGTCAACTTTTTCTAACTCACTGGTTTT GC
	C2-2-20-G08	5	1.89e-18	GCCG ATGTCAACTTTTTCTAACTCACTGGTTTT GC
	C2-2-20-H02	5	1.89e-18	GCCG ATGTCAACTTTTTCTAACTCACTGGTTTT GC
	C2-4-20-H07	5	1.89e-18	GCCG ATGTCAACTTTTTCTAACTCACTGGTTTT GC
	C2-6-40-G02	5	3.94e-18	GCCG ATGTCATTTTTCTAACTCACTGGTTTT GC
	C2-2-20-E11	1	5.75e-13	GCAACCTCTCTTTCAACTTCACTGGTTCT ATTCTC
Motif 4	NAME	START	P-VALUE	SITES
	C2-2-20-G11	3	3.39e-14	GC GGAAAATTAAGTTATTCTGCCCCCTCGA CTCAGCTGAG
	C2-1-20-D07	3	4.61e-14	CT GGATCTTAAAGATTGCATGCGCTCACTA TGGGA
	C2-4-20-H01	3	4.61e-14	CT GGATCTTAAAGATTGCATGCGCTCACTA TGGGA
	C2-2-20-F11	3	1.06e-13	GC AGAAAATTAAGTTATTCTGCCCCCTCGA CTCCG

Figure 2-16. Multiple sequence alignment analysis of sequencing results with MEME Version 3.5.3. Motif 1 refers to aptamer HCA12, motif 2 refers to aptamer HCC03, motif 3 refers to aptamer HCH07, motif 4 refers to aptamer HCH01.

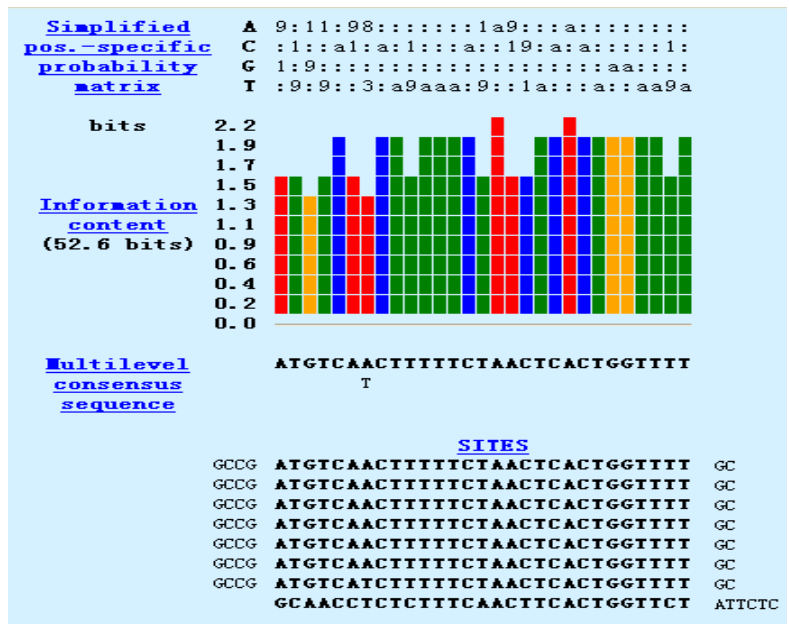


Figure 2-17. Family of aptamer HCH07 shares the same consensus sequence and has high repeats.

After testing, a few of them showed prominent binding ability for SCLC but not for NSCLC (control cell) compared with DNA library, as illustrated by flow cytometry results (Figure 2-18). The dominant peak refers to the binding of aptamer with SCLC cells. A second peak with high fluorescence signal may represent the population of dead cells containing non-specific DNA molecules labeled with fluorescent dye.

In order to see the binding profile of aptamers in a more direct way, we used fluorescence confocal imaging with TAMRA labeled aptamers to confirm the flow cytometry results. According to confocal imaging results, fluorescent dye labeled aptamers bind to target SCLC cells specifically (Figure 2-19). The DNA library control showed limited background signals. Also, the dye labeled aptamers showed the profile of binding to the cell membrane region where the cell surface protein targets are presenting. As seen in flow cytometry, some bright dead cells are full of dye labeled aptamer molecules.

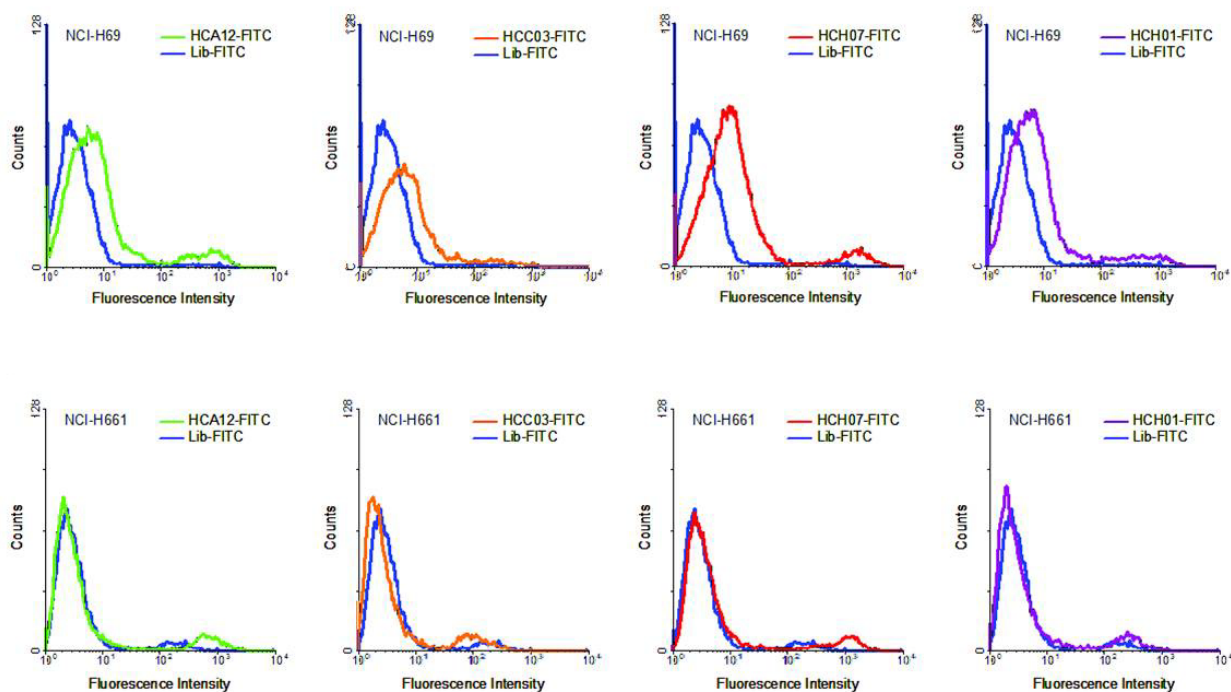


Figure 2-18. Flow cytometry results of molecular aptamers binding specifically to SCLC cells. SCLC cells, NCI-H69 and NSCLC cells, NCI-H661 were incubated with FITC-labeled aptamers and ssDNA library. Aptamer binding was restricted to SCLC cells. As the cells are different, different flow cytometry parameters were used. Comparisons can only be made between the library and the aptamer for each type of cell. The dominant peak refers to the binding of aptamer with SCLC cells. A second peak with high fluorescence signal was also observed, which represents the population of dead cells.

Since the morphology of small cell lung cancer cells studied here are mostly cell aggregates, the fluorescence images only shows the cells on the focal plane, and is not able to show the three-dimensional structure. However, the three-dimensional fluorescent image can be obtained by the accumulation of continuous images of different focal planes as shown in Figure 2-20. These results further confirmed the binding of aptamers selected from cell based SELEX to the target cells.

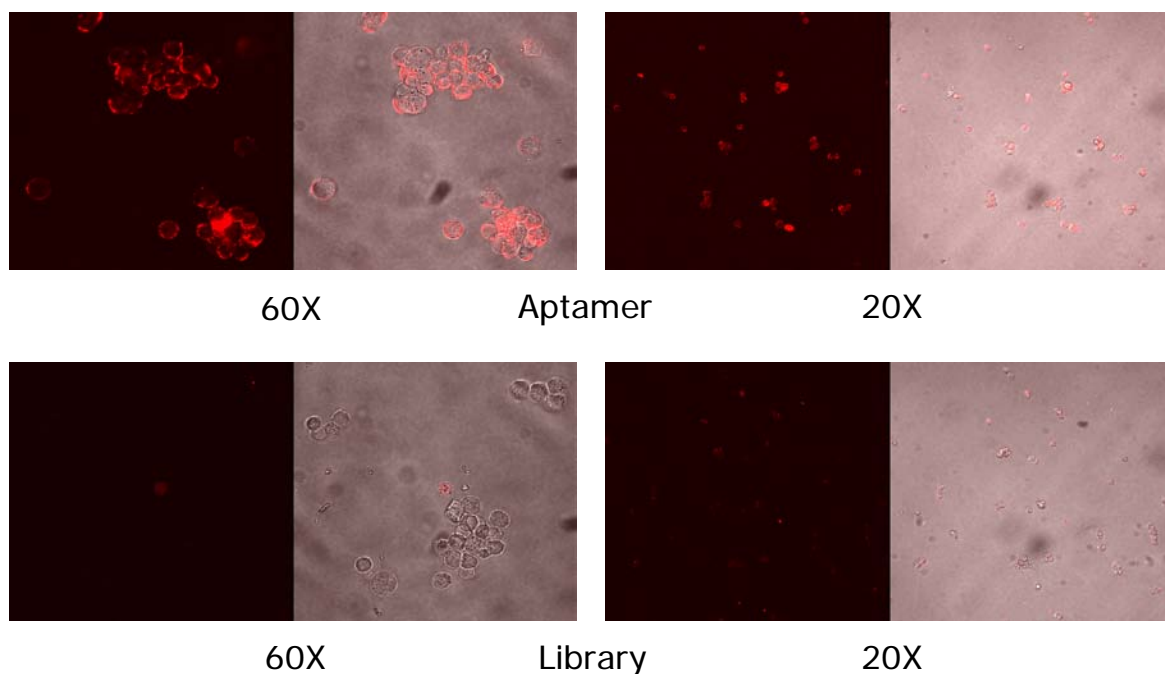


Figure 2-19. Fluorescence confocal imaging of TAMRA labeled aptamer binding to small cell lung cancer cells. SCLC cells, NCI-H69, were incubated with TAMRA-labeled HCH07 aptamer and ssDNA library. The fluorescent dye-labeled aptamers bind to the surface of SCLC cells as determined by confocal imaging at 60 and 20 X magnification. Only background fluorescence was observed on cells incubated with fluorescent dye-labeled ssDNA library due to nonspecific binding.

Identification and Characterization of Aptamers

As shown by both flow cytometry and fluorescence confocal imaging, aptamer HCA12, HCC03, HCH07, and HCH01 can specifically bind to the target cells, small cell lung cancer NCI-H69. None of them can bind to the control cells, non-small cell lung cancer NCI-H661. We also analyzed the secondary structures of these aptamers to check if they have any possible interaction with the protein targets. Generally, aptamers with certain stable secondary structures such as hair-pin structure have more chances to bind with proteins than those with unstable secondary structures.

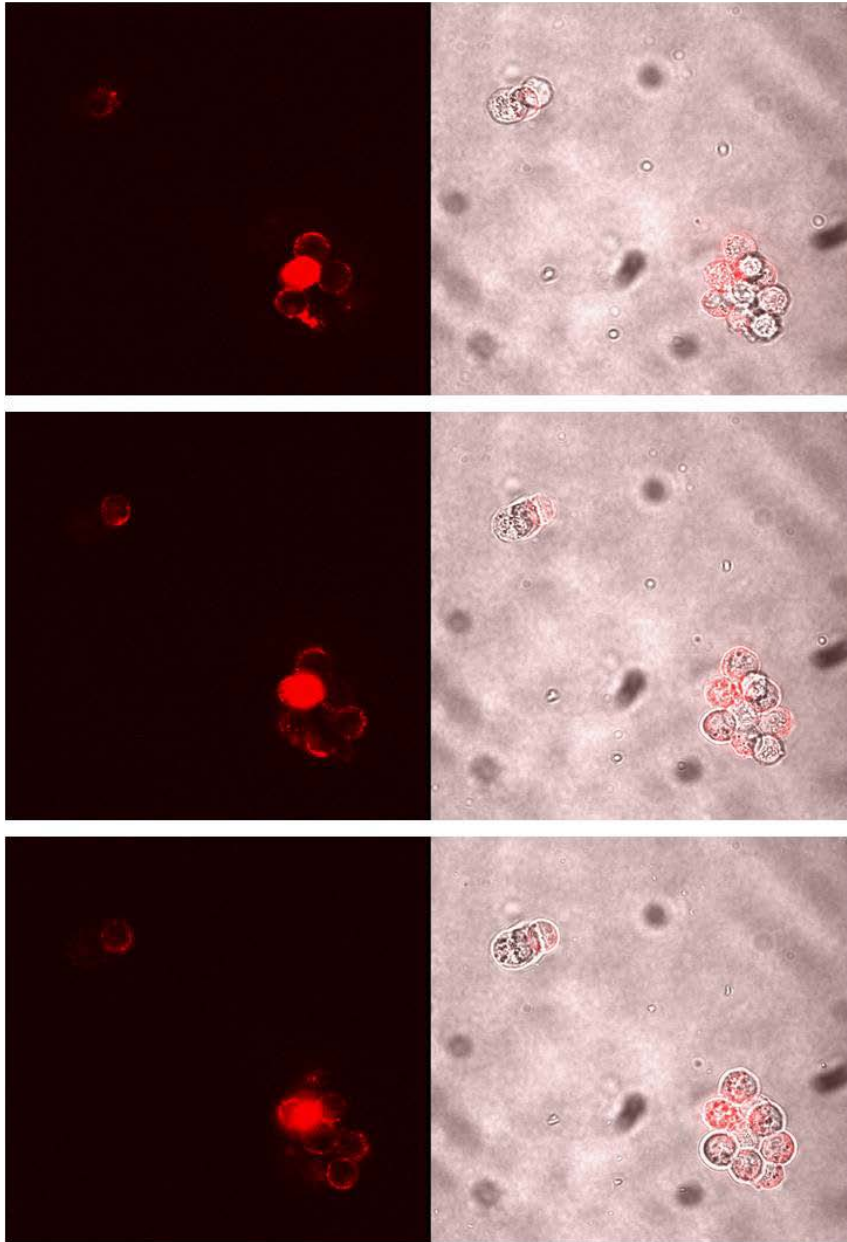


Figure 2-20. Z axis imaging of different focal planes of SCLC cells bound with TAMRA labeled aptamer.

OligoAnalyzer 3.1 software (Integrated DNA Technology) was used to analyze the secondary structures. Figure 2-21 shows the predicted secondary structures of selected aptamers HCA12, HCC03, HCH07, and HCH01. It is observed that all aptamers can form very complicated secondary structures, which may help build up the interaction between aptamers and proteins.

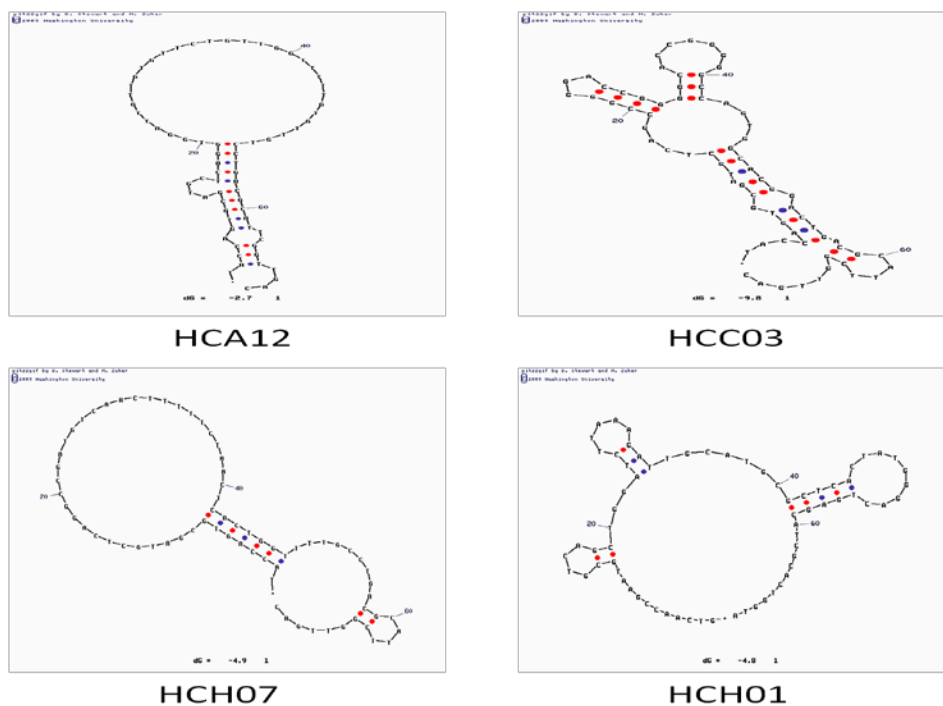


Figure 2-21. Computer software simulated secondary structures of aptamers HCA12, HCC03, HCH07, and HCH01.

In addition, individual aptamers were tested with saturation analysis to measure the relative binding affinities to their target proteins on cell surface. As depicted in Figure 2-22 (A), the traditional K_d determination method for receptor/ligand system was adapted in a few aspects to accommodate the aptamer/cell system. The binding signal of DNA library to the cells was used in this case as background to be subtracted from the total binding signal of aptamers, resulting in the actual aptamer binding curve. In the saturation analysis experiments, cells were first incubated with FITC labeled aptamers at 4°C for 30 minutes, washed three times with 400 μ L washing buffer, and finally re-suspended in 400 μ L binding buffer containing 20% FBS (to minimize the non-specific binding of DNA to cell surface). Cells were then assayed using flow cytometry. Concentrations of FITC labeled aptamers for the relative affinity measurements varied from 0 to 1 μ M. The FITC labeled ssDNA library was used to determine nonspecific

binding. The mean fluorescence intensity of aptamer bound cells (nonspecific binding of DNA library subtracted) was used to calculate bound aptamer fraction at different concentrations. All affinity measurements were performed in triplicate. The results are described as mean \pm s.e.m. The equilibrium dissociation constants (Kd) were obtained by fitting the cell surface binding data of aptamers to a one-site saturation model as shown in Figure 2-22 (B) with SigmaPlot 9.0 (Jandel Scientific).

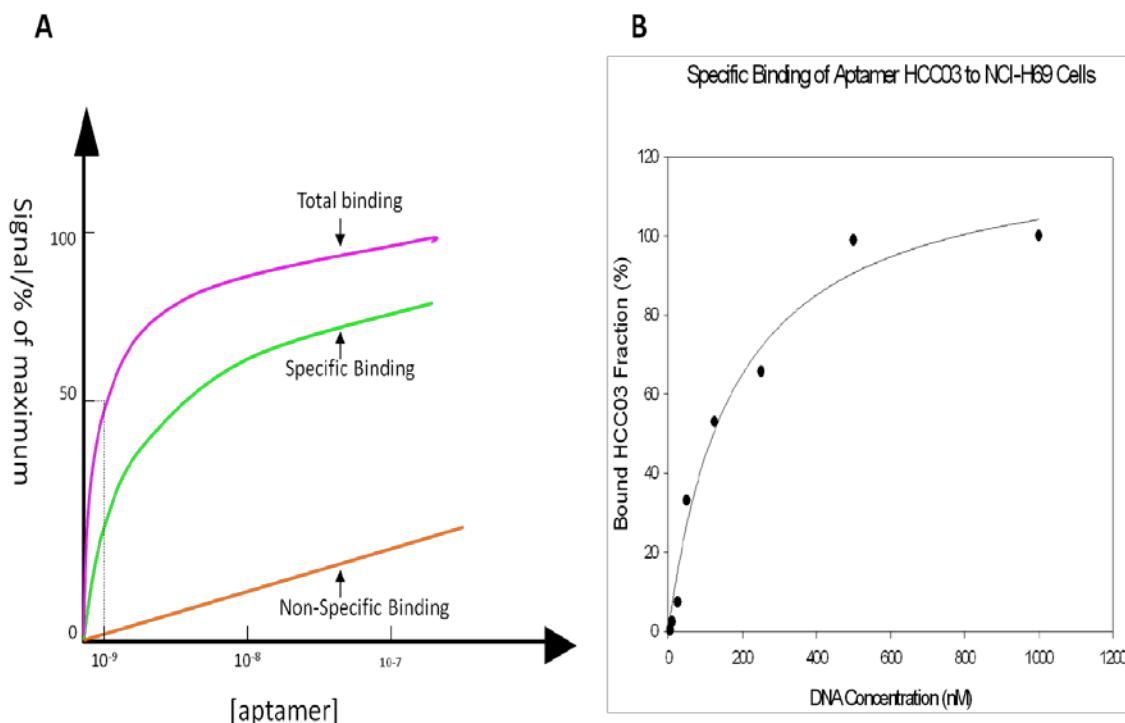


Figure 2-22. Saturation analysis of aptamers. A) Principle of saturation analysis. Cells were analyzed using flow cytometry. The mean fluorescence intensity of aptamers bound with cells (nonspecific binding of DNA library subtracted) was used to calculate bound aptamer fraction at different concentrations. The FITC labeled ssDNA library was used to determine nonspecific binding. B) Saturation analysis result of aptamer HCC03. Concentrations of FITC labeled aptamers for the relative affinity measurements varied from 0 to 1 μ M. All affinity measurements were performed in triplicate. The results are described as mean \pm s.e.m. The equilibrium dissociation constants (Kd) were obtained by fitting the cell surface binding data of aptamers to a one-site saturation model with SigmaPlot 9.0. The apparent Kd obtained in this experiment is considered to be higher than the accurate Kd due to the error brought in by dead cells.

All the selected aptamers were found to have high affinity with equilibrium dissociation constant in the nanomolar range (Table 2-1). These obtained Kds are apparent Kds as the binding data in this case is from aptamers bound with proteins on cell surface. In addition, the poor viability of small cell lung cancer cells makes it difficult to obtain accurate Kd values because the dead cells in cell population contain some nonspecific DNA that can't be eliminated. However this effect can be minimized to an acceptable level and will not affect the use of these aptamers. The accurate Kds of these aptamers can be obtained later by using the purified target proteins for aptamer binding.

Table 2-1: Equilibrium dissociation constant of selected SCLC aptamers

Aptamer sequence name	Kd (nM)
HCA12	~97 nM
HCC03	~123 nM
HCH07	~38 nM
HCH01	~157 nM

Enzyme Analysis of Aptamers

In addition to the Kd characterization of developed aptamers, their putative cell surface targets were examined by enzymatic treatment to further verify the binding of aptamers to SCLC cell surface markers. Before the aptamer binding, cells were first treated by 2 different types of protein digestion enzymes: trypsin and proteinase K. If the target proteins are truly on the cell surface, they will be destroyed by the enzyme treatment, and will no longer be able to bind with aptamers. In the experiments, 1×10^6 Cells were washed with 1 ml of PBS, and treated with 200 μ L of 0.05% trypsin/0.53 mM EDTA in HBSS (Fisher Biotech) or 0.1 mg/mL proteinase K (Fisher Biotech) in PBS at 37°C for 2 minutes. FBS was then added to quench the enzyme activity. After washing with binding buffer, the cells were analyzed for aptamer binding with flow cytometry and confocal imaging as described before. As shown in Figure 2-23 (A), after the treatment of cells with trypsin or proteinase K, diminished binding of aptamers to SCLC cells

was observed by flow cytometry in both cases. We saw the same trend under confocal microscopy, only small amount of fluorescent aptamers retained on enzyme treated cell surfaces (Figure 2-23 (B)). These results suggested that selected aptamers indeed bind to target molecules on cell membrane, and these discovered SCLC cell surface markers can be affected by protease.

Minimal Binding Motif Study

We successfully selected some aptamers for small cell lung cancer cells by using cell based SELEX technique. These aptamers have such great specificity and affinity, that they may be used as molecular probes for diagnosis or escort molecules for targeted drug delivery. However, they may need further optimization and modification before use *in vivo*. The aptamers generated in our experiments contain 71 bases including two 18-base long primer binding sites and one 35-base long randomized region. Both primer binding sites and central region may be involved in the formation of secondary structure, but this may not be necessary.

We decided to seek for the key region of the full length aptamers, which is essential to the binding with protein. We expected to get shorter aptamers with full binding ability. There are several advantages for this study. First, long sequences usually result in low yield and high cost for DNA synthesis while short sequences are more amenable for various applications. Second, the affinity and specificity can be further improved by optimizing the sequences at some key regions. Third, less important region in the sequences can be used for conjugation with functional molecules or replacing with enzyme resistant artificial nucleotides such as locked nucleic acid. In addition, reduced size may increase the tissue penetration rates *in vivo*. To study the minimal binding motif of RNA aptamers, people previously used RNase footprinting and partial hydrolysis.^[125-128] For DNA aptamers, partial fragmentation approach was used to determine the minimal binding motif.^[129]

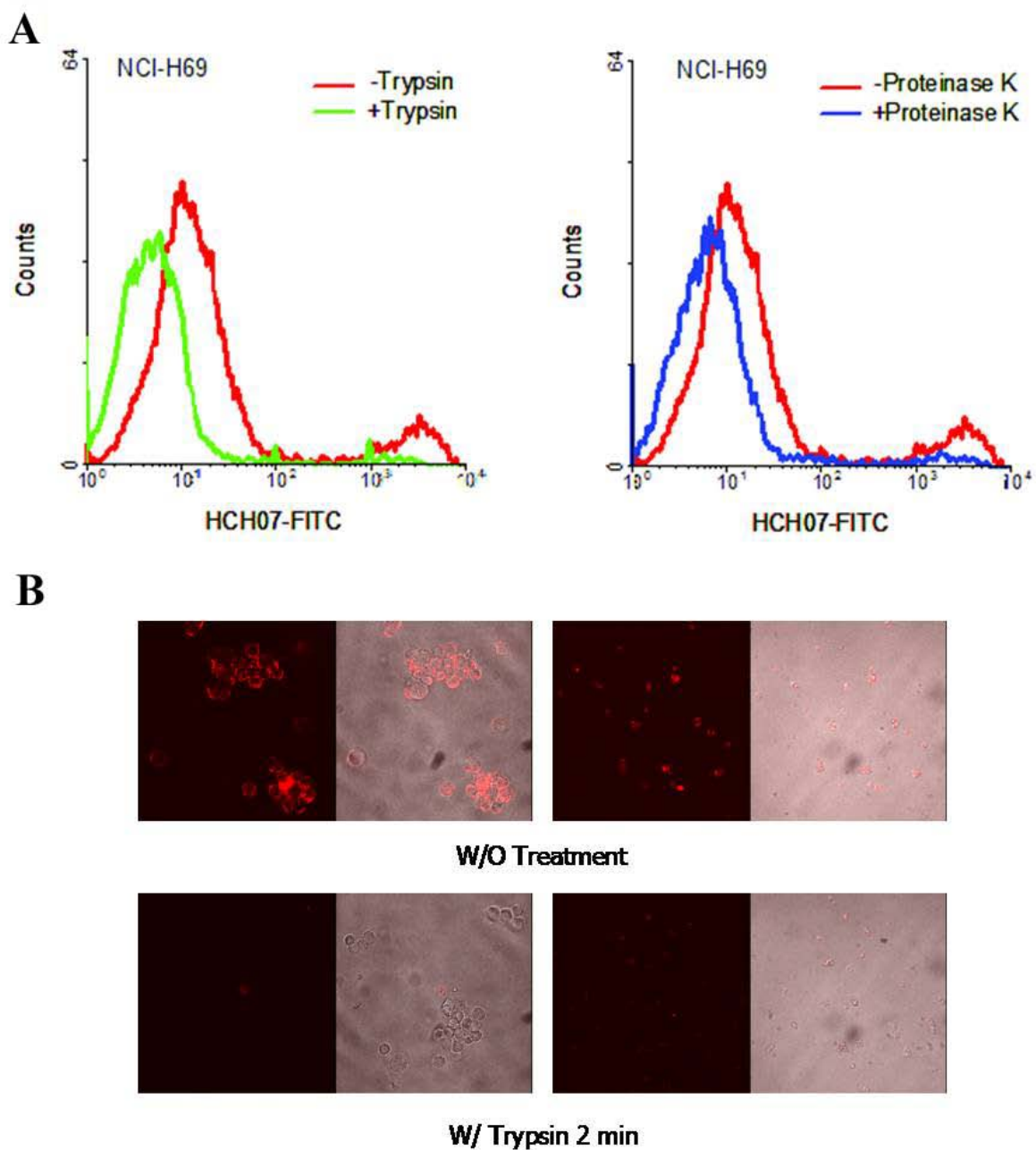


Figure 2-23. Aptamer target protein studies with protease treatment. A) Flow cytometry results of aptamer binding to small cell lung cancer cells with/without trypsin and proteinase K. B) Fluorescence confocal imaging results of aptamer binding to small cell lung cancer cells without trypsin treatment, and with trypsin treatment.

In our study, computer algorithm was used to predict the secondary structure of the aptamer sequences. Based on these structures, several nucleotides were cut off from the ends of

the aptamer sequences that are not involved in forming critical structures such as hair-pin structure. The truncated aptamers were then synthesized for testing the binding ability with cells. We kept cutting the nucleotides from the aptamer sequences until the truncated aptamer lost the binding ability. The rest part of the aptamer then can be reasoned to be the minimal binding motif. As an example, the full sequence of aptamer HCH07 is TACCAGTGCGATGCTCAGGCCGATGTCAACTTTTTCTAACTCACTGGTTTTGCCTGACGCATTCGGTTGAC. The most stable predicted secondary structure based on free energy change (ΔG) contains one hair-pin structure and one extra loop as shown in Figure 2-24. We then synthesized different truncated versions of the aptamer. Structure without loop 2 (ACCAGTGCGATGCTCAGGCCGATGTCAACTTTTTCTAACTCACTGGT) and structure without loop 1 (TTTGCCTGACGCATTCGGTTGAC) were tested with cells for binding, respectively. Both shortened structures lost binding ability completely as shown in Figure 2-24. It seems that both loop1 and loop 2 participated in the forming of critical structure for binding to cell surface protein targets. Only the full length aptamer HCH07 can perform the binding in this case.

Different than HCH07, aptamer HCA12, 71mer (TACCAGTGCGATGCTCAGGTGGA TTGTTGTGTTCTGTTGGTTTTTGTGTTGTCCTGACGCATTCGGTTGAC) can be shortened and modified to structure with perfect stem base pairing, 63mer(GACCAGTGCGTCAGGTGG ATTGTTGTGTTCTGTTGGTTTTTGTGTTGTCCTGACGCACTGGTC) without losing the binding ability as shown in Figure 2-25. In addition, the binding affinity of the aptamer was even improved by artificially creating perfect stem base pairing. With this result, we concluded that the hair-pin structure of HCA12 is critical to cell binding and the shortened HCA12 can fully replace the original aptamer selected from cell based SELEX.

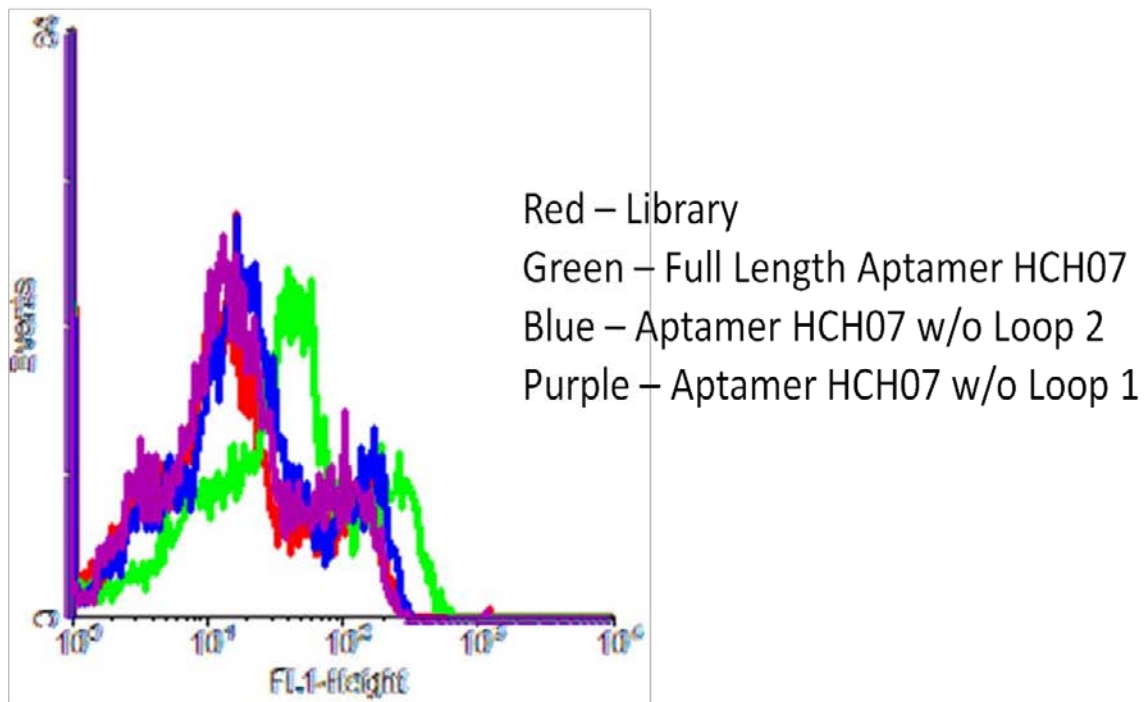
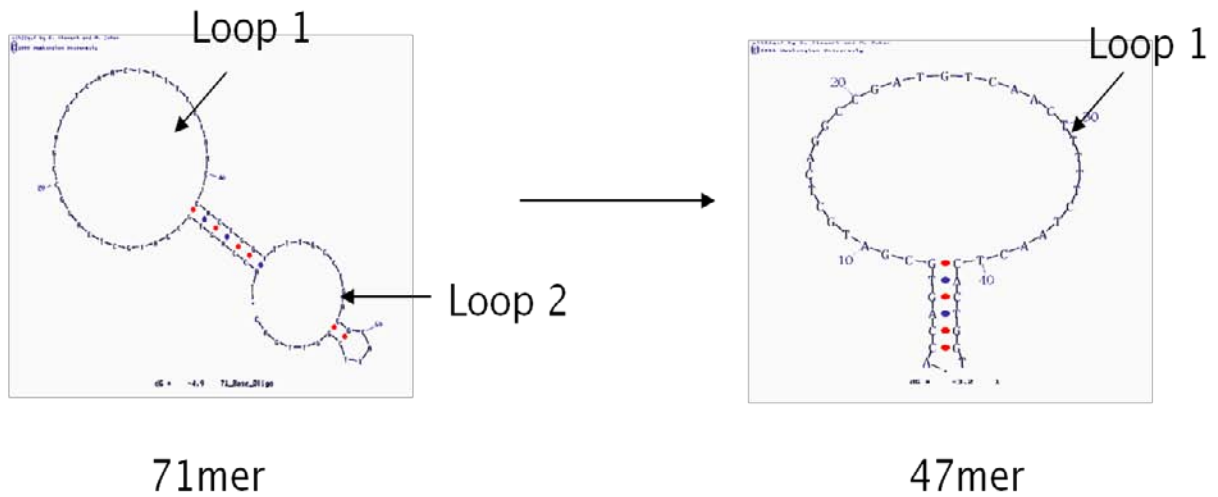


Figure 2-24. Minimal binding motif study of aptamer HCH07. The full length aptamer HCH07 has a hair-pin structure with an extra loop. Truncated aptamers all lost binding ability to cells as tested by flow cytometry.

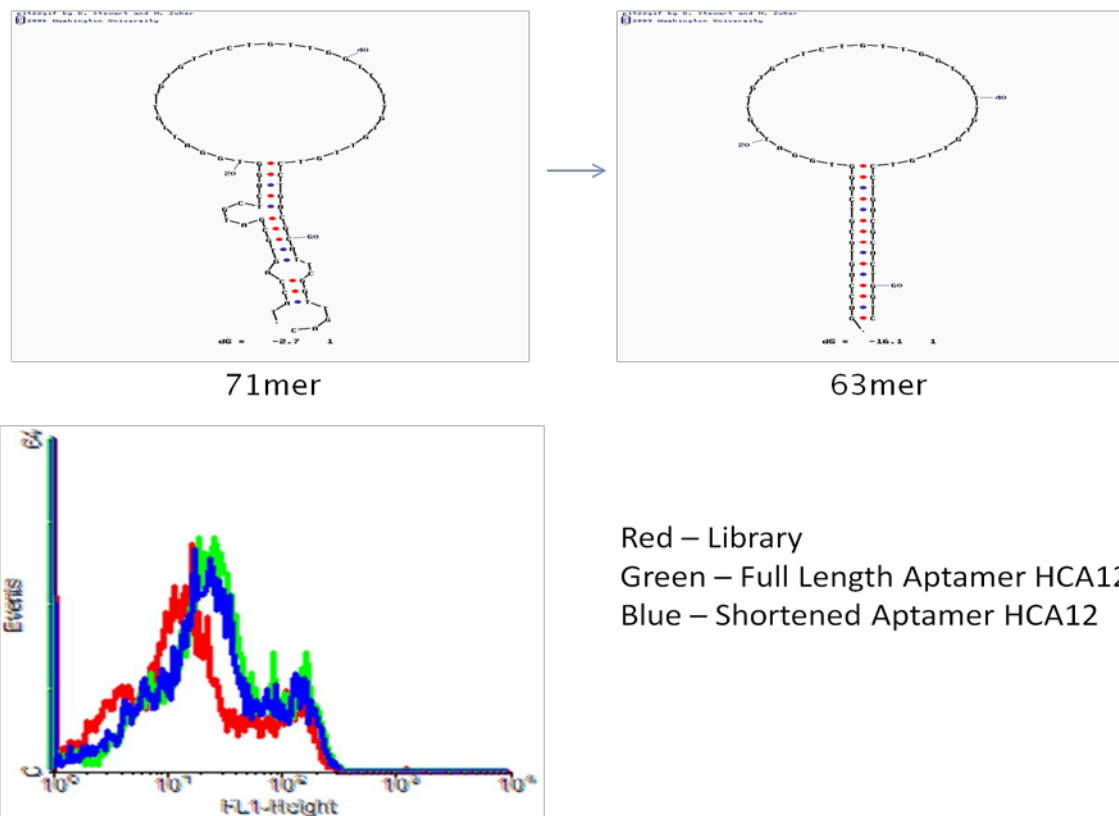


Figure 2-25. Minimal binding motif study of aptamer HCA12. The full length aptamer HCA12 has a hair-pin structure with some small loops in the stem region. The aptamer was shortened and modified by removing the small loops and adding perfect base pairing in stem region. The binding ability was retained by the shortened aptamer.

Competition Study of Selected Aptamers

In order to further confirm that the selected aptamers can bind to target cells specifically, we designed and performed competition experiment. The principle of competition experiment is to have 2 species compete with each other for binding with target cells. The two competitors were labeled with two dyes with different colors, or one was labeled and the other was non-labeled. From the competition experiment results we can tell whether the probe can bind to the target. In the experiments, FITC and TAMRA labeled aptamer HCH07 were prepared. And non-labeled HCH07 was used as the competitor. First, target cells were incubated with dye labeled aptamers, and prominent binding can be observed. For comparison, target cells were incubated

with 100X excess non-labeled aptamer before incubated with dye labeled aptamers. As shown in Figure 2-26, the dye labeled aptamers couldn't compete off the non-labeled aptamers, which suggested that aptamer HCH07 did bind to the target cells specifically.

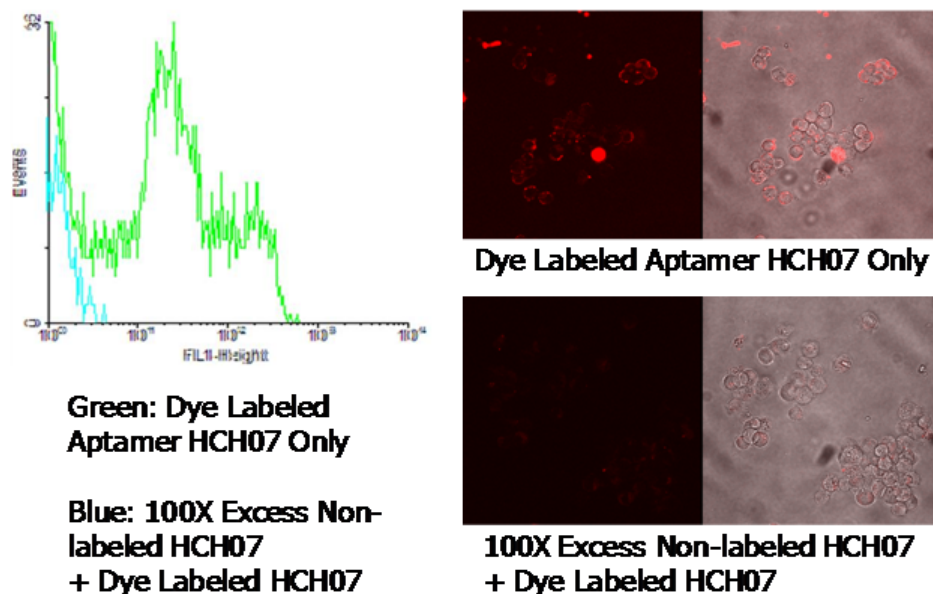


Figure 2-26. Flow cytometry and fluorescence confocal imaging results of competition study of aptamer HCH07. 100X excess non-labeled aptamers were incubated with target cells before incubation with dye labeled aptamers.

Conclusions

We have developed a panel of aptamer probes with specificity to SCLC cells by using cell based SELEX. SCLC was chosen as the model system for its worst prognosis among all lung cancer subtypes. The molecular differences among different types of cells resulted in the evolution of specific aptamer probes. Aptamers developed in this way specifically recognize SCLC cells, whereas NSCLC cells are not recognized. The target molecules of these aptamers are therefore reasoned to be preferentially expressed in SCLC. The interaction between aptamers and their target molecules were further characterized and confirmed. We found that aptamers were indeed binding to their target molecules on cell surface, and this interaction could be

affected by treating cells with protease. Moreover, it was proved that cell based SELEX strategy can be used as an effective tool to select molecular probes for specific SCLC recognition. The method can be used for both cell suspensions as previously demonstrated and cell aggregates, the typical morphology of SCLC.

CHAPTER 3 VALIDATION OF APTAMERS FOR LUNG CANCER RECOGNITION

Introduction

Early detection and local therapy are believed to reduce the overall mortality related with lung cancer, especially SCLC by halting or reversing the progression of premalignant lesions at early stage. Although various imaging based methods have been described for early detection, most of these methods delivered limited effect on the cancer mortality due to their relatively low sensitivity. To improve this situation, molecular approaches were exploited for early detection by detecting specific molecular markers. However, these molecular-marker based techniques also showed unsatisfactory results. For example, among more than 100 monoclonal antibodies for SCLC and NSCLC, none of their antigens are exclusively expressed in SCLC samples.^[130] Therefore, the antibodies used for lung cancer early detection do not have the specificity, and may cross react with normal, mildly atypical, moderately atypical exfoliated epithelial cells, and even normal bronchial epithelium. Additionally, the availability of antibodies is limited to those characterized in previous studies.

By using the new established cell based SELEX approach, we developed aptamers that show great specificity for SCLC but not NSCLC. These aptamers were generated based on the molecular differences between the two subtypes of lung cancer. Although these aptamers show great potential for real clinical applications, they are required to be further validated with more different samples and various assay formats. After the validation, the specificity of these aptamers needs to be further studied to check whether it would eventually prevent cross-reactivity and generate fewer false positives in actual early detection tests.

In this chapter, the selected aptamers were tested with different lung cancer samples ranging from cultured cancer cell lines to clinical samples. Their usefulness in different assay

formats was evaluated, including flow cytometry, fluorescence confocal imaging, and tissue arrays. In addition, the function of aptamers in complex biological environment was also assessed.

Methods and Materials

Chemicals and Reagents

DNA synthesis reagents and DNA labeling reagents (FITC phosphoramidite and TAMRA phosphoramidite) were purchased from Glen Research (Sterling, VA). Ammonium hydroxide, TEAA, ethanol, and solvents for DNA synthesis and HPLC purification were purchased from Fisher Scientific. Formaldehyde, agarose, PBS buffer were purchased from Fisher Biotech. All other chemicals were purchased from Sigma–Aldrich and Fisher Scientific.

In flow cytometry experiments, washing buffer was prepared by dissolving glucose (4.5 g/L), MgCl₂ (5 mM), and bovine serum albumin (1 mg/mL) in Dulbecco's PBS (pH 7.3). Yeast tRNA (0.1 mg/mL) was added in washing buffer to prepare binding buffer to minimize the nonspecific binding effect.

Sodium heparin stabilized human whole blood (IPLA-WB1) was purchased from Innovative Research, Inc.

Cell Culture

NCI-H69 (small-cell carcinoma), NCI-H146 (small-cell carcinoma), NCI-H128 (small-cell carcinoma), NCI-H661 (large-cell carcinoma), NCI-H23 (adenocarcinoma), NCI-H1385 (squamous-cell carcinoma), CCRF-CEM (T-cell acute lymphoblastic leukemia), and Ramos (B-cell human Burkitt's lymphoma) cells were purchased from American Type Culture Collection (ATCC), and maintained at 37°C and 5% CO₂ in RPMI 1640 medium supplemented with 10% heat-inactivated fetal bovine serum (FBS) and penicillin–streptomycin (100 IU/mL). IMEA (liver cancer) and BNL (liver cancer) cells were obtained from the Department of Pathology at

the University of Florida. All cells were cultured in 75 cm² cell flasks. To use cell aggregates for binding experiments, mechanical method and non-enzymatic dissociation reagent were used to break the cell aggregates to single cells for easy handling and minimizing the multi-cell effect on binding results. To use adherent cells for binding experiments, non-enzymatic dissociation reagent was used to detach the cells.

Cell Blocks and Tissue Arrays

Cultured SCLC and NSCLC cell lines were processed into homogeneous cell blocks to evaluate the binding of aptamers to fixed cells. All cell blocks were prepared in the University of Florida Diagnostic Reference Laboratories. 10×10⁶ cells grown in culture were first prepared as cell suspension in minimal amount of medium (adherent cells were detached by trypsin-EDTA treatment first). Cells were then fixed with 4% formaldehyde, and mixed with 1% agarose in isoosmotic PBS. The solidified cell blocks were cut into serial sections and processed on paraffin-embedded slides. Prepared cell blocks were stained with hematoxylin and eosin (H&E) for quality control.

Tissue arrays were purchased from US BioMax. Lung small cell carcinoma tissue array (LC802) contains 35 different small cell lung cancer samples with 2 replicates, 2 tumor adjacent normal and 3 non-malignant normal lung samples with 2 replicates, total 80 cores on one slide. Lung carcinoma multi-tissue combined tissue array (LC803) contains various lung cancer samples including 80 different small cell lung cancer and non-small cell lung cancer samples, total 80 cores on one slide.

Flow Cytometry

To test the binding of aptamers with various cancer cells including small cell lung cancer, non-small cell lung cancer, leukemia, and liver cancer, FITC labeled aptamers and library were incubated with 1×10⁶ cells in 400 μL binding buffer at 4°C for 30 minutes. Cells were then

washed twice and analyzed by flow cytometry. Flow cytometry was performed on a FACScan cytometer controlled by CellQuest software. The binding of selected aptamers to SCLC cells, NSCLC cells, leukemia cells, and liver cancer cells was analyzed by the WinMDI 2.9 software.

Fluorescence Confocal Imaging

The staining of cell blocks and tissue arrays by selected aptamers was evaluated by fluorescence confocal imaging. Fluorescence confocal imaging was performed on a Fluoview 500/IX81 inverted confocal scanning microscope system (Olympus). A 5-mW, 543-nm He-Ne laser was used as excitation source for TAMRA dye. The objective used for imaging was a 60× oil-immersion objective (PLAPO60XO3PH) with a numerical aperture of 1.40 (Olympus). A 20× objective with a numerical aperture of 0.7 (Olympus) was also used for imaging of large field. Images were taken after a five to ten second period during which the instrument was focused to yield the highest intensity from the fluorescence channels.

Array Scanning

For staining of cell blocks and tissue arrays, slides were first treated with xylene and ethanol (100%, 95%, and 70%) for deparaffinization. For antigen retrieval, the dried cell blocks and tissue arrays were rinsed with PBS and kept in 1 mM EDTA Tris buffer (pH 8.0) at 95°C for 15 minutes. Cell blocks and tissue arrays were then incubated with 200 μ L of 0.25 μ M TAMRA labeled aptamers in binding buffer at 4°C for 30 minutes. After washing and dehydration, the stained slides were mounted for evaluation. Aptamer stained cell blocks and tissue arrays were analyzed by array scanning and by confocal imaging. For the array scanning, the stained slides were scanned into a computer with a microarray scanner (2100 BioAnalyzer, Agilent) at 10 μ m scan resolution, and analyzed using Agilent G2567AA Feature Extraction software (v.9.1).

Results and Discussion

Validation of Aptamers with Various Cancer Cells

Several aptamers for small cell lung cancer were identified by using cell based SELEX. Before tested with clinical samples, their specificity needs to be further proved. Thus, we assessed the applicability of developed aptamer probes to other cultured SCLC cell lines (i.e., to validate the target molecules of developed aptamers as exclusive markers for SCLC). NCI-H146 and NCI-H128 were chose for validating aptamers for small cell lung cancer. These two cell lines have similar cell characteristics as NCI-H69, the target cell used in cell based SELEX. FITC labeled aptamers HCA12, HCC03, HCH07, and HCH01 were tested with these two cell lines by flow cytometry. Almost all the aptamers can specifically bind to these small cell lung cancer cells. These results indicate that selected aptamers have consistent binding pattern to all small cell lung cancer cells (Table 3-1).

In contrast to SCLC, two cultured NSCLC cells lines including NCI-H23 (adenocarcinoma) and NCI-H1385 (squamous cell carcinoma) of the same category as large cell carcinoma (the one used as control cell in cell based SELEX), were also tested with selected aptamers by flow cytometry. All these NSCLC cells did not respond to the selected aptamers except one case (aptamer HCH07 bound to NCI-H23) (Table 3-1). From the above results, the selected aptamers did show great specificity for all small cell lung cancer cells in addition to the one used in cell based SELEX experiment.

Moreover, other cancer types including two leukemia cell lines (CCRF-CEM, T cell acute lymphoblastic leukemia; Ramos, B cell human Burkitt's lymphoma) and two liver cancer cell lines (IMEA and BNL) were also tested with selected aptamers by flow cytometry. None of them could be recognized by these aptamers in most cases (Table 3-1). Interestingly, the aptamer that bound to adenocarcinoma NCI-H23 is also able to recognize liver cancer cell lines.

Table 3-1: Tests of developed aptamers with cultured cancer cell lines

Cultured cancer cell lines	Receptors	HCA12	HCC03	HCH07	HCH01
NCI-H69 (small cell carcinoma)	IGF II	+	+	+	+
NCI-H146 (small cell carcinoma, bone marrow)	IGF II	-	+	+	+
NCI-H128 (small cell carcinoma, pleural effusion)	N/A	+	+	+	+
NCI-H661 (large cell carcinoma, lymph node)	N/A	-	-	-	-
NCI-H23 (adenocarcinoma)	PDGF; TGF; EGF	-	-	+	-
NCI-H1385 (squamous cell carcinoma, lymph node)	N/A	-	-	-	-
CCRF-CEM (T cell acute lymphoblastic leukemia)	N/A	-	-	-	-
Ramos (B cell human Burkitt's lymphoma)	N/A	-	-	-	-
IMEA (liver cancer)	N/A	-	-	+	-
BNL (liver cancer)	N/A	-	-	+	-

Considering these cell lines were not used as control cell in cell based SELEX, there is still a chance for some of the selected aptamers to recognize them by the same target molecule SCLC has. This type of cross-reactivity is expected to be minimized by adding additional negative

selection criteria to cell based SELEX. Therefore, we concluded that the selected aptamers have specificity for small cell lung cancer, but not for non-small cell lung cancer and other types of cancer.

Cell Block and Tissue Array Tests

Besides the tests with live cancer cells, it is also interesting to see whether the aptamers developed from live cells can recognize fixed cells, which is the main assay format for retrospective analysis of preserved specimens such as sputum and biopsy in early detection studies. This will be useful for histological examination in the clinical diagnosis of lung cancer. We started with formalin-fixed, paraffin-embedded cell blocks and then tested commercial available tissue microarrays of clinical lung cancer samples (Figure 3-1).

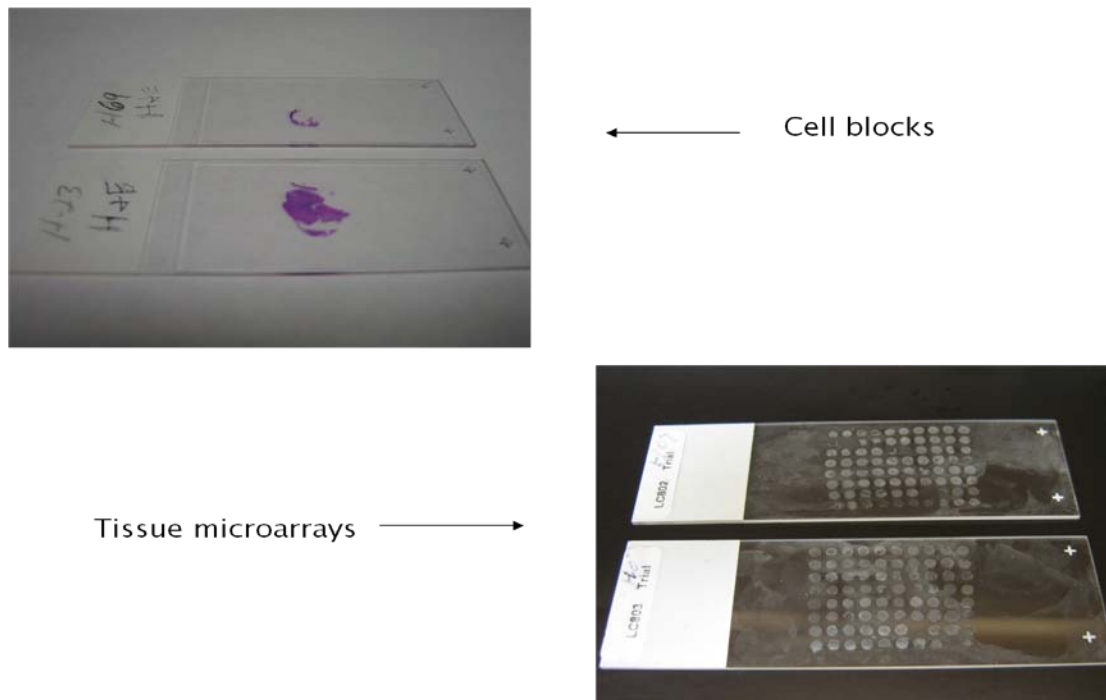


Figure 3-1. Cell blocks and tissue microarrays used for lung cancer aptamer validation.

First, formalin-fixed, paraffin-embedded cell blocks from SCLC and NSCLC samples were processed. Before the preparation of these cell blocks, the cells were tested with aptamers

by flow cytometry for quality control. TAMRA dye labeled aptamers were synthesized and used for slide staining experiments. After incubation with fluorescent dye labeled aptamers, washing, and dehydration, stained slides were mounted for array scanning and confocal imaging. Both the array scanning and confocal imaging results (Figure 3-2) showed that binding of aptamer probes was specific to all SCLC cell blocks including NCI-H69 (used as target cells in cell based SELEX) and NCI-H146. Only background level binding existed for NSCLC cell blocks including NCI-H661 (used as control cells in cell based SELEX) and NCI-H23. These data indicate that specific recognition of cell blocks by aptamers is dependent on the presence of cell surface markers, which are still biochemically active after fixing cells.

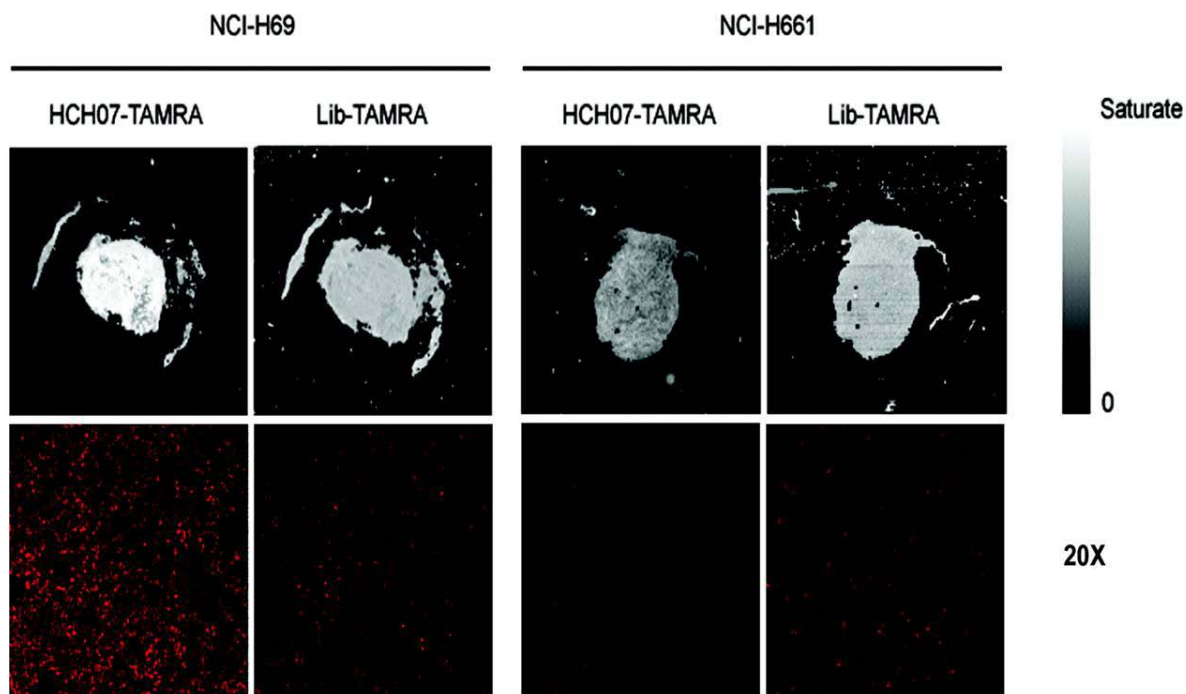


Figure 3-2. Specific binding of molecular aptamers to formalin-fixed, paraffin-embedded SCLC cell blocks. Sections of formalin-fixed SCLC and NSCLC cells embedded in paraffin were stained with TAMRA labeled aptamer and analyzed by array scanning and confocal imaging at 20× magnification. TAMRA labeled ssDNA library was used as a control.

As shown in magnified confocal microscopy image (Figure 3-3), most aptamers bound to the periphery of target cells. This binding pattern is similar to that observed in the tests of live cells, and further confirmed that aptamers indeed bound to their target molecules on fixed cells.

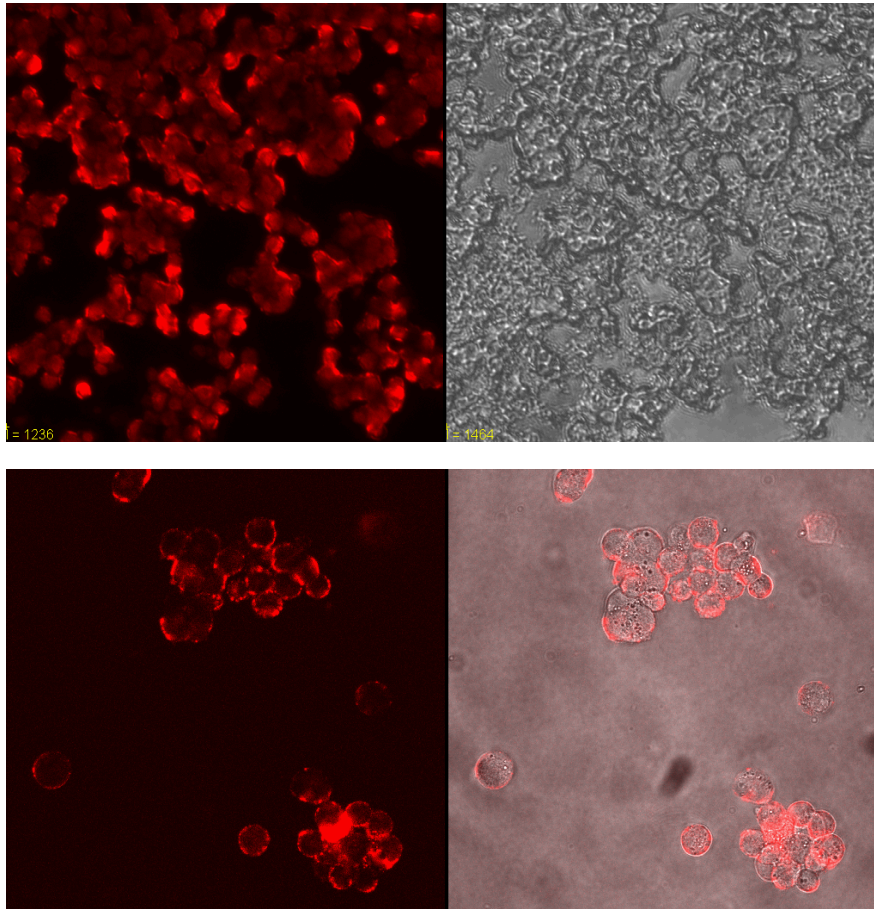


Figure 3-3. Recognition of SCLC fixed cells and live cells by fluorescent dye labeled aptamer. Fluorescent aptamer stained SCLC cell block shows similar binding pattern to live cells by magnified confocal imaging (60× magnification). Note the binding of fluorescent dye labeled aptamers to the periphery of fixed SCLC cells.

After we successfully proved the binding of selected aptamers with fixed cells in cell blocks, we moved to test the tissue microarray made from clinical lung cancer samples. Based on the positive results of cell block experiments, we expected to observe that the selected aptamers can distinguish the clinical sample in the format of tissue microarray. Commercially available

lung small cell carcinoma tissue microarrays containing 40 cases with duplicated cores per case were used for staining experiments with TAMRA dye labeled aptamers. Among the 40 cases, 35 cases are small cell lung carcinoma, 2 are tumor adjacent normal sample, and 3 are non-malignant normal lung tissue. The tissue microarrays were stained with dye labeled aptamers using the similar protocol as cell blocks, and analyzed by both array scanning and fluorescence confocal imaging. From the scanning results (Figure 3-4), we saw clear difference reflected by fluorescence signals between the same tissue microarrays stained with aptamer and DNA library. The tissue microarray stained by dye labeled aptamers showed statistically higher fluorescence signal than the tissue microarray stained by non-specific DNA library. Most of the cores on the positive slide showed strong fluorescence except the normal lung tissue cores used as controls on the same slide. In contrast, the cores on the negative slide maintained low level of average fluorescence signal, explained as not recognized by the DNA library.

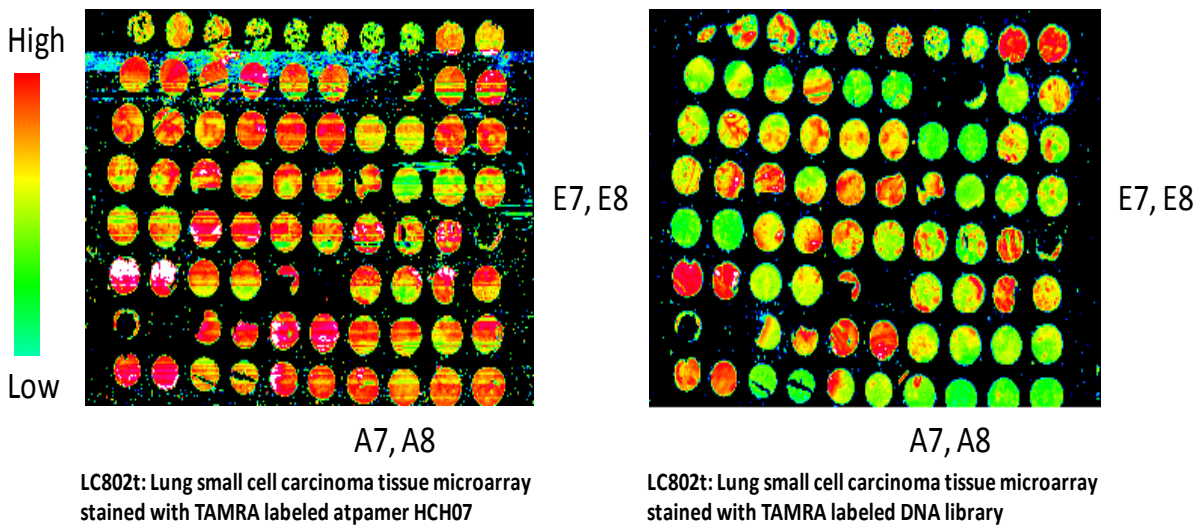


Figure 3-4. Aptamer staining of tissue microarrays. Lung small cell carcinoma tissue microarrays were stained with TAMRA labeled aptamer and TAMRA labeled DNA library. Stained arrays were analyzed by array scanning. Lung small cell carcinoma tissue microarrays contain 40 cases with duplicated cores per case. Among the 40 cases, 2 are tumor adjacent normal sample and 3 are non-malignant normal lung tissue (top row), 35 cases are small cell lung carcinoma (from 2nd – 8th row).

Even on the same slide, different cores showed different response to the aptamer staining. For example, core A7 (A8) had very high fluorescence signal after stained with aptamer while almost no fluorescence signal could be seen after stained with DNA library. But for core E7 (E8), they showed similar response to both aptamer and DNA library. The details of these cores on the tissue microarray were examined by fluorescence confocal imaging (Figure 3-5). As we can see, the core A7 (A8) (top) contains fixed small cell lung cancer cells binding with TAMRA labeled aptamers that give out strong fluorescence signal. In contrast, the cells in core E7 (E8) (bottom) were not stained or stained at a very low level. This is probably due to the subtle pathological difference between these two small cell lung cancer samples. It is well known that patients with even the same type of cancer may have very different clinical presentations. The selected aptamers may not have the ability to tell these subtle molecular differences at this time. However, these selected aptamers have the ability to distinguish some clinical cancer samples and the aptamers are suitable for the assay format of tissue microarray.

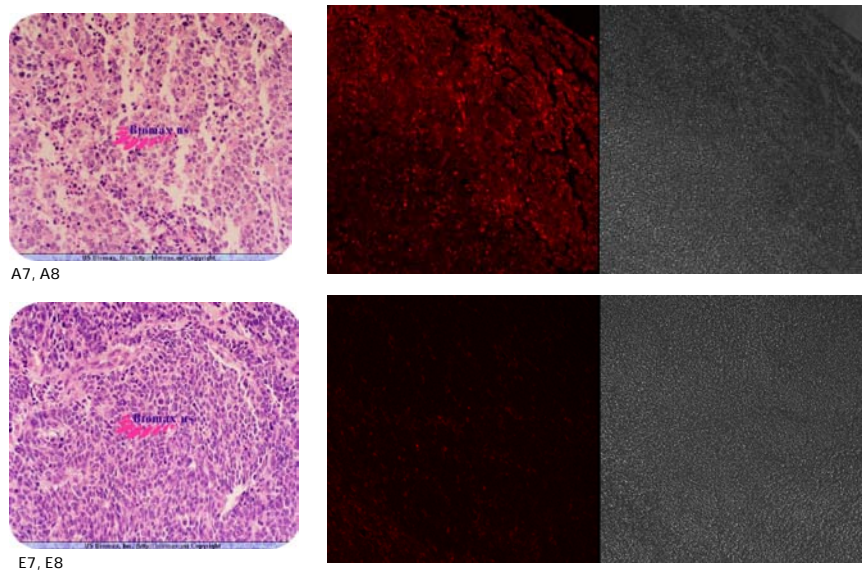


Figure 3-5. Fluorescence confocal imaging of core A7, A8 and core E7, E8 stained with TAMRA labeled aptamer. The left panel is the cell morphology pictures of core A7, A8 and core E7, E8 provided by Biomax.

Clinical Sample Tests

After the demonstration of aptamers on tissue microarray, we assessed the sensitivity and specificity of the aptamers for their ability to detect cancer cells in clinical sample from SCLC patient. SCLC patient samples were obtained from the Diagnostic Reference Laboratories at the University of Florida. The cells were washed and counted before experiments. Small cell lung cancer cells mixed with bone marrow from cancer patient were washed with binding buffer and incubated with FITC labeled aptamers. After washing, the cells were analyzed by flow cytometry as described before. Substantial change in fluorescence intensity was noticed in the SCLC patient sample after incubating with dye labeled aptamers, indicating that aptamers developed for cultured cells are able to recognize the cancer cells from SCLC patients (Figure 3-6).

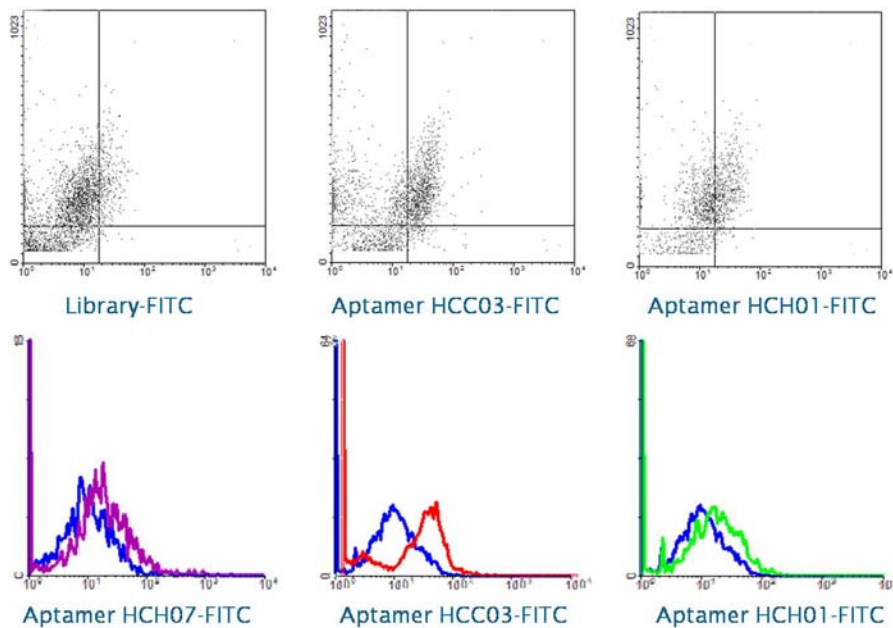


Figure 3-6. Recognition of SCLC cells in patient sample (T06-06195) with aptamers. Clinical samples from SCLC patient (T06-06195) were incubated with either FITC labeled ssDNA library or FITC labeled aptamers (HCC03, HCH01, and HCH07). Samples were then analyzed by flow cytometry. SCLC cells were identified in patient sample by aptamer probes. Flow cytometry results were shown in both dot plot format and histogram format.

For sample T06-06195, small cell lung cancer cells could be recognized by aptamer HCC03, HCH01, and HCH07.

In another patient sample (T6165), small cell lung cancers were also able to be recognized by aptamer HCA12 and HCH07 in the mixture with bone marrow and various blood cells, as shown in Figure 3-7. These results demonstrated the applicability of the selected aptamers to clinical samples, the prerequisite for successful detection of SCLC patient cells in complex biological matrix by the aptamers.

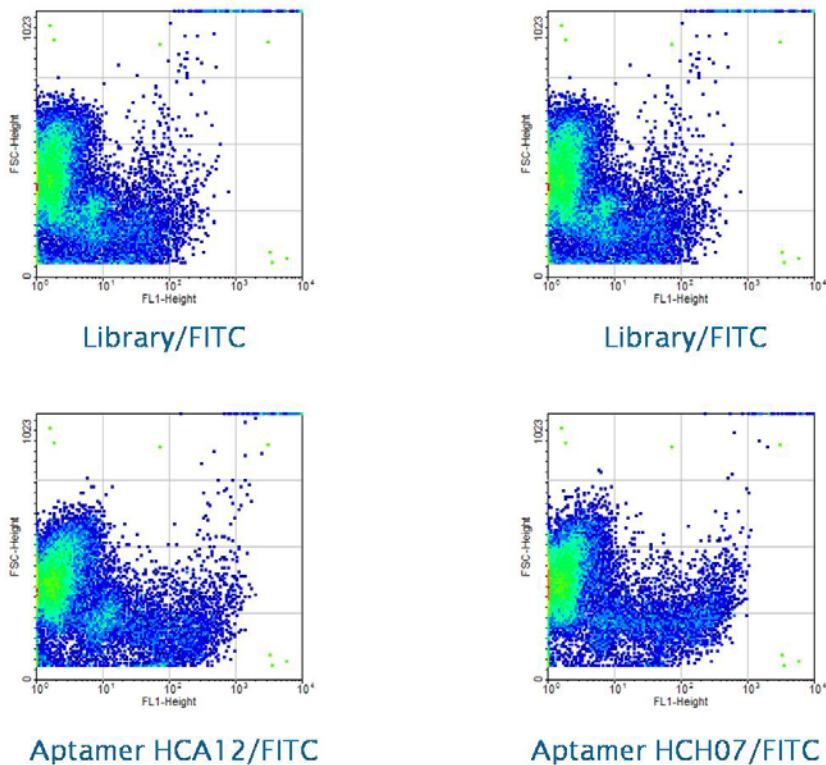


Figure 3-7. Recognition of SCLC cells in patient sample (T6165) with aptamers. Clinical samples from SCLC patient (T6165) were incubated with either FITC labeled ssDNA library or FITC labeled aptamers (HCA12 and HCH07). Samples were then analyzed by flow cytometry. SCLC cells were clearly identified in patient sample by aptamer probes. Flow cytometry results were presented in cell density format.

Detection of Lung Cancer Cells in Whole Blood

In addition to the tests with clinical samples, we sought to determine whether aptamers can retain the ability to specifically recognize SCLC cells in the human blood environment, another criterion for aptamers to be applied in clinical tests. To evaluate the binding capacity of aptamers in complex biological environment, 2×10^6 SCLC cells were prepared and mixed with 3.5 μL human whole blood (IPLA-WB1, Innovative Research, Inc.) in 300 μL of buffer. Human whole blood was prepared by mixing with the anticoagulant, sodium heparin. 100 μL of 1 μM FITC labeled aptamers was added to SCLC cells spiked in human whole blood. After incubation at 4°C and thorough washing, the binding of aptamers to SCLC cells in blood was assessed by flow cytometry. For controls, human whole blood and cells in buffer were incubated with aptamers and analyzed by flow cytometry. Background binding of aptamers to blood cells was negligible. In the mixture, the SCLC cells were gated out for data processing as shown in Figure 3-8, because the binding signal of small amount SCLC cells could be overwhelmed by the enormous amount blood cells. The processed flow cytometry data showed that the aptamers still can recognize the target cells in the blood (Figure 3-8).

Conclusions

Our expanded screening results showed that the aptamers generated for certain SCLC cell line are able to recognize other SCLC cell lines of the same type, but seldom bind to other subtypes of lung cancer as well as other types of cancer (e.g., leukemia and liver cancer). This suggests that the developed aptamer probes have the potential to be used practically with clinical samples. In addition, the aptamers developed from live cells can also recognize fixed cells, the main assay format for retrospective analysis of preserved specimens in early detection study, as well as histological examination in clinical diagnosis of lung cancer. Notably, these aptamers exhibited the same specificity for cancer cells from SCLC patients as they did with cultured

cells. In the complex biological environment such as human whole blood, this specific binding ability of aptamers was not compromised. These results indicate that developed aptamer probes could be practically used in clinical tests.

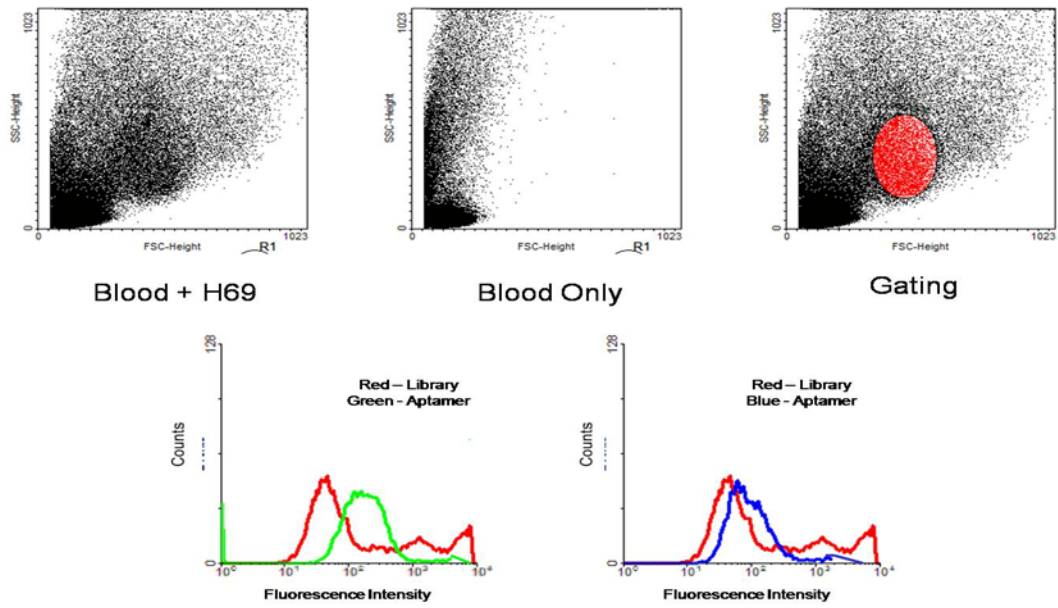


Figure 3-8. Flow cytometry data processing of aptamer binding to small cell lung cancer cells in human whole blood. Flow cytometry data processing (gating) and gated flow cytometry data of aptamer bound small cell lung cancer in blood were shown.

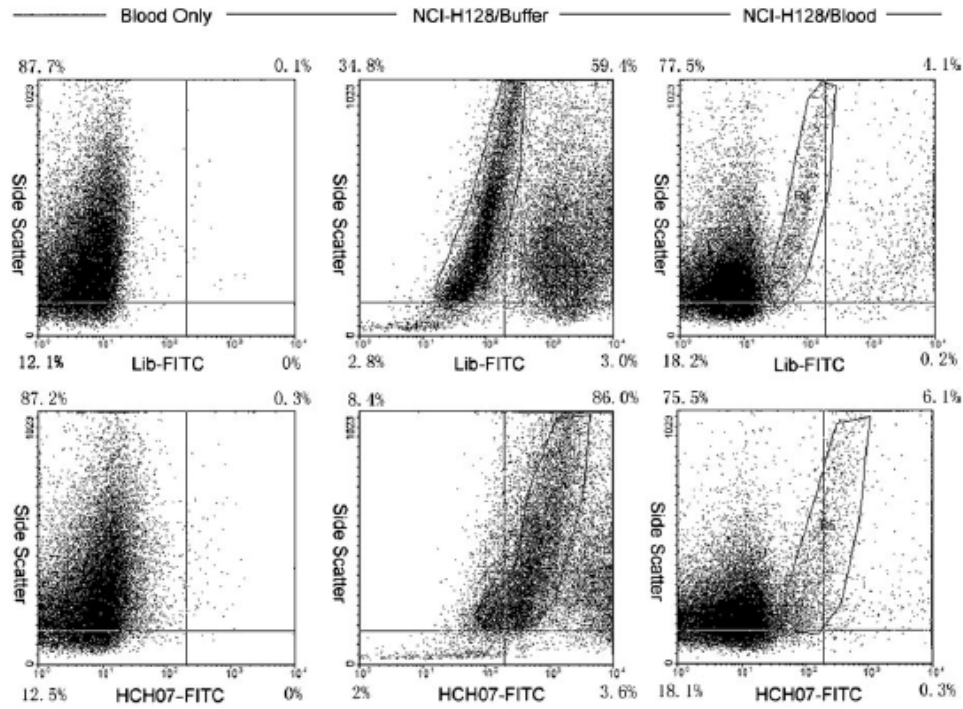


Figure 3-9. Recognition of SCLC cells in whole blood with molecular aptamers. In human whole blood, blood cells were incubated with FITC labeled aptamer and ssDNA library as a control for specificity. SCLC cells in buffer were incubated with FITC labeled aptamer and ssDNA library to compare with SCLC cells in whole blood as a positive control. The binding of aptamer to SCLC cells in human whole blood was also assessed. Circled regions are live SCLC cells. Aptamer retains the specificity to SCLC cells in human whole blood as determined by flow cytometry. No interference from blood cells was observed.

CHAPTER 4 EXTRACTION AND DETECTION OF LUNG CANCER CELLS WITH APTAMER CONJUGATED NANOPARTICLES

Introduction

After we successfully validated the usefulness of the aptamers selected from cell based SELEX, we continued to establish novel platforms for aptamer based assays and applications. One of the applications is using aptamer to detect and capture the trace amount of cancerous cells in human blood or other types of body fluid. In some types of cancers such as ovarian cancer and lung cancer, small amount of malignant cells will disseminate to different organs along with the blood stream, and these circulating cells may serve as the indicator of early stage cancer that is more curable than late stage cancer. For example, during the early stage of lung cancer, malignant lesions begin to shed circulating cells. Encoding valuable information for prognostic prediction, these exfoliated cells should be of great value for early lung cancer diagnosis. Previously, the enrichment and detection of rare exfoliated cells were mainly performed by flow sorting and immunomagnetic cell sorting, which suffered from low sensitivity and specificity.^{[131,}
^{132]} To evaluate the potential of the selected aptamers for early lung cancer detection, we prepared aptamer conjugated magnetic nanoparticles and aptamer conjugated fluorescent nanoparticles to isolate, enrich, and detect rare SCLC cells with a method previously established in our lab.^[133] This method involves the use of two types of aptamer-conjugated nanoparticles. The magnetic nanoparticles assists the capturing and extraction of target cells while the fluorescent nanoparticles help identify the cells captured by magnetic nanoparticles. This strategy is shown in Figure 4-1. This strategy not only provided a fast and easy way to isolate and detect the small amount cancer cells of interest with great sensitivity, but also improved the specificity by having two different binding events simultaneously. Only those cells binding with

both magnetic and fluorescent nanoparticles will be identified in the sample. The non-specific binding of DNA to cells can be significantly reduced by this approach.

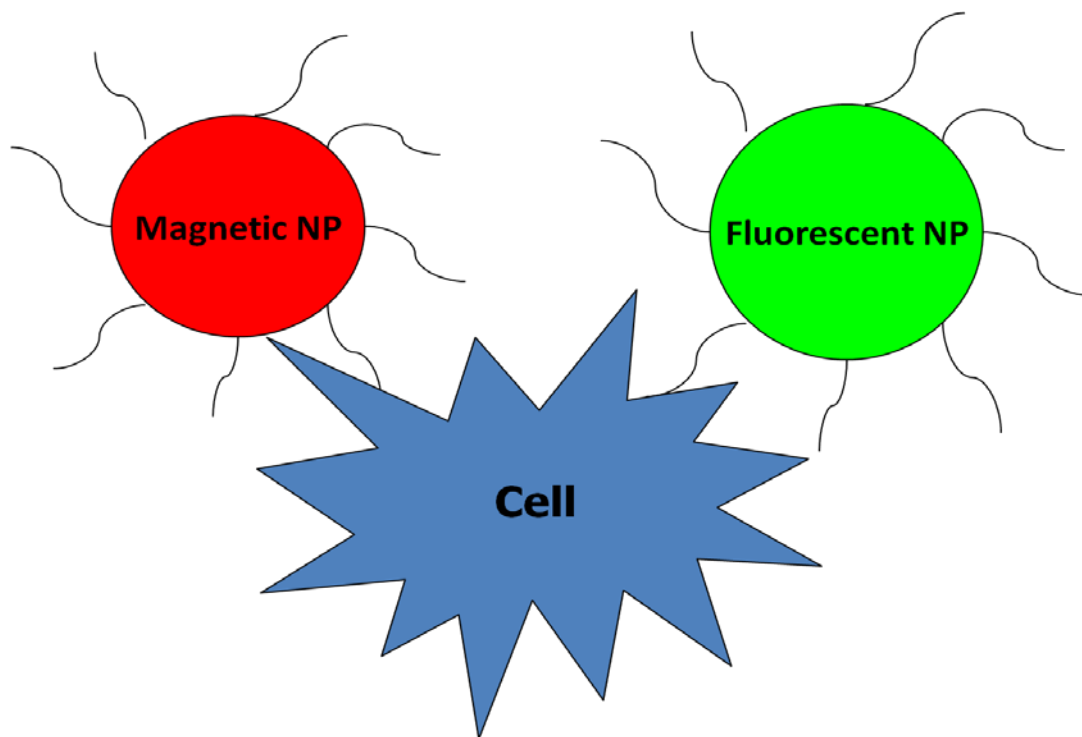


Figure 4-1. Scheme of extraction and detection of lung cancer cells with aptamer conjugated nanoparticles. In the assay, the magnetic (red) and fluorescent (green) nanoparticles bind to the target cell at the same time. Then a magnetic field is applied to immobilize the magnetic nanoparticles bound with the target cells and fluorescent nanoparticles while the unbound cells and fluorescent nanoparticles are washed away.

Methods and Materials

Cell Culture

NCI-H69 (small-cell lung carcinoma), NCI-H128 (small-cell lung carcinoma), and NCI-H661 (non-small cell lung carcinoma) cells were purchased from American Type Culture Collection (ATCC), and maintained at 37°C and 5% CO₂ in RPMI 1640 medium supplemented with 10% heat-inactivated fetal bovine serum (FBS) and penicillin–streptomycin (100 IU/mL). All cells were cultured in 75 cm² cell flasks. Before the experiments, small cell lung cancer cell aggregates were treated with mechanical method and non-enzymatic dissociation reagent to

length square quartz cuvette was used for absorption measurements. Then the product was titrated and suspended in buffer for experimental uses.

Fluorescent Nanoparticle Synthesis

For the synthesis of aptamer conjugated fluorescent nanoparticles, TAMRA dye doped nanoparticles were first prepared by the reverse microemulsion method as previously described.^[133] Tetramethylrhodamine (TMR) doped nanoparticles were synthesized with the following approach: TMR SE was dissolved in DMSO at a concentration of 5 mg/mL, and 3-aminopropyltriethoxysilane (APTS) was added at a molar ratio of 1.2:1 (APTS: dye). The APTS was allowed to react with the amine reactive dye for 24 h in the dark with shaking prior to synthesis of the particles. Glass reaction vessels and Teflon-coated magnetic stir rods were washed with 1 M NaOH solution for 30 min, rinsed with DI water and ethanol, and allowed to dry. This wash step was performed to clean the glass vessel and stir rods and smooth the inside surface of the glass vessel, which prevents unwanted seeding and NP formation. After conjugation, 4.19 mL of ethanol was mixed with 239 μ L of ammonium hydroxide solution in the reaction vessel. A 36 μ L volume of TMR-APTS conjugate was added to the reaction vessels, yielding 3.44×10^{-7} mol of dye/reaction (ratio of 2300 mol of silica/mole of dye). A 177 μ L volume of TEOS was added rapidly to the reaction mixture, and the vessels were sealed. The reaction was allowed to proceed for 48 hours in the dark before the particles were recovered by centrifugation at 14000 rpm. The particles were washed three times with phosphate buffer to remove any dye molecules that are weakly bound. The synthesis method was found to reproducibly produce fluorescent nanoparticles with average particle size of $50 \text{ nm} \pm 5 \text{ nm}$ with a monomodal distribution, as measured by a Honeywell UPA 150 dynamic light scattering instrument. After silica polymerization and stabilization treatment with TEOS, the dye doped

nanoparticles were coated with avidin as detailed below. Avidin coated dye doped nanoparticles were further conjugated with excess biotinylated DNA aptamers and ssDNA library.

Magnetic Nanoparticle Synthesis

For the synthesis of aptamer conjugated magnetic nanoparticles, the 65-nm iron oxide doped magnetic nanoparticles were first prepared by precipitating iron oxide as previously described.^[133] The iron oxide core magnetic nanoparticles were prepared by means of precipitating iron oxide by mixing ammonia hydroxide (2.5%) and iron chloride at 350 rpm using a mechanical stirrer (10 minutes). The iron chloride solution contains ferric chloride hexahydrate (0.5 M), ferrous chloride tetrahydrate (0.25 M), and HCl (0.33 M). After three washes with water and once with ethanol, an ethanol solution containing ~1.2 % ammonium hydroxide was added to the iron oxide nanoparticles, yielding a final concentration of ~7.5 mg/mL. The magnetite core particles were then coated with silica by the hydrolysis of tetraethoxyorthosilicate, and treated with TEOS. To create the silica coating for the magnetite core particles, 200 μ L tetraethoxyorthosilicate was added, and the mixture was sonicated for 90 minutes to complete the hydrolysis process. For post coating, an additional aliquot of 10 μ L TEOS was added and additional sonication was performed for 90 minutes. The resulting nanoparticles were washed three times with ethanol to remove excess reactants.

Conjugation of Aptamers with Nanoparticles

The prepared fluorescent and magnetic nanoparticles were then further modified with functional groups to react with DNA library and aptamers. We used the avidin/biotin strategy for the conjugation of aptamer with nanoparticles. After washing the synthesized nanoparticles, avidin coating was performed by incubating 0.1 mg/mL nanoparticle solution with 5 mg/mL avidin solution at 4°C for 12 hours. The avidin coated nanoparticles were then washed with PBS, and stabilized by crosslinking with 1% glutaraldehyde at 25°C for 1 hour. After washing with

Tris-HCl buffer, the 0.2 mg/mL avidin coated nanoparticles were incubated with excess biotinylated DNA aptamers and ssDNA library at 4°C for 12 hours. The prepared aptamer conjugated nanoparticles were washed and stored at a final concentration of 0.2 mg/mL for magnetic nanoparticles and 10 mg/mL for fluorescent nanoparticles at 4°C for use.

Fluorescence Confocal Imaging

Detection of target cells captured by magnetic nanoparticles and illuminated by fluorescent nanoparticles was performed on an Olympus IX-81 automated fluorescence microscope with a Fluoview 500 confocal scanning unit. The TMR dye doped nanoparticles were excited at 543 nm and collected at 570 nm. Images were taken after a five to ten second period during which the instrument was focused to yield the highest intensity from the fluorescence channels.

Plate Reader Measurements

Fluorescence measurements were also performed by plate reader in our lab. A Tecan Safire Microplate Reader was used to measure the fluorescence in a 384 well small volume plate. 20 μ L aliquots from each sample were deposited in each well and the fluorescence signals in each well at defined wavelengths were measured at a constant gain at 5 nm slit widths. TMR dye doped nanoparticles were excited with 550 nm light source and the emission was collected at 575 nm.

Results and Discussion

Aptamer Conjugated Nanoparticle Assay Development

We successfully synthesized both fluorescent and magnetic nanoparticles using the previously developed methods. The nanoparticles were then functionalized with aptamers on the surface. The extraction and detection assay using aptamer conjugated fluorescent and magnetic nanoparticles was first tested for proof of concept. The key step in this experiment is to assure that the aptamer conjugated nanoparticles truly bind to the target cells, but not control cells, and the nanoparticle bound cells can be extracted and identified in the assay. To demonstrate this

method, small cell lung cancer NCI-H69 and non-small cell lung cancer NCI-H661 were used as the model system using the following described protocol, and analyzed by confocal imaging and plate reader.

For every experiment, 1.0×10^5 cells were prepared and dispersed in 200 μL of cell media buffer. The specified amount of aptamer conjugated magnetic and fluorescent nanoparticles was then simultaneously added to the cell suspension. After 30 minute incubation and washing, cells were isolated from cell media buffer by magnetic extraction, and recovered in 20 μL of buffer for confocal imaging and fluorescence measurement. A 2 μL aliquot of the extracted sample was assessed by confocal imaging as described before. The rest of samples were then added to 96-well plate, and the fluorescence of dye doped nanoparticles bound to extracted cells was measured by a plate reader. Figure 4-2 (A) shows a representative confocal image of extracted target cells which are illuminated by fluorescent nanoparticles. In contrast, Figure 4-2 (B) shows the results of the control cells after the extraction.

The confocal imaging results showed clear difference of amount of cells extracted between the target cells and control cells. This assay can extract large amount of target cells while only a few control cells got extracted. In addition, these control cells carry no or very low fluorescent signal, which means that they were nonspecifically binding to magnetic nanoparticles, and not binding to fluorescent nanoparticles. Therefore, the advantage of using two types of aptamer conjugated nanoparticles in one assay can prevent the false positive results in an effect way, which is important in real clinical practice.

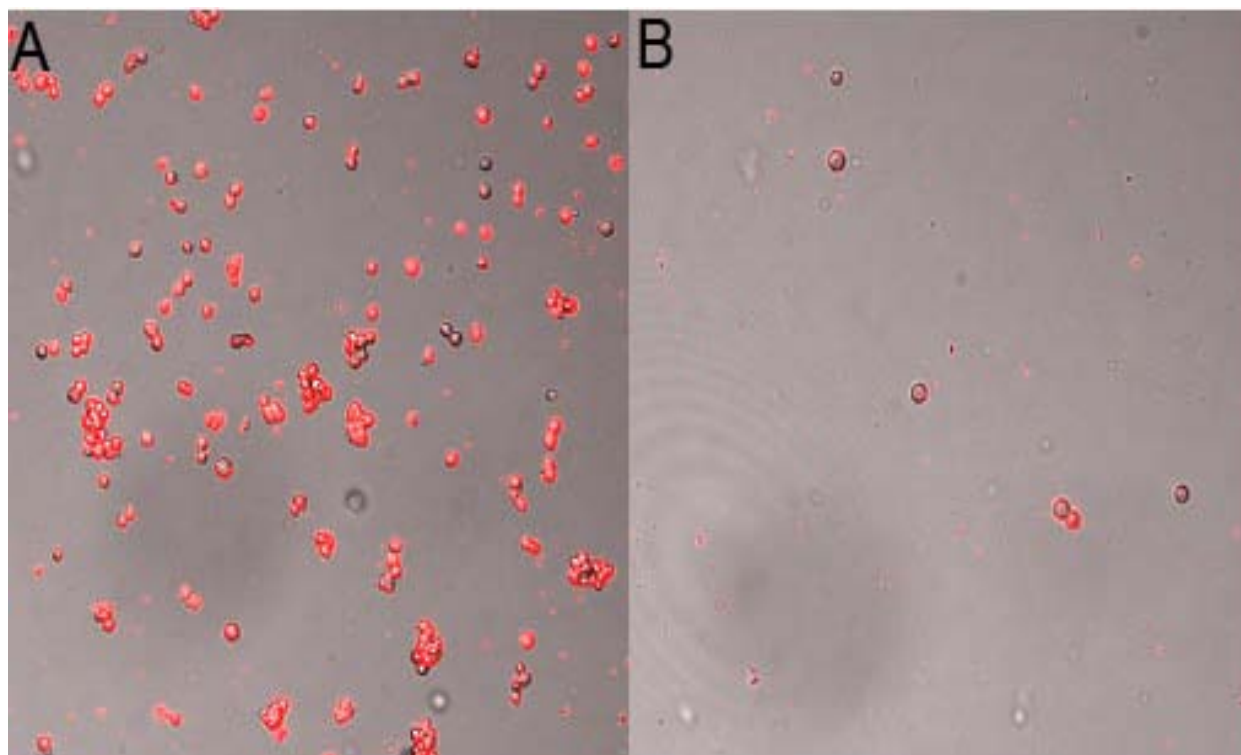


Figure 4-2. Confocal images of extracted target cells. A) Target cells after incubation with aptamer conjugated magnetic and fluorescent nanoparticles. B) Control cells.

Characterization of Extraction and Detection Assay

After successfully demonstrated the proof of concept, we continued to test more samples and characterize the assay results. Small cell lung cancer NCI-H69, NCI-H128, and non-small cell lung cancer NCI-H661 were tested separately with aptamer conjugated magnetic and fluorescent nanoparticles. ssDNA library conjugated magnetic and fluorescent nanoparticles were used for control experiments. The spiked tumor cells were first incubated with aptamer conjugated magnetic and fluorescent nanoparticles. Magnetic nanoparticle bound cells were then isolated by magnetic separation. After recovery, we measured the fluorescence of the dye doped nanoparticles, which also bound to the isolated cells through aptamers. Whereas two different types of SCLC cells were effectively isolated and detected, the extraction of NSCLC cells was inefficient (Figure 4-3). Additionally, low background fluorescence signal was observed in the

control experiment using DNA library conjugated nanoparticles, suggesting that nonspecific extraction of tumor cells is rare with this method.

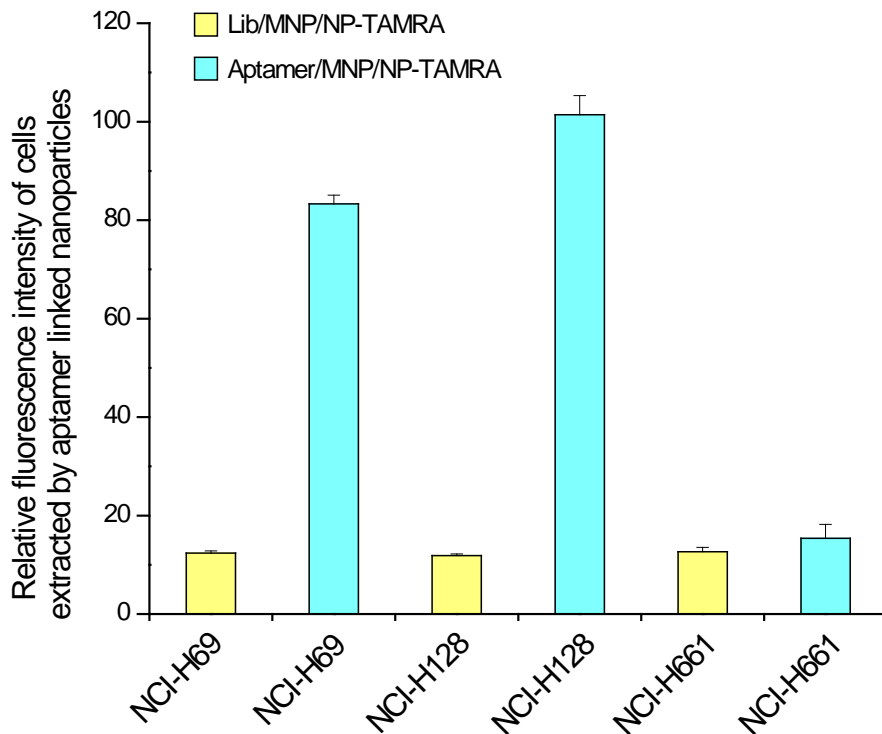


Figure 4-3. Extraction and detection of SCLC cells for enrichment and early diagnosis with aptamer conjugated magnetic/fluorescent nanoparticles. Same amount of the spiked SCLC (NCI-H69 and NCI-H128) and NSCLC (NCI-H661) cells were incubated with aptamer conjugated magnetic and fluorescent nanoparticles. Aptamer bound cells were subsequently isolated by magnetic separation. Total extracted cell amount after magnetic separation was determined by measuring the fluorescence signal of dye doped nanoparticles that also bind to cells. Aptamer conjugated nanoparticles effectively extracted SCLC cells but not NSCLC cells (cyan). ssDNA library conjugated nanoparticles were used in control experiments and showed only limited non-specific extraction of tumor cells (yellow).

Effective enrichment and detection of SCLC cells were verified by confocal imaging results, which showed that the extracted tumor cells were indeed binding to aptamer conjugated nanoparticles (Figure 4-4). Moreover, the dye doped nanoparticles confer great sensitivity to the detection of extracted tumor cells. Therefore, this aptamer conjugated nanoparticle approach

demonstrated its capability to enrich and detect rare lung cancer cells, which is critical for early diagnosis of lung cancer.

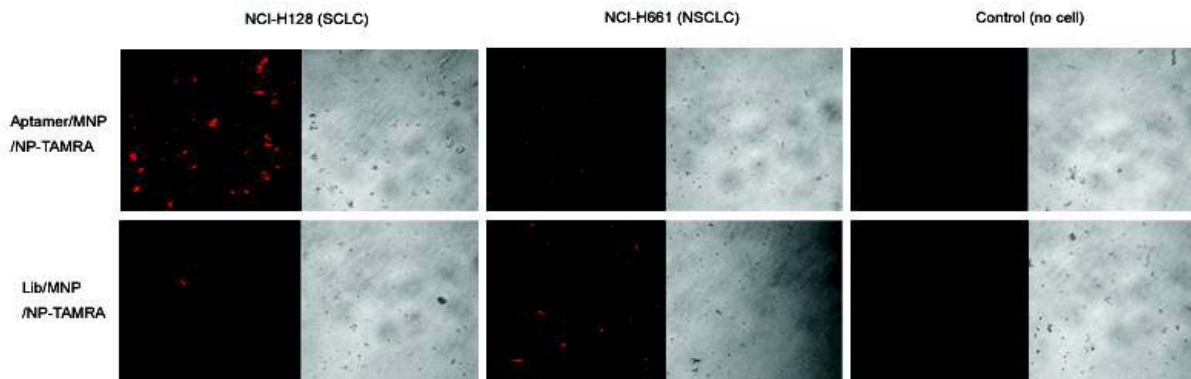


Figure 4-4. Confocal imaging of cells extracted by aptamer conjugated nanoparticles and ssDNA library conjugated nanoparticles. Extraction and detection of SCLC cells with this aptamer based approach were verified.

To further confirm that the aptamer conjugated nanoparticles truly bind to the cells, we examined the binding details with confocal imaging, and compared the binding pattern of nanoparticles with cells to that of aptamers only with cells. Figure 4-5 shows that the aptamer conjugated nanoparticles bind to the target cell surface in a similar way as the dye labeled aptamers bind to the target cell surface. In contrast, no binding can be observed for DNA library and DNA library conjugated nanoparticles. These results again confirmed the effectiveness of this extraction and detection assay using magnetic and fluorescent nanoparticles.

Conclusions

In this study, we tested aptamers for possible application in lung cancer early detection, particularly enrichment and detection of exfoliated tumor cells, by using aptamer conjugated magnetic nanoparticles and fluorescent nanoparticles. The high affinity and great specificity of aptamers resulted in effective extraction of SCLC cells by magnetic separation, and the dye doped nanoparticles provided the sensitive detection after cell extraction. Thus, the aptamer

conjugated nanoparticle strategy may substantially improve the efficiency of detecting circulating tumor cells; thereby potentially benefit the early detection of lung cancer.

Target Cells

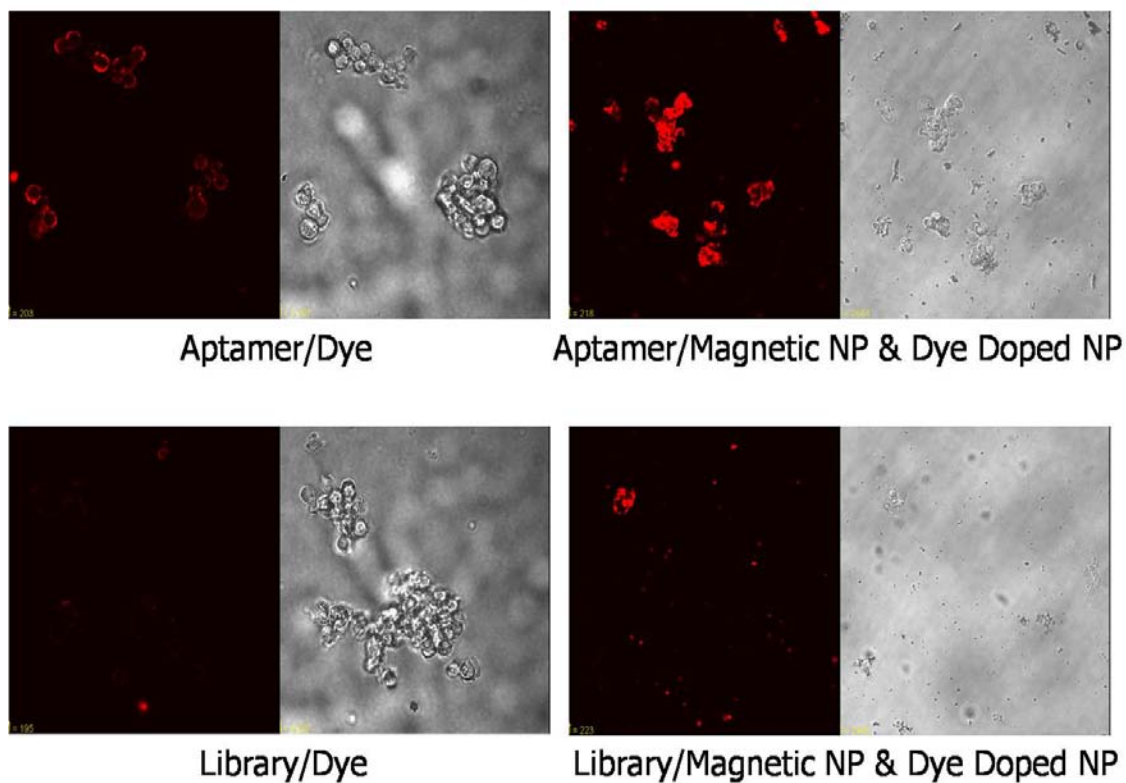


Figure 4-5. Comparison of binding pattern with target cells between dye labeled aptamer and aptamer conjugated nanoparticles. Dye labeled library and library conjugated nanoparticles were used as control.

CHAPTER 5
APTAMER-PCR ASSAY FOR CANCER CELL DETECTION USING APTAMERS FROM
CELL BASED SELEX

Introduction

During the past few decades, the rapid development of molecular sensing systems has resulted in diversified platforms for both basic biomedical studies and advanced bioanalytical applications. Generally, molecular sensing systems are composed of molecular recognition elements and signal transduction mechanisms. To achieve specific detection, different biological molecular recognition elements have been exploited, among which aptamers are more applicable than others for the design of bioanalytical sensors and can be developed for almost any target molecules. For example, the aptamers developed from cell based SELEX have great specificity and affinity for various cancer cells. Aptamers are easily synthesized, and are suitable for biomedical applications in undesirable conditions.

Meanwhile, effective diagnosis, therapy, and prevention of diseases require the understanding of diseases at the molecular level. Particularly for the diagnosis of cancer, accurate and simple assays are indispensable. Assays currently used for cancer diagnosis are mostly based on genetic characteristics instead of proteomic characteristics, and are complicated and insufficient for clinical practices. For example, detection of mRNA copies of cancerous gene is a widely used way for cancer diagnosis. Regardless of its high sensitivity, it is very difficult to quantify the amount of the rare cancer cells in the sample, which is very important for early diagnosis of certain types of cancer. Also, it requires additional pre-treatment procedure to isolate mRNA from cancer cells, which is time consuming. Recently, novel assays targeting cancer related proteins were developed. Immuno-PCR assay is an assay based on antibody recognition of cancer biomarker proteins. It has comparable sensitivity as real-time PCR

detection of mRNA. However, this method requires the conjugation of antibody with reporter DNA sequences, and this assay is limited by the lack of well-defined cancer biomarker proteins and specific antibodies to recognize and identify them. In addition, it is difficult to quantify the cancerous cells because this assay is mainly targeting excreted proteins other than the cells.

By using the aptamers developed from cell based SELEX, we developed a novel assay for detection and quantification of rare cancer cells. In this aptamer-PCR assay, the aptamers purposely selected for certain cancer cells showed great specificity as well as sensitivity with the help of certain signal transduction mechanisms such as real-time PCR and proximity dependent ligation reactions. The aptamers are not only the binders but also the reporters in this assay. They bind to the cancer cell surface and serve as the signaling molecules in the real-time PCR reaction. The aptamer bound cancer cells can be easily quantified in this way. It is simple and no pretreatment procedure is required. More importantly, for any type of cancer cells of interest, aptamers can be readily developed and used for this assay. This advantage from cell based SELEX significantly improved the applicability of this assay. Previously, it was very challenging to discover enough cancer biomarker proteins for detection purposes due to the limits of current biomarker discovery techniques, even though cancer diagnosis by recognition of molecular signatures is relatively simple and direct. Now with the help of this efficient and reliable method to develop specific aptamer probes for cancer biomarkers without prior knowledge, the new assay is expected to exhibit its potential in real application of cancer diagnosis.

Methods and Materials

Cell Culture

CCRF-CEM (T-cell acute lymphoblastic leukemia), and Ramos (B-cell human Burkitt's lymphoma) cells were purchased from American Type Culture Collection (ATCC), and maintained at 37°C and 5% CO₂ in RPMI 1640 medium (ATCC) supplemented with 10% heat-

Primers: 5'-primer (5' ATACCAGCTTATTCAATT3'); 3'-primer (5' AGATTGCACTTACTATCT3')

Aptamer SGC8 (88mer) with K_d of 0.80 nM selected in cell based SELEX against CCRF-CEM cells was used as lead probe in the experiment selecting paired aptamers for proximity dependent ligation reaction. Based on the minimal binding motif study results, a shortened version of SGC8 (61mer) with K_d of 0.62 nM was used in place of the full length SGC8. To serve as lead probe, it was extended with a 10 base spacer and 18 base hybridization region including Apa I enzyme recognition site.

Lead probe:

5'ACACTTAGAGTTCTAACTGCTGCGCCGCCGGGAAAATACTGTACGGTTAGATAGTAAGTGC3'

ssDNA library used for paired aptamer selection contains a randomized sequence of 35 bases, a 10 base spacer, a 18 base hybridization region for lead probe/forward primer binding site, a reverse primer binding site, as well as a 8 base coding region.

ssDNA library:

5'TGTTCTGGGCCCTTCGTGAAAAAAAAAATTACCTTANNCTATCCGCTCGCATACTC3'

A fluorescein isothiocyanate (FITC) labeled 5'-primer (5'FAM-TGTTCTGGGCCCTTCGTG3'); and a triple biotinylated (trB) 3'-primer (5'trB-GAGTATGCGAGCGGATAG3') were used in the PCR reactions for the amplification of double-labeled DNA molecules.

DNA library, aptamers, and primers were all synthesized in house on an ABI 3400 DNA/RNA synthesizer using solid-state phosphoramidite chemistry at 1 μ mol scale. The

synthesized product was then subjected to two times of reverse phase HPLC (RP-HPLC) purification process on a ProStar HPLC with a C18 column (Econosil, 5 μ , 250 \times 4.6 mm) and optimized elution gradient in 0.1 M TEAA solution. The HPLC-purified product was then dried, trityl group deprotected, and re-suspended in water for quantification. Quantification was done by measuring the UV/Vis absorbance on a Cary Bio-300 UV spectrometer. A 1 cm path length square quartz cuvette was used for absorption measurements. Then the product was titrated and suspended in buffer for experimental uses.

Real-time PCR Reaction

To quantify the amount of aptamers bound with target cells, they were examined by real-time PCR reaction. After carefully washing off non-specific binding sequences, the specific binding sequences were collected and run real-time PCR together with standard samples. Standard samples contain a series of dilutions of DNA with known concentrations. Because the starting quantity of template DNA in real-time PCR is proportional to the PCR threshold cycles, the amount of target cell bound aptamers can be calculated by comparing with standard curves. In our experiments, we used iTaq DNA polymerase (Bio-Rad) and a MyiQ real-time PCR system (Bio-Rad) for real-time PCR experiments. SYBR green (Molecular Probes) was used for the detection of PCR products by intercalating into double stranded DNA product of PCR reaction.

Proximity Dependent Evolution of Paired Aptamers

Lead probe SGC8 and ssDNA library were synthesized on the ABI DNA synthesizer and purified by reverse phase HPLC. Denatured PAGE was used to further purify the lead probe and ssDNA library to minimize the interference of impurity to hybridization product and SELEX. The purified lead probe and ssDNA library were denatured at 95°C for 10 minutes and cooled

down to 37 °C immediately. After that, the hybridization of lead probe with ssDNA library was performed by mixing 1:1 ratio of two components in 1×PBS at 37°C for 30 minutes.

After incubation of lead probe/ssDNA library with target cells, the complex was washed with modified NEB 4 buffer in which restriction enzyme Apa I had 100% activity at 25°C (50 mM potassium acetate, 50 mM sodium chloride, 20 mM Tris-acetate, 10 mM magnesium acetate, 1 mM DTT, 0.1 mg/mL BSA, pH 7.9). Excess amount of restriction enzyme Apa I obtained from New England Biolab was added to cell suspension after wash. During 1 hour incubation at 25°C, the 5'-GGGCCC-3' restriction enzyme recognition site embedded in the 18 base pair hybridization region will be specifically recognized and cleaved. Thereby, those ssDNA molecules with low affinity to the target protein of lead probe *sgc8* can be washed off after the linkers between them and lead probes are cleaved. Only those aptamer candidates with very high affinity to the target protein will retain with lead probes. After washing with ligation buffer (50 mM Tris-HCl, 100 mM sodium chloride, 10 mM magnesium chloride, 10 mM DTT, 1 mM ATP, 0.025 mg/mL BSA, pH 7.5), the sticky ends generated by previous restriction cleavage of hybridization complex of lead probes and aptamers were ligated at the presence of excess amount of T4 DNA ligase (New England Biolab) at 16°C for 30 minutes. After selection, aptamers still bound with target cells were amplified by PCR and processed to perform next round of selection. The binding abilities of selected new aptamer as well as resulted aptamer pairs were screened with flow cytometer. Thereafter, the highly enriched library will be cloned and sequenced. New selected aptamers are then synthesized, hybridized with lead probes, and tested with target cells using FRET based proximity dependent assay to confirm the simultaneous binding of two aptamers with same target protein.

Principle of Aptamer-PCR Assay

To make use of the aptamers selected for the cancer cells using cell based SELEX, we developed a novel assay format involving both the aptamer and real-time PCR techniques to detect the rare cancer cells which exfoliated in body fluid such as peripheral blood. With this assay format, any kind of target cells can be detected since the aptamers can be readily developed for these cells using cell based SELEX.

This assay does not require any modification of the aptamers for them to report the existence of target cells. The aptamers are allowed to bind to their target proteins on the surface of cancer cells, similar to the flow cytometry assay. After washing off weak binding or non-specific binding sequences, the specific binding aptamers are collected for real-time PCR reaction. Meanwhile, samples with known amount of DNA are tested together with unknown sample, serving as standard samples to help determine the amount of specific binding aptamers.

Compared with previously reported cancer cell detection techniques that relies on tumor specific gene identification (Figure 5-1), the new aptamer-PCR assay has several advantages. First of all, this method allows the quantification of the detected cancer cells. Unlike in the gene detection assay, the samples can be analyzed without pre-treatment such as target cell isolation by antibody modified magnetic beads. Other treatments including cell lysis and mRNA extraction are not required as well. The process is much easier in the case of aptamer-PCR assay, including only 3 steps: binding, washing, and real-time PCR. The easy procedures and simple instrumentation make it possible to develop the standard protocol. In addition, the specificity of this technique may be greatly improved if multiple aptamers are available, which can be easily achieved by cell based SELEX.

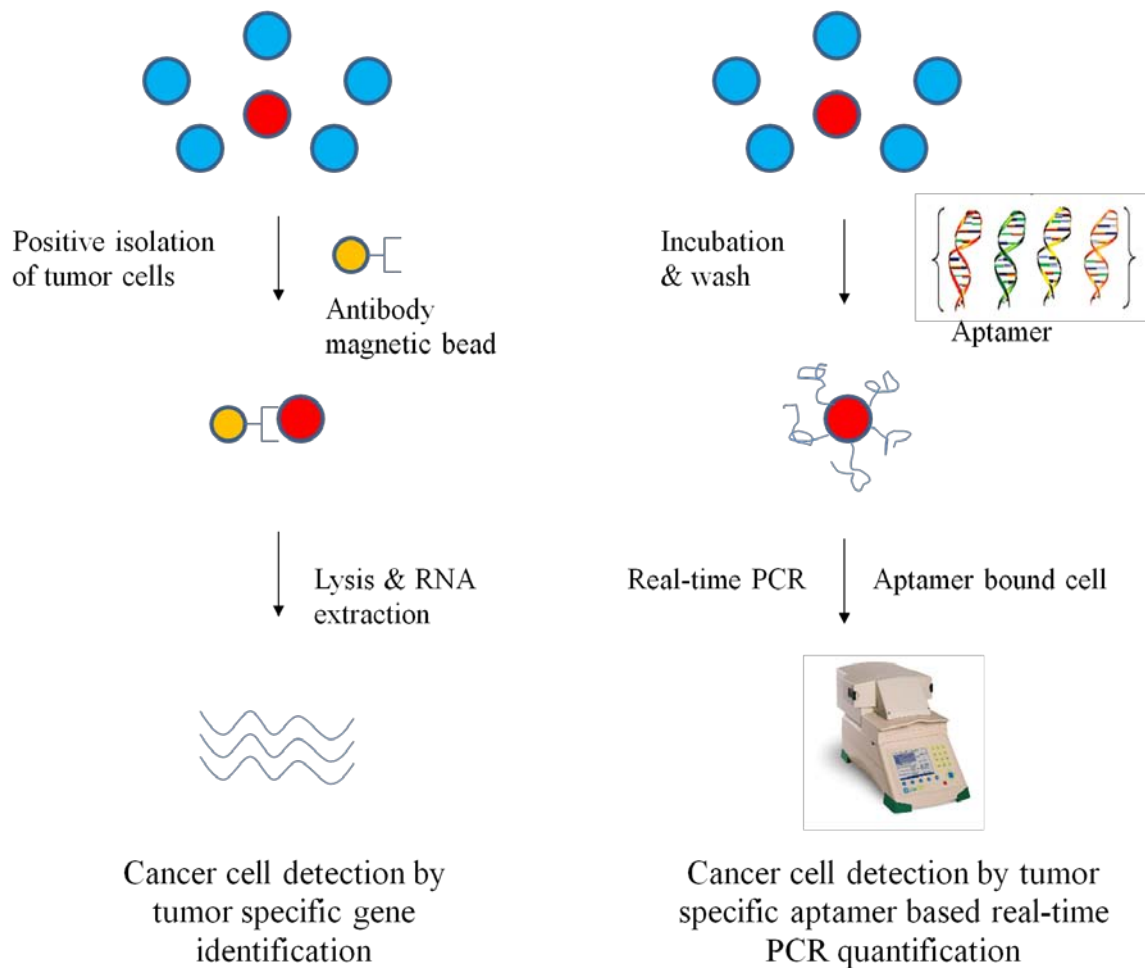


Figure 5-1. Comparison of cancer cell detection by tumor specific gene identification and cancer cell detection by tumor specific aptamer based real-time PCR quantification.

Detection and Quantification of Cancer Cells by Aptamer-PCR Assay

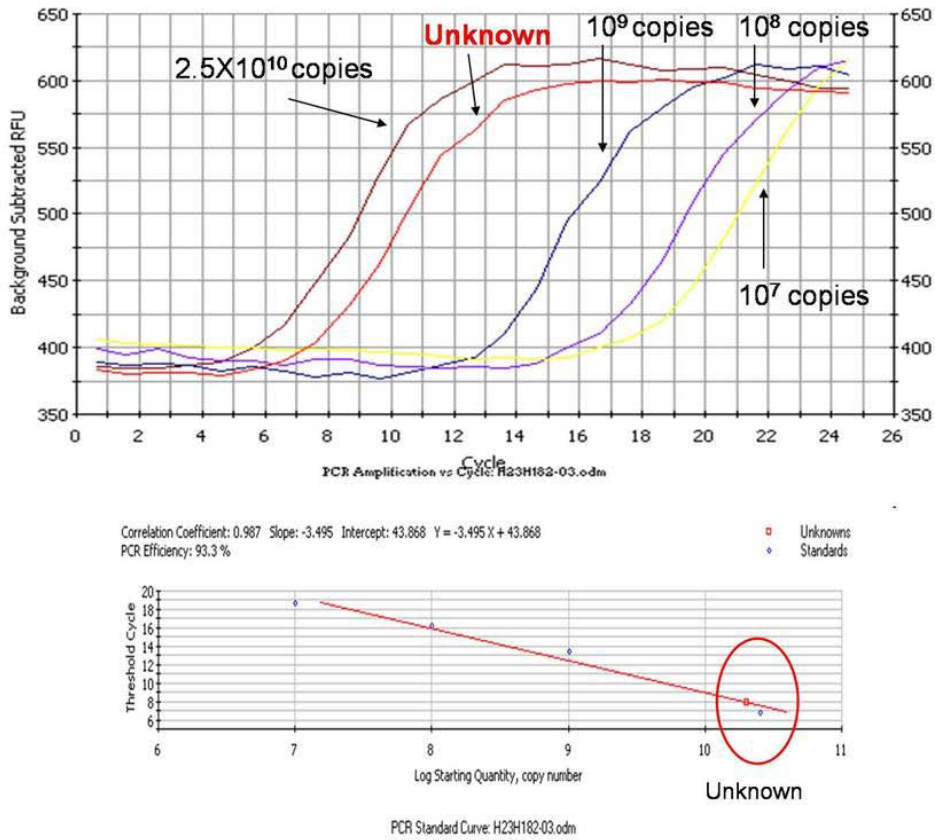
To demonstrate this aptamer-PCR assay, we started with the leukemia cells spiked in buffer as the model system. CCRF-CEM (T-cell acute lymphoblastic leukemia) was used as target cell, and Ramos (B-cell human Burkitt's lymphoma) was used as control cell. We chose aptamer SGC8 (88mer) as the probe to detect the target cells in this system. Aptamer SGC8 was developed by cell based SELEX and has a K_d of 0.80 nM. It shows great specificity for CEM cells but not for Ramos cells. In this assay, the aptamer SGC8 was allowed to bind to the target

protein PTK7 (protein tyrosine kinase 7) on the surface of CEM cells. After washing off non-specific binding DNA, the specific binding aptamers were analyzed by real-time PCR reaction. In order to determine the amount of specific binding aptamers on cell surface, we run a series of standard samples with known concentrations together with the sample to be detected in real-time PCR. Because the starting quantity of DNA template in real-time PCR is proportional to the threshold cycle, the amount of specific binding aptamers can be calculated by comparing it with the standard curve from known samples as demonstrated in Figure 5-2.

Before the experiments, we synthesized the aptamer SGC8 and library. To test the binding ability, the synthesized aptamers and library were first modified with biotin. The biotinylated aptamer and library were then allowed to bind with target cells and control cells. After washing, the cell/aptamer complex was further incubated with streptavidin modified FITC dye to give out the binding signals. This signal transduction mechanism was used because only non-fluorescent DNA is allowed in real-time PCR reaction. In real-time PCR reaction, only fluorescent signals allowed are from the intercalating dye such as SYBR green that emits fluorescence signals when bind to double stranded DNA. As shown in Figure 5-3, the synthesized aptamer SGC8-biotin possesses great binding ability for the target CEM cells, compared with the background binding of library-biotin. Both SGC8 and library show low background binding signals against control RAMOS cells. The results confirmed the quality of the synthesized aptamer and library control for the assay.

In order to perform the real-time PCR reaction and determine the amount of specific binding aptamers bound to cell surface, we prepared standard samples of different concentrations. Dilutions of SGC8 with copies ranging from 10^{12} to 10^1 were prepared as standard samples for SGC8. These standard samples were run together with unknown samples in

PCR reaction, and used to derive the standard curve for determination of aptamer amount in unknown samples. We also prepared the same standard samples for DNA library because the DNA sequence compositions are different for DNA library than for the SGC8 that has an individual sequence.



Type	Identifier	Replicate #	Threshold	Cycle (Ct)	Starting Quantity
C3	Standard	1	6.83	10.401	2.52E+10
C4	Standard	2	13.44	9.000	1.00E+09
C5	Standard	3	16.23	8.000	1.00E+08
C6	Standard	4	18.76	7.000	1.00E+07
C7	Unknown	1	7.88	10.299	1.99E+10

Figure 5-2. Standard curve of real-time PCR for calculating the amount of specific binding aptamers in aptamer-PCR assay.

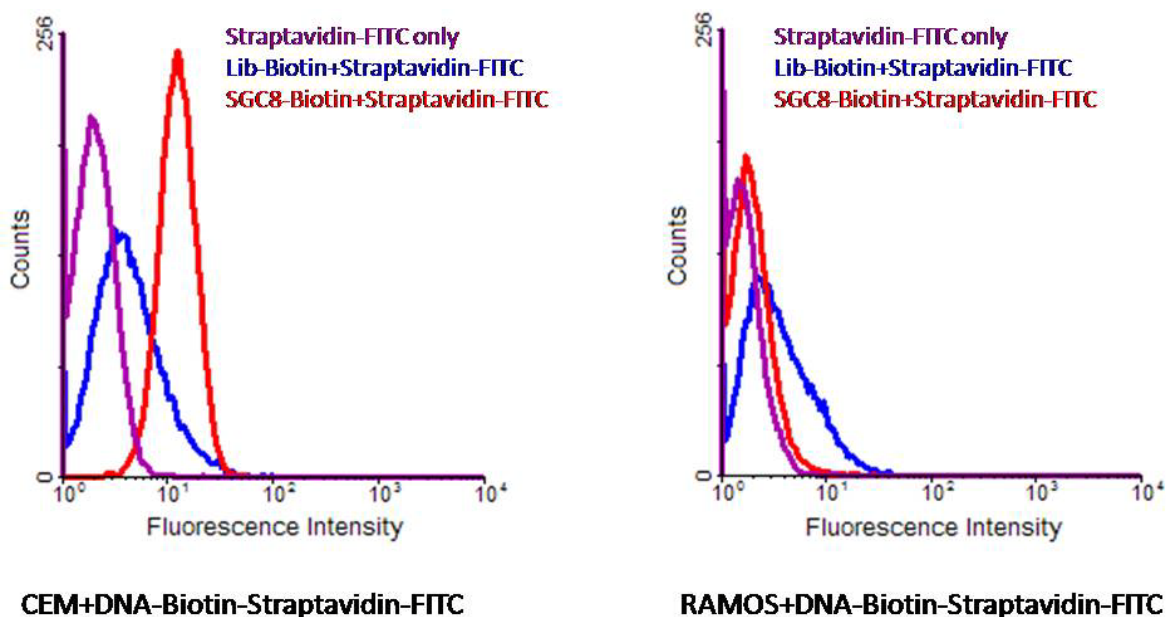


Figure 5-3. Flow cytometry results of aptamer SGC8 and library bound to CEM and RAMOS cells. During experiments, SGC8-biotin and library-biotin were first allowed to bind with target cells and control cells. Cells were washed and then incubated with straptavidin-FITC. The resulted SGC8-biotin/straptavidin-FITC and library-biotin/straptavidin-FITC were then analyzed by flow cytometry. Straptavidin-FITC only was incubated with cells as negative control.

Due to the heterogeneous population of DNA library, the PCR efficiency of DNA library is different than that of SGC8. This difference of PCR efficiency eventually affects the determination of the starting quantity in PCR reaction. For quality control purpose, a negative control not containing any DNA was used in all the experiments to assure no contamination in reagents.

To perform the binding experiments, the aptamer SGC8 and library were incubated with CEM and RAMOS cells. The cell amount varied from 10⁶ to 10¹ for both target cells and control cells. However, the amount of DNA for incubation was fixed for different cell samples, so that the binding of aptamers to cells was always saturated. The final amount of binding aptamer sequences on cell surface after washing was expected to be proportional to the amount of cells in

every sample. After incubation, the cells were thoroughly washed and heated to elute the binding sequences for real-time PCR reactions. Same amount of different samples were added into the PCR cocktail mixture containing the SYBR green dye. The PCR mixtures of different samples were put into individual wells of a 96-well PCR plate with the layout shown as in Figure 5-4.

	1	2	3	4	5	6	7	8	9	10	11	12
CEM/SGC8	A	Unknown 1	Unknown 2	Unknown 3	Unknown 4	Unknown 5	Unknown 6	Unknown 7				
	Quantity	N/A	N/A	N/A	N/A	N/A	N/A	N/A				
	Identifier	EXCLUDED	EXCLUDED	EXCLUDED	EXCLUDED	EXCLUDED	EXCLUDED	EXCLUDED				
CEM/LIB	B		Unknown 2	Unknown 3	Unknown 4	Unknown 5	Unknown 6	Unknown 7				
	Quantity		N/A	N/A	N/A	N/A	N/A	N/A				
	Identifier		EXCLUDED	EXCLUDED	EXCLUDED	EXCLUDED	EXCLUDED	EXCLUDED				
RAM/SGC8	C	Unknown 1	Unknown 2	Unknown 3	Unknown 4	Unknown 5	Unknown 6	Unknown 7				
	Quantity	N/A	N/A	N/A	N/A	N/A	N/A	N/A				
	Identifier	EXCLUDED	EXCLUDED	EXCLUDED	EXCLUDED	EXCLUDED	EXCLUDED	EXCLUDED				
RAM/LIB	D		Unknown 2	Unknown 3	Unknown 4	Unknown 5	Unknown 6	Unknown 7				
	Quantity		N/A	N/A	N/A	N/A	N/A	N/A				
	Identifier		EXCLUDED	EXCLUDED	EXCLUDED	EXCLUDED	EXCLUDED	EXCLUDED				
ST SGC8	E											
	Quantity											
	Identifier											
ST LIB	F	Standard 1	Standard 2	Standard 3	Standard 4	Standard 5	Standard 6	Standard 7	Standard 8	Standard 9	Standard 10	Standard 11
	Quantity	1.00e+12	1.00e+11	1.00e+10	1.00e+09	1.00e+08	1.00e+07	1.00e+06	1.00e+05	1.00e+04	1.00e+03	1.00e+02
	Identifier	EXCLUDED	EXCLUDED	EXCLUDED	EXCLUDED	EXCLUDED	EXCLUDED	EXCLUDED	EXCLUDED	EXCLUDED	EXCLUDED	EXCLUDED
NEGATIVE	G	Standard 1	Standard 2	Standard 3	Standard 4	Standard 5	Standard 6	Standard 7	Standard 8	Standard 9	Standard 10	Standard 11
	Quantity	1.00e+12	1.00e+11	1.00e+10	1.00e+09	1.00e+08	1.00e+07	1.00e+06	1.00e+05	1.00e+04	1.00e+03	1.00e+02
	Identifier	EXCLUDED	EXCLUDED	EXCLUDED	EXCLUDED	EXCLUDED	EXCLUDED	EXCLUDED	EXCLUDED	EXCLUDED	EXCLUDED	EXCLUDED
NEGATIVE	H	Neg Control										
	Quantity	N/A										
	Identifier											

Figure 5-4. Sample layout of real-time PCR reaction. Same amount of aptamer SGC8 and library were incubated with different amount (10^6 to 10^1) of target cell (CEM) and control cell (Ramos). Standard samples of SGC8 and library were prepared to containing DNA copies ranging from 10^{12} to 10^1 . Negative control with no DNA template was included.

All the samples were analyzed by real-time PCR reactions and the fluorescence signals were recorded and processed by MyiQ software (Bio-Rad). The fluorescence signals of standard samples and unknown samples were recorded separately and processed before overlay for analysis (Figure 5-5). The baseline signal was optimized by software to derive the threshold cycle number. A standard curve of threshold cycle numbers Vs. Log starting quantity copies was

generated and fit to give an equation. DNA copies in unknown samples were then calculated using this equation.

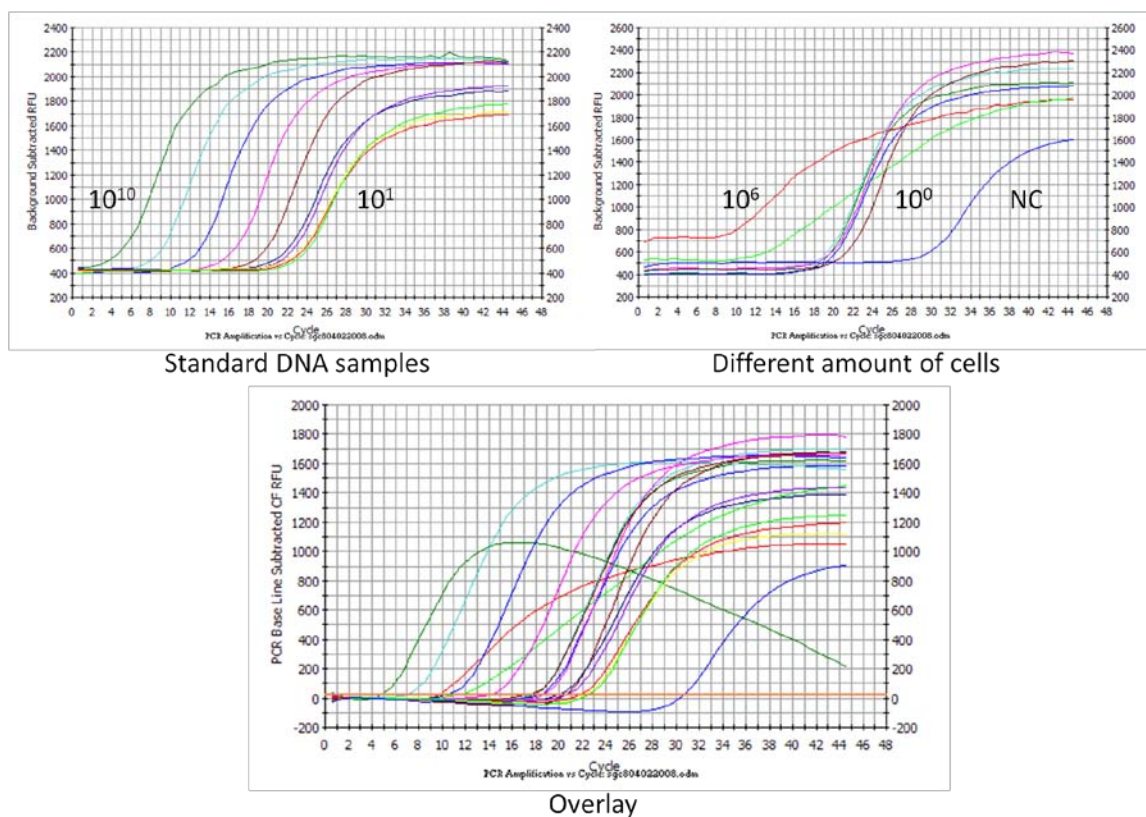


Figure 5-5. Real-time PCR results of standard DNA samples and unknown amount of specific binding aptamer SGC8 sequences for CEM cells. Amount of aptamer SGC8 sequences bound to different amount (10^6 to 10^1) of target cells (CEM) were recorded. Standard samples of SGC8 ranging from 10^{12} to 10^1 copies were also recorded. Negative control with no DNA template was included.

The starting quantity of DNA sequences in each well was calculated as mentioned above and listed in Table 5-1. The results showed that the amount of binding aptamer sequences was proportional to the amount of cells started with in the experiments. Thus, the amount of cells in unknown samples could be determined based on this data. Unlike the aptamers, the DNA library showed no significant difference between different amounts of cells. The DNA library data could be subtracted from the aptamer data as background in the real application of this assay. Although

the assay successfully demonstrated its capability of detecting cancer cells using aptamer and real-time PCR technique, the sensitivity of this method was limited to 10^4 cells. As shown in Table 5-1, samples with cell quantity below 10^4 could not be distinguished from each other, only those samples containing more than 10^4 cells could be successfully detected and quantified. This limitation may be an important challenge for the application of this assay to real patient samples because patient samples usually contain rare amount of exfoliated cancer cells. To improve the assay sensitivity, we may introduce a signal amplification mechanism as well as reduce the background signal resulted from non-specific binding of DNA molecules.

Table 5-1: Copy numbers (Log) of specific binding aptamers on different amount of cells

Cells	10^6	10^5	10^4	10^3	10^2
CEM/SGC8	8.5	7.7	4.7	4.7	4.5
CEM/LIB	5.8	5.4	4.6	4.5	4.1

Development of Paired Aptamers for Ultra-Sensitive Aptamer-PCR Assay

As we discussed in previous session, the aptamer-PCR assay has the ability to detect and quantify the large amount of cancer cells, generally more than 10^4 cells. Although the real-time PCR reaction allows the quantification of cell binding aptamers, the non-specific amplification of PCR technique is the main cause of high background signal in aptamer-PCR assay. Any non-specific binding DNA molecules could be amplified by PCR reaction and counted as the signal of specific binding aptamers. Although the background signal can be reduced to some extent by using a DNA library, it cannot be completely solved. The detection limit of aptamer-PCR assay can be further improved by either amplifying the signal or reducing the background. Methods such as rolling-circle PCR could be the choice to amplify the signal. However, it may need to change the whole assay platform. Recently, proximity-dependent DNA ligation assays were developed to achieve ultra-sensitive detection of proteins with higher sensitivity than immuno-

PCR, rolling-circle PCR, and immunodetection amplified by T7 RNA polymerase. Proximity-dependent DNA ligation assay improves the assay sensitivity mainly by reducing the background binding signal. We then introduced the mechanism of proximity-dependent DNA ligation to the aptamer-PCR assay to improve the assay sensitivity.

The general idea of proximity dependent ligation mechanism is to generate signal by binding of different epitopes of same target molecule with a set of two proximity probes. Linked aptamer probes that bind to same cell surface biomarker will result in decreased dissociation rate, which can give rise to higher sensitivity. However, aptamers selected against pure proteins and complex targets often bind to single epitopes, which limits the applications of proximity dependent probes. Thus, we designed proximity-dependent evolution experiment to generate paired aptamer probes for ultra-sensitive aptamer-PCR assay of cancer cells. It is achieved by using a previously selected aptamer as lead probe to facilitate the binding of aptamer candidates in library to the same target on cell membrane.

T-cell lymphoblast (CCRF-CEM) was chosen as the target cell. One aptamer with high affinity selected by cell based SELEX was used as lead probe in this experiment. By hybridizing to the new DNA library, the lead probes function to guide the new aptamer selection for the same cell surface target protein (Figure 5-6). In the first a few rounds of cell based SELEX, the amount of aptamer candidates is very low. Thus the chances for those aptamers with high affinity to bind with the target proteins are very small. The potential loss of them due to the separation and amplification procedures can further lower the chances. However, it can be improved by lead probe facilitated, site specific selection of aptamer. In addition, unlike the cell based SELEX, in which little information of the target protein is available before the aptamers are selected out, the aptamers isolated in proximity dependent evolution will only recognize the same target protein

of lead probe as the lead probe works as a tag to help identify the aptamer for the same target protein. The resulted paired aptamers may have improved affinity which should be at least two times higher than single aptamer probe. Synergetic or allosteric binding effect between lead probe and potential aptamer is also possible. Another advantage of this strategy is the capability of selecting multiple aptamers for one target protein instead of the one to one model in traditional cell based SELEX. When working together with restriction cleavage-ligation strategy as shown in Figure 5-6, the proximity dependent evolution can exclude the binding of aptamers with low affinity as well as non-specific binding, thus improve the efficiency of selection and make it easy to identify the aptamers with high affinity in the enriched pool.

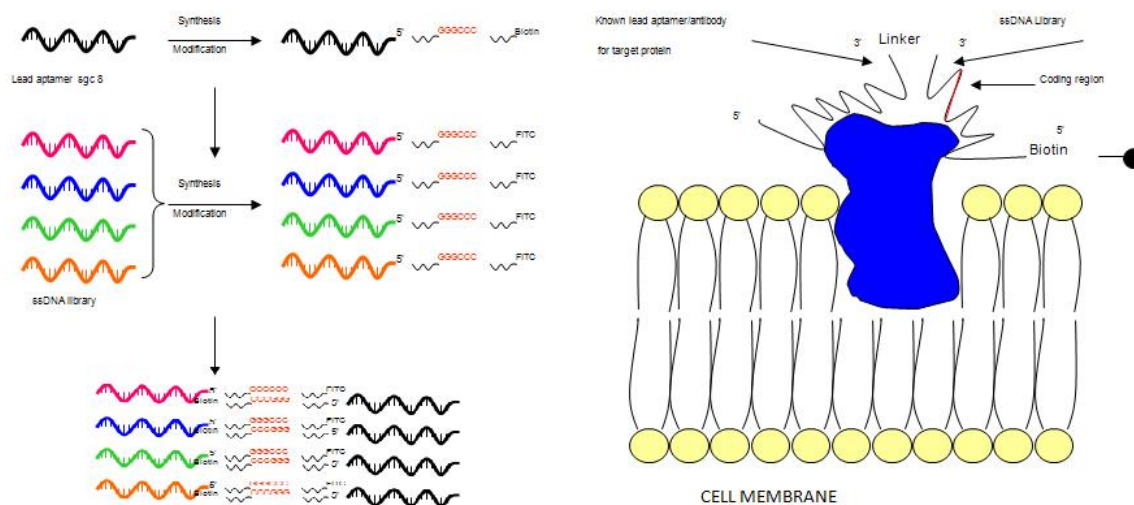


Figure 5-6. Proximity dependent evolution of paired aptamer probes for ultra-sensitive aptamer-PCR assay. Lead probe hybridizes with DNA library to perform facilitated aptamer selection for same target protein on cell surface.

Conclusions

In this chapter, we described a novel assay format for rare cancer cell detection. Rare cancer cell detection is critical for the early diagnosis of certain types of cancer, which exfoliate small amount of cancer cells into blood or other bodily fluid at the early stage of cancer. This

aptamer-PCR assay utilizes the aptamers developed from cell based SELEX to detect the existence of target cancer cells, meanwhile using real-time PCR technique to quantify the amount of target cancer cells detected by aptamers. Compared to other approaches, this method is simple, accurate, and specific. With readily developed aptamers from cell based SELEX, this assay format can be used for any target cell of interest. This assay shows great sensitivity ($>10^4$ cells), however it still lacks the ability to detect trace amount of target cells. To improve the detection limit, proximity dependent evolution experiment was designed to develop paired aptamers that bind to the same target protein on cell surface. With the added proximity dependent binding mechanism, the aptamer-PCR assay should have better sensitivity and specificity for cancer cell detection.

CHAPTER 6 SUMMARY AND FUTURE DIRECTIONS

Summary

Aptamers are synthetic DNA or RNA molecules evolved from a random library of 10^{15} - 10^{18} candidates. The binding ability of aptamers comes from their tertiary structures in the presence of target molecules, which derive from the combinatorial secondary structures of nucleic acid molecules during the systematic evolution of ligands by exponential enrichment (SELEX). Besides its early applications in bioanalytical chemistry as a basic molecular recognition element, aptamers have recently begun to be utilized in personalized disease diagnosis and therapy. Single stranded nucleic acid aptamers can be evolved to have high specificity and affinity against different disease related metabolites, biomarker proteins, and even whole live cells expressing a variety of surface proteins of interest. When coupled with suitable signal transduction mechanisms, aptamers show great potential as a new tool for biomedical studies.

We recently developed some new aptamers as recognition elements to probe the molecular signatures of different lung cancer cells in a direct and simple manner. These molecular signatures expressed on live cell membranes may imply important disease mechanisms if validated as biomarkers. Theoretically, any molecular level variance among different types or subtypes of cancer cells could be revealed by a similar methodology, something that was impractical before. To develop such aptamer probes for molecular differences between two types of cancer, a methodology called cell based SELEX dealing with whole live cancer cells was used. This methodology is unlike previous attempts of SELEX against other complex targets. Another distinct aspect of this methodology is the use of a counter-selection strategy to screen out those aptamers binding with common target proteins expressed on the cell membranes of

different cancer cells. In this specific case, two different lung cancer cell lines were chosen to study the molecular level differences. A cultured small cell lung cancer cell line was used as a positive target while a cultured non-small cell lung cancer cell line was used as the negative control. After iterative binding with both positive and negative cell lines, a panel of aptamer probes became enriched, among which probes can be used either individually for bioanalytical applications, or together in multi-probe based assays to provide more information for diagnostics.

Most of the aptamers selected by this methodology only recognized target cells and were not interfered by the excess of DNA library. These aptamers exhibited not only great specificity but also high affinity for the target cells, which ranges from sub-micromolar to sub-nanomolar. As the aptamers were generated against whole live cells in their native state, the clinical assays can be directly performed. In complicated environment, target cells were still recognized by aptamer probes.

To demonstrate the widespread usefulness of these selected aptamer probes, they were tested for other lung cancer cell lines, which are similar to the cells used in aptamer selection, as well as some other types of cancer. The results showed that these aptamers recognized most “target cell like cell lines” and did not recognize either most “control cell like cell lines” or other types of cancer. It was encouraging to see that real clinical patient samples also responded to the aptamer probes. Thus, the capability of aptamers generated by cell based SELEX for the recognition of molecular differences among cancer cells was clearly demonstrated.

We have shown that aptamers developed in this work are suitable for multiple types of early detection studies. First, retrospective analysis of preserved specimens could be done with these aptamers by using assay formats including flow cytometry and confocal imaging as

demonstrated in this work. Second, aptamer conjugated nanoparticles are able to isolate, enrich, and detect exfoliated tumor cells in peripheral blood. Third, aptamer-PCR assay can readily detect and quantify the cancer cells for early diagnosis. Combining the molecular recognition ability of aptamers with specific signal transduction mechanisms provides simple, rapid, sensitive, and selective assays for cancer diagnosis.

Future Directions

Not only can a group of aptamers selected from cell differences be used as molecular probes for the detection of specific disease cells, but also they can be used to purify and identify biomarkers, which have not been studied before the probes were generated. The developed aptamer probes, demonstrating high specificity and affinity to lung cancer cells, will be used to purify and identify the target proteins on the cell surface through affinity chromatography coupled with LC-MS/MS.

The aptamer assisted biomarker discovery strategy is expected to greatly facilitate biomarker discovery by identifying more biologically relevant biomarkers for specific types of diseases and reducing the effort required for biomarker screening and biomarker validation. As distinct biomarkers can be discovered for specific diseases, they will eventually help achieve more accurate diagnoses and more effective treatments, which are essential for the goal of personalized medicine. It is clear that the integration of probe development and biomarker discovery gives rise to extra advantages resulting in a shortened time gap between laboratory research and clinical application.

In the future, we will continue to work on selecting aptamers probes for other types of lung cancer such as non-small cell lung cancer. These aptamers could be very useful for lung cancer subtyping during screening^[134] and planning appropriate treatment, for example, avoiding excessive therapy in the case of resectable NSCLC.

Although the benefits of using this aptamer approach for lung cancer early detection remains to be determined in prospective trial, it might also be able to detect pre-invasive lesions even before the malignant cells exfoliated when local therapy has limited effect, or indicate the possible relapse in early stage^[135] for proper therapy to prevent it if specific cell surface markers can be identified eventually. In addition, this approach would provide valuable information for the understanding of progressive neoplastic differentiation of lung cancer during early stage. However, the use of aptamer for lung cancer screening and whether it can eventually reduce the overall mortality must first be determined in a randomized clinical trial.

In conjunction with the further selection of aptamers, biomarker identification, and assay development, the development of new drugs and novel targeted drug delivery methods may be accelerated in the future. The proteomics presented by aptamer approach, together with genomics, molecular imaging, and clinical factors, will in principle achieve the molecular profiling of lung cancer and provide tailored treatments, and therefore realize the personalized medicine.^[136]

Conclusions

With cell based SELEX technique, molecular aptamers can be readily developed for any cancer cells of interest without prior knowledge of cell surface marker proteins, and thus are more flexible and practical to use than other molecule marker based methods. It is noteworthy that a panel of aptamer probes for multiple cell surface differentiation markers can be developed by our strategy. The combination of multiple markers ultimately will be more accurate and predictive than single marker. An additional, notable advantage of this aptamer based approach is that molecular markers are recognized at their native state on living cell surfaces. The molecular aptamers have many advantages over other methods for early lung cancer detection in terms of sensitivity, reproducibility, simplicity, robustness, production, and flexible

modification. These merits lead to aptamers' recruitment as one of the most desirable molecular recognition elements. When coupled with appropriate assay formats, aptamers show great potential to be used in clinical tests. In the future, the development of specific aptamer probes for molecular signatures of disease cells will allow us to find more biomarkers, define diseases, and create tailored treatment regime for more "personalized" medicine.

LIST OF REFERENCES

- [1] A. Jemal, R. Siegel, E. Ward, T. Murray, J. Q. Xu, M. J. Thun, *CA-Cancer J. Clin.* **2007**, 57, 43–66.
- [2] F. R. Hirsch, W. A. Franklin, A. F. Gazdar, P. A. Bunn, *Clin. Cancer Res.* **2001**, 7, 5–22.
- [3] D. M. Jackman, B. E. Johnson, *Lancet* **2005**, 366, 1385–1396.
- [4] A. McWilliams, C. MacAulay, A. F. Gazdar, S. Lam, *Oncogene* **2002**, 21, 6949–6959.
- [5] J. L. Mulshine, *Nat. Rev. Cancer* **2003**, 3, 65–73.
- [6] E. F. Patz, P. C. Goodman, G. Bepler, *N. Engl. J. Med.* **2000**, 343, 1627–1633.
- [7] S. D. Bernal, A. D. Elias, *J. Clin. Oncol.* 1988, 6, 1676–1678.
- [8] I. I. Wistuba, J. Berry, C. Behrens, A. Maitra, N. Shivapurkar, S. Milchgrub, B. Mackay, J. D. Minna, A. F. Gazdar, *Clin. Cancer Res.* **2000**, 6, 2604–2610.
- [9] L. Mao, *Oncogene* **2002**, 21, 6960–6969.
- [10] L. Mao, R. H. Hruban, J. O. Boyle, M. Tockman, D. Sidransky, *Cancer Res.* **1994**, 54, 1634–1637.
- [11] N. A. Levin, P. M. Brzoska, M. L. Warnock, J. W. Gray, M. F. Christman, *Genes Chromosomes Cancer* **1995**, 13, 175–185.
- [12] M. S. Tockman, P. K. Gupta, J. D. Myers, J. K. Frost, S. B. Baylin, E. B. Gold, A. M. Chase, P. H. Wilkinson, J. L. Mulshine, *J. Clin. Oncol.* **1988**, 6, 1685–1693.
- [13] K. Yanagisawa, Y. Shyr, B. G. J. Xu, P. P. Massion, P. H. Larsen, B. C. White, J. R. Roberts, M. Edgerton, A. Gonzalez, S. Nadaf, J. H. Moore, R. M. Caprioli, D. P. Carbone, *Lancet* **2003**, 362, 433–439.
- [14] T. D. Chanin, D. T. Merrick, W. A. Franklin, F. R. Hirsch, *Curr. Opin. Pulm. Med.* **2004**, 10, 242–247.
- [15] L. Stryer, *Biochemistry* 4th edn (New York: Freeman) 1995
- [16] A. D. Ellington, J. Szostak, *Nature*, **1990**, 346, 818–822.
- [17] D. S. Wilson, J. W. Szostak, *Annu. Rev. Biochem.* **1999**, 68, 611–647.
- [18] D. Shangguan, Y. Li, Z. W. Tang, Z. H. C. Cao, H. W. Chen, P. Mallikaratchy, K. Sefah, C. Y. J. Yang, W. H. Tan, *Proc. Natl. Acad. Sci. USA* **2006**, 103, 11838–11843.
- [19] M. Hendrix, E. S. Priestley, G. F. Joyce, C. H. Wong, *Journal of American Chemical Society* **1997**, 119, 3641–3648.

- [20] M. Liss, B. Petersen, H. Wolf, E. Prohaska, *Analytical Chemistry* **2002**, 74, 4488-4495.
- [21] C. A. Savran, S. M. Knudsen, A. D. Ellington, S. R. Manalis, *Analytical Chemistry* **2004**, 76, 3194-3198.
- [22] D. K. Xu, D. W. Xu, X. B. Yu, Z. H. Liu, W. He, Z. Q. Ma, *Analytical Chemistry* **2005**, 77, 5107-5113.
- [23] H. M. So, B. K. Kim, K. Won, Y. H. Kim, B. H. Ryu, P. S. Na, H. Kim, J. O. Lee, *Journal of American Chemical Society* **2005**, 127, 11906-11907.
- [24] S. B. Lee, D. T. Mitchell, L. Trofin, T. K. Nevanen, H. Soderlund, C. R. Martin, *Science* **2002**, 296, 2198-2200.
- [25] Y. Cui, Q. Q. Wei, H. K. Park, C. M. Lieber, *Science* **2001**, 293, 1289-1292.
- [26] O. C. Farokhzad, S. Jon, A. Khademhosseini, T. T. Tran, D. A. LaVan, R. Langer, *Cancer Research*, **2004**, 64, 7668-7672.
- [27] P. Alivisatos, *Nature Biotechnology* **2004**, 22, 47-52.
- [28] S. E. Stiriba, H. Frey, R. Haag, *Ange. Chemie Int. Ed.* **2002**, 41, 1329-1334.
- [29] M. Bruchez, M. Moronne, P. Gin, S. Weiss, A. P. Alivisatos, *Science* **1998**, 281, 2013-2016.
- [30] L. X. Tiefenauer, G. Kuhne, R. Y. Andres, *Bioconjugate Chem.* **1993**, 4, 347-352.
- [31] Simard, J.; Briggs, C.; Boal, A.K.; Rotello, V.M. *Chem. Commun.* 2000, 1943-1944.
- [32] A. L. Stepanov, J. R. Krenn, H. Ditlbacher, A. Hohenau, A. Drezet, B. Steinberger, A. Leitner, F. R. Aussenegg, *Optics Letters* **2005**, 30, 1524-1526.
- [33] X. J. Zhao, R. Tapeç-Dytioco, W. T. Tan, *Journal of American Chemical Society* **2003**, 125, 11474-11475.
- [34] A. A. Schvedova, E. R. Kisin, R. Mercer, A. R. Murray, V. J. Johnson, A. I. Potapovich, Y. Y. Tyurina, O. Gorelik, S. Arepalli, D. Schwegler-Berry, A. F. Hubbs, J. Antonini, D. E. Evans, B. K. Ku, D. Ramsey, A. Maynard, V. E. Kagan, V. Castranova, P. Baron, *Am. J. Physiol. Lung Cell Mol. Physiol.* **2005**, 289, L698-L708.
- [35] W. C. W. Chan, D. J. Maxwell, X. H. Gao, R. E. Bailey, M. Y. Han, S. M. Nie, *Curr. Opin. Biotechnol.* **2002**, 13, 40-46.
- [36] M. Bruchez, M. Jr, Moronne, P. Gin, S. Weiss, A. P. Alivisatos, *Science*, **1998**, 281, 2013-2015.
- [37] H. Mattoussi, *J. Am. Chem. Soc.* **2000**, 122, 12142-12150.

- [38] M. E. Akerman, W. C. W. Chan, P. Laakkonen, S. N. Bhatia, E. Ruoslahti, *Proc. Natl. Acad. Sci. USA* **2002**, 99, 12617-12621.
- [39] S. J. Rosenthal, *J. Am. Chem. Soc.* **2002**, 124, 4586-4594.
- [40] X. H. Gao, Y. Y. Cui, R. M. Levenson, L. W. K. Chung, S. M. Nie, *Nature Biotechnology* **2004**, 22, 969-976.
- [41] C. M. Niemeyer, *Angew. Chem. Int. Ed. Engl.* **2001**, 40, 4128-4158.
- [42] M. Y. Han, X. H. Gao, J. Z. Su, S. M. Nie, *Nat. Biotechnol.* **2001**, 19, 631-635.
- [43] J. Turkevitch, P. C. Stevenson, J. Hillier, *Discuss. Faraday Soc.* **1951**, 11, 55-75.
- [44] Gomez, S.; Philippot, K.; Colliere, V.; Chaudret, B.; Senocq, F.; Lecante, P. *Chem. Commun.* 2000, 1945-1946.
- [45] Franzen, S.; Folmer, J.C.W.; Glomm, W.R.; O'Neal, R. J. *Phys. Chem. A* 2002, 106, 6533-6540.
- [46] Tkachenko, A.G.; Xie, H., Coleman, D.; Glomm, W.; Ryan, J.; Anderson, M.F.; Franzen, S.; Feldheim, D.L. *J. Am. Chem. Soc.* 2003, 125, 4700-4701.
- [47] Storhoff, J.J.; Mirkin, C.A. *Chem. Rev.* 1999, 99, 1849-1862.
- [48] Hayat, M.A. *Colloidal Gold: Principles, Methods and Applications*; New York: Academic Press; 1989, Vol. 1.
- [49] Wang, G.L.; Zhang, J.; Murray, R.W. *Anal. Chem.* 2002, 74, 4320-4327.
- [50] K. L. Kelly, E. Coronado, L. L. Zhao, G. C. Schatz, *J. Physical Chem. B* **2003**, 107, 668-677.
- [51] A. J. Haes, R. P. A. Van Duyne, *J. Am. Chem. Soc.* **2002**, 124, 10596-10604.
- [52] R. Elghanian, J. J. Storhoff, R. C. Music, R. L. Letsinger, C. A. Mirkin, *Science* **1997**, 277, 1078-1081.
- [53] Y. W. C. Cao, R. C. Jin, C. A. Mirkin, *Science* **2002**, 297, 1536-1540.
- [54] A. K. Gupta, M. Gupta, *Biomaterials*, **2005**, 26, 3995-4021.
- [55] Z. Li, L. Wei, M. Y. Gao, H. Lei, *Adv. Mater.* **2005**, 17, 1001-1005.
- [56] S. Jing, S. Gider, K. Babcock, D. D. Awschalom, *Science* **1996**, 271, 937-941.
- [57] W. T. Coffey, *Physical Rev. Lett.* **1998**, 80, 5655-5658.

- [58] F. Grasset, N. Labhsetwar, D. Li, D. C. Park, N. Saito, H. Haneda, O. Cador, T. Roisnel, S. Mornet, E. Duguet, J. Portier, J. Etourneau, *Langmuir* **2002**, 18, 8209-8216.
- [59] A. Bee, R. Massart, S. J. Neveu, *J. Magn. Magn. Mater.* **1995**, 149, 6-9.
- [60] J. Lee, T. Isobe, M. Senna, *Colloids Surf. A* **1996**, 109, 121-127.
- [61] D. Langevin, *Annu. Rev. Phys. Chem.* **1992**, 43, 341-369.
- [62] X. Wang, J. Zhuang, Q. Peng, Y. Li, *Nature*, **2005**, 437, 121-124.
- [63] D. W. Elliott, W. X. Zhang, *Environ. Sci. Technol.* **2001**, 35, 4922-4926.
- [64] M. Takafuji, S. Ide, H. Ihara, Z. Xu, *Chem. Mater.* **2004**, 16, 1977-1983.
- [65] D. C. Jiles, *Acta Mater.* **2003**, 51, 5907-5910.
- [66] O. V. Salata, *J. Nanobiotechnol.* **204**, 2, 3-13.
- [67] G. Barratt, *Cell. Mol. Life Sci.* **2003**, 60, 21-37.
- [68] T. Neuberger, B. Schopf, H. Hofmann, M. Hofmann, B. Von Rechenberg, *J. Magn. Magn. Mater.* **2005**, 293, 483-496.
- [69] C. C. Berry, *J. Mater. Chem.* **2005**, 15, 543-547.
- [70] D. L. Huber, *Small* **2005**, 1, 482-501.
- [71] H. Yamauchi, T. Ishikawa, S. Kondo, *J. Colloids Surf.* **1989**, 37, 71-80.
- [72] A. van Blaaderen, A. Vrij, *Langmuir* **1992**, 8, 2921-2931.
- [73] I. Roy, T. Y. Ohulchansky, D. J. Bharali, H. E. Pudavar, R. A. Mistretta, N. Kaur, P. N. Prasad, *Proc. Nat. Aca. Sci.* **2005**, 102, 279-284.
- [74] T. Ohno, M. Takeshi, S. Hisao, F. masayuki, *Adv. Powder Tech.* **2006**, 17, 167-179.
- [75] G. T. Hermanson, *Bioconjugate Techniques*, Academic Press: San Diego, CA, **1996**.
- [76] R. Tapes, X. J. Zhao, W. Tan, *J Nanosci Nanotechnol.* **2002**, 2, 405-409.
- [77] K. A. Davis, Y. Lin, B. Abrams, S. D. Jayasena, *Nucleic Acids Res.* **1998**, 26, 3915-3924.
- [78] D. W. Drolet, L. Moon-McDermott, T. S. Romig, *Nat. Biotechnol.* **1996**, 14, 1021-1025.
- [79] Y. Lin, A. Padmapriya, K. M. Morden, S. D. Jayasena, *Proc. Natl. Acad. Sci. USA* **1995**, 92, 11044-11048.

- [80] R. J. Fulton, R. L. McDade, P. L. Smith, L. J. Kienker, J. R. Kettman, *Clin. Chem.* **1997**, 43, 1749-1756.
- [81] D. H. Wilson, W. Groskopf, S. Hsu, D. Caplan, T. Langner, M. Bauman, *Clin. Chem.* **1998**, 44, 86-91.
- [82] S. Tyagi, F. R. Kramer, *Nat. Biotechnol.* **1996**, 14, 303-308.
- [83] L. B. Koutny, D. Schmalzing, T. A. Taylor, M. Fuchs, *Anal. Chem.* **1996**, 68, 18-22.
- [84] K. Shimura, B. L. Karger, *Anal. Chem.* **1994**, 66, 9-15.
- [85] S. Fredriksson, M. Gullberg, J. Jarvius, C. Olsson, K. Pietras, S. M. Gustafsdottir, A. Ostman, U. Landegren, *Nature Biotechnology* **2002**, 20, 473-477.
- [86] A. Dove, *Nat. Biotechnol.* **1999**, 17, 233-236.
- [87] L. C. Bock, L. C. Griffin, J. A. Latham, E. H. Vermaas, J. J. Toole, *Nature* **1992**, 355, 564-566.
- [88] K. A. Davis, B. Abrams, Y. Lin, S. D. Jayasena, *Nucleic Acids Res.* **1996**, 24, 702-706.
- [89] D. Shangguan, Z. W. Tang, P. Mallikaratchy, Z. Y. Xiao, W. H. Tan, *ChemBioChem* **2007**, 8, 603-606.
- [90] T. Sano, C. L. Smith, C. L. Cantor, *Science* **1992**, 258, 120-122.
- [91] H. T. Zhang, J. E. Kacharina, K. Miyashiro, M. I. Greene, J. Eberwine, *Proc. Natl. Acad. Sci. USA* **2001**, 98, 5497-5502.
- [92] B. Schweitzer, *Proc. Natl. Acad. Sci. USA* **2000**, 97, 10113-10119.
- [93] R. Etzioni, *Nat. Rev. Cancer* **2003**, 3, 243-252.
- [94] S. Ramaswamy, C. M. Perou, *Lancet* **2003**, 361, 1576-1577.
- [95] M. Baker, *Nature Biotechnology* **2005**, 23, 297-304.
- [96] N. Rifai, M. A. Gillette, S. A. Carr, *Nature Biotechnology* **2006**, 24, 971-983.
- [97] N. L. Anderson, N. G. Anderson, *Mol. Cell. Proteomics* **2002**, 1, 845-867.
- [98] E. F. Petricoin, *Lancet* **2002**, 359, 572-577.
- [99] J. Villanueva, *Anal. Chem.* **2004**, 76, 1560-1570.
- [100] N. C. VerBerkmoes, *J. Proteome Res.* **2002**, 1, 239-252.
- [101] J. N. Adkins, *Mol. Cell. Proteomics* **2002**, 1, 947-955.

- [102] Y. Shen, *Anal. Chem.* **2004**, 76, 1134-1144.
- [103] D. H. Shangguan, Z. H. Cao, L. Meng, P. Mallikaratchy, K. Sefah, H. Wang, Y. Li, W. H. Tan, *J. Proteome Res.* **2008**, 7, 2133-2139.
- [104] P. Mallikaratchy, Z. W. Tang, K. Sefah, L. Meng, D. H. Shangguan, W. H. Tan, *Mol. Cell. Proteomics* **2007**, 6, 2230-2238.
- [105] J. Luo, W. B. Isaacs, J. M. Trent, D. J. Duggan, *Cancer Invest.* **2003**, 21, 937-949.
- [106] V. Espina, D. Geho, A. I. Mehta, E. F. Petricoin, L. A. III, Liotta, K. P. Tosenblatt, *Cancer Invest.* **2005**, 23, 36-46.
- [107] S. E. Cwirla, E. A. Peters, R. W. Barrett, W. J. Dower, *Proc. Natl. Acad. Sci. USA* **1990**, 87, 6378-6382.
- [108] J. K. Scott, G. P. Smith, *Science* **1990**, 249, 386-390.
- [109] D. A. Daniels, D. P. Lane, *Exp. Opin. Ther. Pat.* **1995**, 5, 901-912.
- [110] J. D. Marks, H. R. Hoogenboom, T. P. Bonnert, J. McCafferty, A. D. Griffiths, G. Winter, *J. Mol. Biol.* **1991**, 222, 581-597.
- [111] G. Winter, A. D. Griffiths, R. E. Hawkins, H. R. Hoogenboom, *Ann. Rev. Immunol.* **1994**, 12, 433-455.
- [112] A. D. Ellington, *Curr. Biol.* **1994**, 4, 427-429.
- [113] L. Gold, *J. Biol. Chem.* **1995**, 270, 13581-13584.
- [114] A. D. Ellington, J. W. Szostak, *Nature* **1990**, 346, 818-822.
- [115] C. Tuerk, L. Gold, *Science* **1990**, 249, 505-510.
- [116] S. D. Mendonsa, M. T. Bowser, *Journal of American Chemical Society* **2004**, 126, 20-21.
- [117] B. Vant-Hull, A. Payano-Baez, R. H. Davis, L. Gold, *J. Mol. Biol.* **1998**, 279, 579-597.
- [118] K. N. Morris, K. B. Jensen, C. M. Julin, M. Weil, L. Gold, *Proc. Natl. Acad. Sci. USA* **1998**, 95, 2902-2907.
- [119] M. Homann, H. U. Goring, *Nucleic Acids Res.* **1999**, 27, 2006-2104.
- [120] M. Blank, T. Weinschenk, M. Priemer, H. Schluesener, *J. Biol. Chem.* **2001**, 276, 16464-16468.
- [121] D. A. Daniels, H. Chen, B. J. Hicke, K. M. Swiderek, L. Gold, *Proc. Natl. Acad. Sci. USA* **2003**, 100, 15416-15421.

- [122] C. Wang, M. Zhang, G. Yang, D. Zhang, H. Ding, H. Wang, M. Fan, B. Shen, N. Shao, *J. Biotechnol.* **2003**, 102, 15-22.
- [123] D. N. Carney, *Lancet* **1992**, 339, 843–846.
- [124] D. S. Ettinger, J. Aisner, *J. Clin. Oncol.* **2006**, 24, 4526–4527.
- [125] J. C. Manimala, S. L. Wiskur, A. D. Ellington, E. V. Anslyn, *J. Am. Chem. Soc.* **2004**, 126, 16515-16519.
- [126] B. J. Hicke, A. W. Stephens, *J. Clin. Invest.* **2000**, 106, 923-928.
- [127] N. M. Sayer, M. Cubin, A. Rhie, M. Bullock, A. Tahiri-Alaoui, W. James, *J. Biol. Chem.* **2004**, 279, 13102-13109.
- [128] M. Legiewicz, M. Yarus, *J. Biol. Chem.* **2005**, 280, 19815-19822.
- [129] L. S. Green, D. Jellinek, R. Jenison, A. Ostman, *Biochemistry* **1996**, 35, 14413-14424.
- [130] R. L. Souhami, P. C. L. Beverley, L. G. Bobrow, *Lancet* **1987**, 330, 325–326.
- [131] P. S. Kraemer, C. A. Sanchez, G. E. Goodman, J. Jett, P. S. Rabinovitch, B. J. Reid, *Cytometry Part A* **2004**, 60, 1–7.
- [132] H. Iinuma, K. Okinaga, M. Adachi, K. Suda, T. Sekine, K. Sakagawa, Y. Baba, J. Tamura, H. Kumagai, A. Ida, *Int. J. Cancer* **2000**, 89, 337–344.
- [133] J. K. Herr, J. E. Smith, C. D. Medley, D. H. Shangguan, W. H. Tan, *Anal. Chem.* **2006**, 78, 2918–2924.
- [134] L. A. Doyle, D. Giangiulo, A. Hussain, H. J. Park, R. W. C. Yen, M. Borges, *Cancer Res.* **1989**, 49, 6745–6751.
- [135] H. Y. Chen, S. L. Yu, C. H. Chen, G. C. Chang, C. Y. Chen, A. Yuan, C. L. Cheng, C. H. Wang, H. J. Terng, S. F. Kao, W. K. Chan, H. N. Li, C. C. Liu, S. Singh, W. J. Chen, J. J. W. Chen, P. C. Yang, *N. Engl. J. Med.* **2007**, 356, 11–20.
- [136] R. S. Herbst, S. M. Lippman, *N. Engl. J. Med.* **2007**, 356, 76–78.

BIOGRAPHICAL SKETCH

Hui Chen was born in Jiangsu Province, China, in September, 1978. He went to Soochow University in 1996 to study chemistry. After four years of chemistry major study, he entered the graduate program in the same university in 2000. After he obtained the M.S. degree, Hui entered the University of Florida in 2003 and joined Dr. Weihong Tan's research group. He received his Ph.D. from the University of Florida in the spring of 2009.